Technische Universität München
TUM School of Medicine and Health

The role of transient fetal hypoxia in the development of pulmonary hypertension dependent on p22phox

Katharina Patricia Haufe

Vollständiger Abdruck der von der TUM School of Medicine and Health der Technischen Universität München zur Erlangung einer Doktorin der Medizinischen Wissenschaft (Dr. med. sci.) genehmigten Dissertation.

Vorsitz: Prof. Dr. Michael Joner

Prüfende der Dissertation:

1. Prof. Dr. Agnes Görlach
2. Priv.-Doz. Dr. Katja Steiger

Die Dissertation wurde am 07.08.2024 bei der Technischen Universität München eingereicht und durch die TUM School of Medicine and Health am 04.12.2024 angenommen.

Index

1 Abbreviations

8-oxoG	8-Oxo-2’-oxyguanosine
8-oxodG	8-Oxo-2’-deoxyguanosine
Ao	Aortic
Bcl-2	B-cell lymphoma 2 gene
BMPR2	Bone morphogenic protein receptor 2
BPD	Bronchopulmonary dysplasia
BSA	Bovine serum albumin
BW	Body weight
CCB	Calcium channel blocker
cDNA	Cyclic deoxyribonucleic acid
CGD	Chronic granulomatous disease
cGMP	Cyclic guanine monophosphate
CHD	Congenital heart defect
CMH	3-Carbamoymethyl-5-Methyohexanoic Acid
COMT	Catechol-o-methyltransferase
CPP	Cycloparaphenylene
CTEPH	Chronic thromboembolic pulmonary hypertension
cTnT	Cardiac troponin T
DAPI	4,6-Diamidin-2-phenyoindol
DES	Diethylstilbetrol
DETC	Diethyldithiocarbamic acid
DMPO	5,5-Dimethyl-1-pyrroline N-oxide
DMSO	Dimethylsulfoxide
DNA	Deoxyribonucleic acid
DTT	Dithiothreitol
EB	Embryoid body
EDTA	Ethylenediaminetetraacetic acid

eNOS	Endothelial nitric oxygen synthase
EPO	Erythropoietin
EPR	Electron paramagnetic resonance
ET (A)	Endothelin A
ET (B)	Endothelin B
ET-1	Endothelin-1
FC	Functional class
FCS	Fetal calf serum
FiO2	Fraction of inspired oxygen
GIH	Gestational intermittent hypoxia
GPx	Glutathione peroxidase
GSH	Glutathione
GTP	Guanine Triphosphate
HE	Haematoxylin eosin
Hif1	Hypoxia inducible factor 1
Hif1-α	Hypoxia inducible factor 1-α
Hif1-β	Hypoxia inducible factor 1-β
Hnf-1	Hepatocyte nuclear factor 1
HR	Heart rate
Hsp70	Heat shock protein 70
Hx	Hypoxia
HxHx	Fetal hypoxia (10% oxygen 24 h E10.5-11.5), 21 days of hypoxia (10% oxygen) at an age of 8 weeks
HxNx	Fetal hypoxia (10% oxygen 24 h E10.5-11.5), adult normoxia
i.p.	Intraperitoneal
IRI	Ischemia reperfusion injury
IUGR	Intrauterine growth restriction
LHD	Left heart disease
Lif	Leukaemia inhibitory factor

LV	Left ventricle
MEF	Murine embryonic fibroblast
mESC	Murine embryonic stem cells
MI	Myocardial infarction
miRNA	Micro ribonucleic acid
mPAP	Mean pulmonary arterial pressure
mRNA	Messenger ribonucleic acid
NAD	Nicotinamide adenine nucleotide
NADPH	Nicotinamide adenine dinucleotide phosphate
NO	Nitric oxygen
Nx	Normoxia
NxHx	Fetal normoxia, 21 days of hypoxia (10% oxygen) at an age of 8 weeks
NxNx	Normoxic control group
Oct4	Octamer binding transcription factor 4
OFT	Outflow tract
OSA	Obstructive sleep apnea
Otx2	Orthodenticle homeobox 2
PAH	Pulmonary arterial hypertension
PaO2	Partial pressure of oxygen
PAS	Periodic acid Schiff’s reaction
PASMC	Pulmonary artery small muscle cell
PAWP	Pulmonary arterial wedge pressure
PBMC	Peripheral blood mononuclear cells
PBS	Phosphate buffered saline
PCR	Polymerase chain reaction
PDE-5	Phosphodiesterase-5
PDGF	Platelet-derived growth factor
PFA	Paraformaldehyde
PH	Pulmonary hypertension

PKCε	Protein kinase C ε
PMSF	Phenylmethylsulfonyl fluoride
PTEN	Phosphatase and tensin homologue
PVR	Pulmonary vascular resistance
qPCR	Quantitative polymerase chain reaction
RNA	Ribonucleic acid
ROS	Reactive oxygen species
RV	Right ventricle
SDS	Sodium dodecyl sulfate
sGC	Soluble guanylate cyclase
siRNA	Small interfering ribonucleic acid
SOD	Superoxide dismutase
SP A-C	Surfactant protein A-C
TEMED	N,N,N',N'-Tetramethylethylenediamine
TRIS	Tris(hydroxymethyl)aminomethane
UA	Uterine artery
VE	Demineralized water
VEGF	Vascular endothelial growth factor
VEGFR2	Vascular endothelial growth receptor 2
WB	Western blot
WGA	Wheat germ agglutinin
WHO	World health organization
WT	Wildtype
XO	Xanthine oxidase
α-MHC	α-Myosin heavy chain
α-smc	α-Smooth muscle cell
β-MHC	β-Myosin heavy chain

2 Summary

Fetal hypoxia is a common complication of many pregnancies. Epidemiological studies have shown that oxygen deprivation during pregnancy can increase the risk of developing cardiovascular dysfunction later on. However, little is known about molecular mechanisms that could underlie this so-called fetal programming.

Hypoxia can lead to a subsequent increase in the formation of reactive oxygen species (ROS). ROS serve as signalling molecules in small quantities, but in larger quantities they can be harmful to cells. An enzyme group with the primary function of producing reactive oxygen species are NADPH oxidases. NADPH oxidases play a role in the pathogenesis of various cardiovascular diseases in adults. The role they play in fetal development and fetal programming is not understood. The aim of this study was therefore to investigate the role of NADPH oxidases in the fetal programming of cardiovascular diseases by fetal hypoxia.

For this purpose, pregnant wild-type mice and mice that have a mutation in the gene of the NADPH oxidase subunit p22phox and thus lack a functional NADPH oxidase, were exposed to 10% oxygen between E10.5 and E11.5. Wild-type mice exposed to transient fetal hypoxia showed intrauterine growth inhibition, signs of delayed cardiac and pulmonary development, and signs of pulmonary hypertension with right heart hypertrophy in adulthood. Fetal hypoxia led to increased ROS formation in the embryo at E11.5 and E17.5, as well as to oxidative DNA damage not only in the E11.5 embryo, but also in the heart of E17.5 embryos and in the adult offspring. Mice with mutated p22phox gene did not show increased ROS formation and were protected from the effects of fetal hypoxia in both embryonic and adult age. These studies suggest that NADPH oxidases play an important role in fetal programming of pulmonary hypertension by fetal hypoxia. Inhibition of NADPH oxidases may represent an important protective mechanism against the development of late effects after fetal hypoxia.

2.1 Zusammenfassung

Fetale Hypoxie ist eine weit verbreitete Komplikation vieler Schwangerschaften. Epidemiologische Studien zeigten, dass Sauerstoffmangel während der Schwangerschaft das Risiko erhöhen kann, später u.a. an kardiovaskulären Dysfunktionen zu erkranken. Noch ist jedoch wenig bekannt über molekulare Mechanismen, die dieser sog. fetalen Programmierung zugrunde liegen könnten.

Hypoxie kann zu einer nachfolgenden Vermehrung der Bildung von reaktiven Sauerstoffspezies (ROS) führen. ROS dienen in geringen Mengen als Signalmoleküle, in größeren Mengen können sie aber zellschädlich sein. Eine Enzymgruppe mit der vornehmlichen Funktion, reaktive Sauerstoffspezies zu produzieren, sind die NADPH Oxidasen. NADPH Oxidasen spielen eine Rolle in der Pathogenese verschiedener kardiovaskulärer Erkrankungen im Erwachsenen. Welche Rolle sie bei der fetalen Entwicklung und der fetalen Programmierung spielen, ist nicht verstanden.

Ziel dieser Arbeit war daher zu untersuchen, welche Rolle NADPH Oxidasen bei der fetalen Programmierung kardiovaskulärer Erkrankungen durch fetale Hypoxie spielen.

Dazu wurden trächtige Wildtypmäuse und Mäuse, die eine Mutation im Gen der NADPH Oxidase Untereinheit p22phox und damit keine funktionale NADPH Oxidase besitzen, zwischen E10.5 und E11.5 10% Sauerstoff ausgesetzt.

Wildtypmäuse, die transienter fetaler Hypoxie von Entwicklungstag 10.5-11.5 ausgesetzt waren, zeigten eine intrauterine Wachstumshemmung, Zeichen einer verzögerten Herz- und Lungenentwicklung sowie Anzeichen einer pulmonalen Hypertension mit Rechtsherzhypertrophie im Erwachsenenalter. Fetale Hypoxie führte zu einer erhöhten ROS-Bildung im Embryo in E11.5 und E17.5, sowie zu oxidativen DNA-Schäden nicht nur im E11.5 Embryo, sondern auch im Herzen von E17.5 Embryonen und im adulten Nachwuchs. Mäuse mit mutiertem p22phox Gen zeigten keine erhöhte ROS-Bildung und waren vor den Auswirkungen der fetalen Hypoxie sowohl im Embryonal- wie auch im Erwachsenenalter geschützt. Diese Untersuchungen lassen vermuten, dass NADPH Oxidasen eine wichtige Rolle bei der fetalen Programmierung der pulmonalen Hypertension durch fetale Hypoxie spielen. Hemmung der NADPH Oxidasen könnte einen wichtiger Schutzmechanismus vor der Entwicklung von Spätfolgen nach fetaler Hypoxie darstellen.

3 Introduction

3.1 Fetal development – a comparison between humans and mice

Since decades of research, mice are serving as experimental models for human development due to their comparability. Although the development of humans and mice has many similarities, there are some important differences between them. To apply results from in vivo experiments in rodents to humans, it is of an outstanding importance to understand these differences and to consider them in the experimental design. Human gestation lasts for about 40 weeks, being one of the longest pregnancies among mammals. In contrast, rodents like mice have a gestation about 18 to 21 days, depending on the strain and conditions (Murray, Morgan et al. 2010). Therefore, it is very difficult to mimic especially the last two thirds of human pregnancy in animal studies, because this stage is simply not existent for example in rodent gestation. Because of that, earlier time points during organ formation and differentiation are more comparable between humans and mice (Xue, Cai et al. 2013).

3.1.1 Cardiac development

Despite the different time humans and mice develop in utero, the steps during organogenesis and cardiac formation are almost the same (Krishnan, Samtani et al. 2014).

Giving a very short summary of the heart development applicable to humans and mice, firstly the primitive heart tube is formed (Patterson and Zhang 2010). Cardiac progenitor cells differentiate into myocardial cells and fuse for the formation of the heart tube. Then, looping of the heart tube takes place to set the in which the chambers can develop. Trabeculation begins to increase the surface to volume ratio so the myocardium can grow prior to the establishment of the separation of blood flow and the coronary circulation before septation (Patterson and Zhang 2010). To form the coronary arteries, the vessels undergo extensive remodelling and there is evidence suggesting that the physiological hypoxia during gestation is giving the initial signal mediating angioblast invasion of the embryonic heart (Nanka, Valasek et al. 2006, Patterson and Zhang 2010). The primary cardiac progenitor cells develop to fetal cardiomyocytes. They differ from adult cardiomyocytes, having less and fewer organized myofibrils with lower developed sarcoplasmatic reticulum and T tubules. The most important difference is that fetal cardiomyocytes proliferate rapidly throughout early stages of development, and they become increasingly differentiated and lose their ability to propagate

towards the end of gestation (Patterson and Zhang 2010, Gittenberger-de Groot, Bartelings et al. 2013). The reasons for the loss of the proliferation capacity are unclear. For a short comparison of the cardiac development between mice and humans, Figure 1 shows the different days of pregnancy in mice, starting at E 9.5, and the Carnegie stages, which describe the steps in human development in the first 8 weeks of pregnancy.

There are a few morphological differences between human and mouse hearts, excellently described by Krishnan et. al. Mice have a single pulmonary venous orifice, while humans have 2-4 venous orifices. Furthermore, mice are lacking the moderator band, and they have a bilateral superior vena cava. The thickness of the atrioventricular septum is thick and muscular in the mouse, while human septum is thin and fibrous (Krishnan, Samtani et al. 2014).

Beside the similarities, mouse models which refer to the human heart development are limited at late gestation, because within a few days after completion of cardiac morphogenesis, mice are born, but in humans several months of gestation remain. Nevertheless, the mouse model is one of the best for examining cardiovascular development and congenital heart defects (CHD) because the most vulnerable phase in human gestation is early to midterm pregnancy (Wessels and Sedmera 2003).

E 9.5–10.5	-E 11.5	-E 12.5	-E 13.5	-E 14.5	-E 17.5	E 18-21
Cardiac looping	Progressive septation of atria and ventricles, muscular interventricular septum formation, septation of the outflow tract	Progressive septation of the outflow tract atrioventricular canal septation	Completion of ventricular septum formation, remodelling of atrioventricular cushions, bilaterally asymmetrical aortic arch system	All definitive major cardiac structures identifiable, atrial septation complete	Myocardial compaction, AV/ semilunar valve refinement, coronary arteries are modified	Continued myocardial compaction semilunar valve refinement
CS 13-17	CS 15-16	CS 17-18	CS 19-21	CS 22	CS 23	

Fig. 1: Cardiac development in mice and humans

Comparison of cardiac development starts at E 9.5 in mice with cardiac looping. Until E11.5 there are a few steps in the mouse development which take place during CS 13-17 in humans, for example septation of the atria and ventricles, progressive septation of the outflow tract and muscular interventricular septum formation. Until E12.5 (CS 17-18) the septation of the OFT proceeds and the AV canal septation takes place. The ventricular septum is completed until E13.5 (CS 19-21) and the bilateral asymmetrical aortic arch system is formed. At E14.5 (CS 22) all major cardiac structures are identifiable and atrial septation is completed. E17.5 is the timepoint where coronary arteries are being modified and AV and semilunar valves are refined. Birth takes place in mice gestation from E18-21, depending on the line and the size of the litter. In humans this is comparable with the first 8 weeks of development. The 23 Carnegie stages represent the first 8 weeks of embryonic development. P.c.= post conceptionem, CS = Carnegie Stages, E = days p.c. (Krishnan, Samtani et al. 2014)

3.1.2 Lung Development

The maturation of the embryonic lungs is comparable between mice and humans (Figure 2). In murine pregnancy, lung development starts at E9.5 with the formation of the primordium, in human gestation it starts on day 28 post conceptionem (p.c.) (Ten Have-Opbroek 1991, Chao, El Agha et al. 2015, Pan, Deutsch et al. 2019). At this developmental stage, a protrusion of the foregut appears and develops into the prospective trachea and two lung buds. Each of them forms a branching tubular system with tubules, called primordial tubules lined by undifferentiated columnar epithelium. Vascular connection between the heart and the lung has been described as early as day 34 gestation in human and E10.5 in mice (Herriges and Morrisey 2014). At E14.5, differentiation of the primordial system into the bronchial system and the respiratory system starts. From E16.5, the prospective pulmonary acinus shows dramatic changes in shape, transforming the acinar tubules into structures with a duct-, sac-, or pouch-like shape. It is very likely that this transformation process is influenced by the proximity of capillaries in the alveolar walls. The formation of the terminal sac is ended 5 days after birth, followed by the alveolar developmental stage which is protruding until day 30 of life (Ten Have-Opbroek 1991).

The co-development of heart and lung is illustrated when the lung endoderm protrudes into the cardiac mesoderm as the two organs develop parallel to form the cardiopulmonary circulation. Interestingly, in mice, the pulmonary vasculature develops even in the absence of lung development. This process is induced by a special population of multipotent cardiopulmonary mesoderm progenitors (CPPs). It was shown through lineage tracing and clonal analysis that cardiomyocytes as well as pulmonary vascular and airway smooth muscle, proximal vascular endothelium, and pericyte-like cells originate from these CPPs (Peng, Tian et al. 2013).

Embryonic	Pseudoglandular	Canalicular	Saccular	Alveolar
E9 - 11.5	E 11.5 - 16.5	E 16.5 - E 17.5	E17.5 - PND 5	PND 5 - PND 28
Respiratory diverticulum appears on the ventral wall of the foregut, lobar division occurs	extensive airway branching, mesenchyme is surrounding epithelial tubes	Bronchioles form, capillaries in contact with cuboidal epithelium, alveolar epithelium development	Formation of alveolar ducts and air sacs	secondary septation occurs, increase of the number and size of capillaries and alveoli
W 4 - 5	W 5 - 17	W 17 - 24	W 24 - 40	Late fetal – 8 y

Fig. 2: Lung development in mice and humans

Lung development in mice starts with the formation of the respiratory diverticulum from the foregut at E9-11.5 in the embryonic phase, which is comparable to week 4-5 of human gestation. Next, pseudoglandular stage is reached with airway branching and mesenchyme formation from E11.5 to E16.5 (finished around week 17 in humans). Then, canalicular stage with differentiation of bronchioles and alveolar epithelium appears until E17.5 or weeks 24 in humans. Different to human gestation, where the alveolar ducts and air sacs are developed in utero until week 40, the saccular stage ends with postnatal day 5 in mice. The last stage takes the most time, ending at day 28 postnatally in mice and by eight years in humans (Ten Have-Opbroek 1991, deMello, Sawyer et al. 1997, Hislop 2005, Smith, McKay et al. 2010, Herriges and Morrisey 2014, Krishnan, Samtani et al. 2014, Pan, Deutsch et al.

3.2 Fetal hypoxia

Originally, Sir Joseph Barcroft was the first to describe the oxygen situation of the developing fetus in utero. He was coining the phrase ‘Everest in utero’, comparing the developing fetus to a mountain climber acclimatized to high altitudes (Giussani, Bennet et al. 2016). The physiological fetal arterial oxygen tension (25 mmHg) is lower compared to the adult (95 mmHg). This physiological environment of lower oxygen is crucial for proper fetal development, but further decline in oxygen availability has detrimental effects on the fetus (Ducsay, Goyal et al. 2018).

3.2.1 Gestational hypoxia – studies in humans

Hypoxia during pregnancy is a rather common but underestimated issue. It can be caused by a variety of reasons such as maternal smoking, adiposity, preeclampsia, anemia, gestational diabetes, obstructive sleep apnea (OSA), asthma, placental deformations or environmental factors like living at high altitude (Mikhed, Gorlach et al. 2015). Hypoxia during gestation is linked to an increased risk of CHD (Vento and Teramo 2013, Torres-Cuevas, Parra-Llorca et al. 2017) and it has also an impact on the risk of developing cardiovascular diseases later in life by fetal heart programming (Patterson and Zhang 2010). Many studies have shown that hypoxia during gestation leads to a decreased birth weight and intrauterine growth restriction (IUGR) (Julian, Wilson et al. 2009, Moore, Charles et al. 2011).

Studies examining the effects of hypoxia during development in humans started in the 1950ies with John Litchy who found out why newborns in Colorado had the highest prematurity rate (defined as a birth weight lower than 2500 g) (Lichty 1957). It is also known that multigenerational residents at high altitude can compensate chronic hypoxia, mainly through a rise in the uterine artery (UA) blood flow (Julian, Wilson et al. 2009, Browne, Julian et al. 2015).

Studies performed at high altitude are an important contribution to our understanding of the mechanisms and effects of chronic hypoxia and the adaptation mechanisms multigenerational high-altitude residents can develop. There are 140 million people living above 2500 m, putting numerous persons at risk of fetal growth restriction. Additionally, large number of tourists visit high altitude during gestation, increasing the risk of intermittent hypoxia due to anemia or cardiopulmonary diseases (Moore, Charles et al. 2011). Therefore, understanding the detailed mechanisms underlying hypoxia during gestation is of great importance. First recognized in the late 50ies, it became more and more obvious that beside such factors as ethnicity and inadequate medical care, high altitude itself is responsible for fetal growth restriction (Lichty

1957, Lichty, Ting et al. 1957). More recent studies showed that birth weight decreases on average 102 g per 1000 m height gain and that the number of babies born small for their gestational age has tripled at high altitude (Krampl 2002, Julian, Vargas et al. 2007). Although there are factors like nutrition, socioeconomic status, and health care also contributing to this observation, such factors cannot account for the altitude-associated fall. Furthermore, about half the fall can be attributed to a tripling of the incidence of preeclampsia, also causing fetal hypoxia (Jensen and Moore 1997, Keyes, Armaza et al. 2003, Moore, Charles et al. 2011).

Interestingly, multigenerational residents of high-altitude like Andean women undergo a doubling of uterine artery (UA) diameter during pregnancy whereas European women are only showing about half as much increase at high altitude (Vargas, Vargas et al. 2007, Wilson, Lopez et al. 2007, Moore, Charles et al. 2011). This leads to a greater oxygen delivery through a much higher UA blood flow in Andean compared to Europeans at high altitude. Ancestry-group related differences in UA blood flow are already present by week 20, which is well before altitude-associated reductions in fetal growth are apparent (Julian, Wilson et al. 2009, Julian, Wilson et al. 2009, Moore, Charles et al. 2011). It is possible that a high UA blood flow protects the fetus against intermittent hypoxia and ischemia reperfusion injury (IRI), leading to a stimulation of reactive oxygen species (ROS) production, damaging the endothelium, reducing vasodilator production or activity, and decreasing uterine vessel diameter and flow (Jeffreys, Stepanchak et al. 2006, Moore, Charles et al. 2011). Also, Andean residents had a higher antioxidant activity compared to Europeans suggesting that this might be one mechanism to prevent oxidative damage and preserving larger UA diameters and flow (Julian, Wilson et al. 2009).

Sustaining fetal growth, UA blood flow is clearly important, and the observation that there was a greater increase in long than in short-resident high-altitude population suggests, that the UA blood flow could be an important factor to the relative protection from altitude-associated fetal growth restriction (Julian, Vargas et al. 2007, Vargas, Vargas et al. 2007, Wilson, Lopez et al. 2007, Julian, Wilson et al. 2009, Browne, Julian et al. 2015). However, precise mechanisms are presently unknown.

It is estimated that intrauterine hypoxia affects 0.6-0.8% of pregnancies and is correlated with an increased risk of IUGR, perinatal mortality, impaired neurodevelopment, and elevated risk of adult cardiovascular disease (Ream, Ray et al. 2008, Cahill, Zhou et al. 2014). Gestational hypoxia itself is a difficult model to study. Out of several reasons many epidemiological studies which were made in humans are limited in their validity. Most of these studies were made at areas where there is not only chronic hypoxia due to high altitude, but also a high prevalence

of maternal undernutrition and poor socioeconomic status, which could also influence the development of the fetus (Keyes, Armaza et al. 2003, Vargas, Vargas et al. 2007, Julian, Wilson et al. 2009). Also, many diseases like preeclampsia, placental insufficiency and maternal obesity are linked to a lower fetal oxygen supply as well as nutritional supply. Therefore, it is difficult to study the isolated effects of hypoxia on the fetus. Nevertheless, that is the reason why animal studies come closest to gestational hypoxia in humans (Jensen and Moore 1997).

About 1% of newborns suffer from a congenital heart defect (CHD), making it an important health concern (Wu, He et al. 2020). CHDs include a wide range of phenotypes with varying severity and potentially different aetiologies, such as atrial or ventricular septum defects, transposition of the grand arteries or Fallot's tetralogy. They can be caused by genetically and environmental factors, making it hard to define the underlying mechanisms and for most CHD the reasons remain unknown. But the risk of a CHD is increased by antenatal hypoxia, which can be caused by maternal smoking, preeclampsia and diabetes (Correa, Levis et al. 2015). Although the fetal heart develops under physiologically hypoxic conditions, further abnormal oxygen saturation has adversely and detrimental effects on cardiogenesis (Torres-Cuevas, Parra-Llorca et al. 2017).

Preeclampsia is one of the most frequent causes of chronic gestational hypoxia (Osol and Mandala 2009). Due to changes of the lumen of spiral arteries, a low intermittent uterine blood flow to the placenta occurs. These fluctuant perfusion causes a low-grade IRI that provokes oxidative stress. Some studies also suggest that ROS may cause preeclampsia by different mechanisms such as consolidating the inflammatory and vascular endothelium response or activating syncytiotrophoblast pro-apoptotic pathways during placentation thus impairing normal arteriolar remodelling (Kublickiene, Lindblom et al. 2000, Pennington, Schlitt et al. 2012, Torres-Cuevas, Parra-Llorca et al. 2017).

The detailed mechanisms behind chronic fetal hypoxia caused by diabetes are still not completely revealed, but epidemiological reports have shown that diabetic pregnancies have an increased risk of stillbirth and early neonatal (Mathiesen, Ringholm et al. 2011, Luo, Zhao et al. 2013, Torres-Cuevas, Parra-Llorca et al. 2017). Hyperinsulinemia as well as hyperglycemia can negatively influence fetal development which could result in fetal macrosomia and hypoxia (Torres-Cuevas, Parra-Llorca et al. 2017). High blood glucose levels are correlated with oxidative stress and ROS production. The intensity and duration of fetal hypoxia can be measured by fetal plasmatic and amniotic fluid erythropoietin (EPO) levels. EPO is not stored and cannot cross the placental barrier, so it is reflecting fetal production and

elimination (Escobar, Teramo et al. 2013, Suzuki 2015). Hyperglycemia causes an increased production of advanced glycation end products and activates hexosamine biosynthesis. Conclusively, nicotine amid dinucleotide (NAD) synthesis and rebuilding of GSH by the GSH-reductase are reduced. In the end, activation of the protein kinase C pathway and NADPH oxidase activation contribute an enhanced ROS production leading to oxidative stress (Escobar, Teramo et al. 2013, Torres-Cuevas, Parra-Llorca et al. 2017). Furthermore, insulin resistance is triggered by the activation of nuclear factor κB (NFκB), activator protein-1 and HIF-1α. EPO levels were increased in pregnant women with gestational or type I diabetes treated with insulin. It indicated that intrauterine hypoxia in insulin dependent diabetic pregnancies caused fetal oxidative stress and increased neonatal morbidities (Torres-Cuevas, Parra-Llorca et al. 2017). Despite these relevant findings, more studies must be performed, especially about the effects of acute hypoxia during gestation. An adequate oxygen availability during the embryonic, fetal and postnatal phases is essential for normal metabolism, growth and development.

Overall, the impact of unphysiological fetal hypoxia is detrimental to the fetal development and may even have long term effects in the adult offspring. Depending on the time point and duration of fetal hypoxia, it affects organogenesis, fetal growth, lung maturation or metabolic function.

3.2.2 Gestational hypoxia – studies in animals

Overall, there are few studies dealing with the effect of gestational hypoxia. The most common animal model are rodents like mice and rats, but also pregnant sheep are a common model in this field. The studies vary in time points, duration, and oxygen content, but all of them conclude that unphysiological gestational hypoxia has a detrimental effect on the developing fetus in various ways. Table 1 shows some examples of studies in rodents, which were set under fetal hypoxia at different time points with different percentages of oxygen. Overall, fetal hypoxia leads to impaired cardiac and pulmonary development and growth retardation, which could affect the offspring persistently.

Table 1: Studies of gestational hypoxia in rodents: LV= left ventricle, RV= right ventricle, HR= heart rate, Ao= aortic, BP= blood pressure, BPD= bronchopulmonary dysplasia,

Hypoxia model	Results
12% O_2 E15 – E21 (Rueda-Clausen, Stanley et al. 2014)	• males are more sensitive to prenatal hypoxia than females: smaller body weights, signs of left ventricular hypertrophy, • signs of LV diastolic dysfunction in the offspring • signs of PAH by 12 months of age (decreased pulmonary artery acceleration time, increased diastolic RV diameter) in the offspring • lower HR (offspring) • bigger Ao end diastolic/systolic diameter (offspring) • higher Ao peak ejection velocity (offspring)
10.5% O_2 E10.5 – E18.5 (Rueda-Clausen, Dolinsky et al. 2011)	• increased BP • proteinuria in C57BL/6J and eNOS -/- mice • fetal survival significantly reduced particularly in eNOS -/- mice (<10%) • decreased body mass at birth • placentas from COMT -/- mice demonstrated increased peroxynitrite • crown to rump length and abdominal circumference was significantly reduced
8% O_2 E11.5 – E17.5 for 24 h (Ream, Ray et al. 2008)	• 89% of E13.5 embryos died • 5% of E11.5 embryos died • 51% of E17.5 embryos died • decreased birth weight (26%) and total protein (45%) • signs of heart failure, including loss of yolk sac circulation, haemorrhage, and oedema
10% O_2 E14.5 – E18.5 (Schmiedl, Roolfs et al. 2017)	• BPD like alterations (retardation of morphological pulmonary development) in 2 week old mice • E18 post hypoxia: no morphological retardation of pulmonary development • significantly lower body weight after hypoxia
10% O_2 at E16.5 for 24h (Tsao and Wei 2013)	• Lung development: control mice were in the pseudoglandular stage and progressed to the canalicular stage to E17.5 • Hypoxic lungs failed to progress beyond the late pseudoglandular or early canalicular stages • inhibitory effect of prenatal hypoxia persisted after the return to normoxia at E18.5

Another common model for developmental hypoxia is intermittent hypoxia, mimicking obstructive sleep apnoea (OSA). Several studies showed OSA is connected to metabolic dysfunction, insulin resistance and a rise in cholesterol and triacylglycerides (Drager, Jun et al. 2010). Furthermore, it has detrimental effects on the fetus: in mice, intermittent hypoxia between day 13-18 (5% FiO_2 for 12 hours during light phase) of gestation induced metabolic dysfunction showed by an increased body weight and adiposity index in adult male offspring and altered proinflammatory macrophages (Khalyfa, Cortese et al. 2017).

One study showed that postnatal hypoxia is also affecting the adult offspring in a detrimental way. It is known that premature infants are at a very high risk of hypoxia because of their

immature lungs and surfactant deficiency. Neonates were exposed to intermittent hypoxia in alternating cycles of 8% and 21% FiO_2 with 120s-cycle duration for 6 hours per day for the first 4 weeks of life. At 3 months age, various cardiovascular measurements were obtained. The adult mice showed signs of endothelial dysfunction as shown by impaired vasodilatory responses to acetylcholine, reduced reperfusion indices after tail vessel occlusion, higher systolic blood pressure, an altered baroreflex and autonomic nervous system regulation (Chu, Gozal et al. 2015).

Another study has shown that in chicken embryos chronic fetal hypoxia leads to a reduced number of cardiomyocytes due to reduced proliferation and premature cardiomyocyte maturation. The ventricle-to-body-mass ratio was increased, which is explained by the fact that the fetal cardiomyocytes are inhibited in proliferation, leading to hyperplasia as a compensation mechanism. Interestingly, there were no signs of ventricular wall remodelling or myocardial fibrosis detected, and also no increase in binucleated cardiomyocytes was found (Osterman, Lindgren et al. 2015). This is also in contrast to the findings of studies summarized above (Martin, Yu et al. 1998, Bae, Xiao et al. 2003).

In chronic hypoxic vs. normoxic guinea pigs, there was a decrease by 50% in pregnancy-associated UA DNA synthesis. Also, proliferation of vascular smooth muscle cells as a response to serum stimulation in cultured UA was diminished, suggesting that this process is limited due to hypoxia (Rockwell, Dempsey et al. 2006, Moore, Charles et al. 2011). There was also an increased production of ROS, leading to a diminished NO activity. This led to the observation, that pregnancies affected by chronic gestational hypoxia also show less vasodilator response to flow (White, McCullough et al. 2000, Mateev, Sillau et al. 2003, Moore, Charles et al. 2011), similarly to studies in myometrial arteries from pregnancies affected by preeclampsia (Kublickiene, Lindblom et al. 2000, Kublickiene, Nisell et al. 2000).

The physiological mechanisms which underlie the connection of IUGR and the risk of cardiovascular diseases in the offspring are poorly characterized. Fetal evolvement takes place under slightly hypoxic conditions, being beneficial to the expression of Hif1-α, VEGF and other factors that contribute to angiogenesis and vasculogenesis (Compernolle, Brusselmans et al. 2003, Sugishita, Leifer et al. 2004). Pathophysiological hypoxia has indeed the adverse effect, inhibiting the pluripotency of embryonic stem cells and can lead to changes in structure, function and gene expression which might persist in the offspring (Infantes, Prados et al. 2015).

Many recent studies concentrated on the formation of the outflow tract (OFT) and coronary vessel formation. Indeed, apoptosis of OFT cardiomyocytes is necessary for remodelling and

the shortening and rotation needed for the aorta to join the left ventricle and pulmonary vessels to connect to the right ventricle (Patterson and Zhang 2010). Some studies suggest that HIF-1 and other hypoxia-regulated genes might be responsible for OFT remodelling (Watanabe, Jafri et al. 2001, Barbosky, Lawrence et al. 2006). But there are also OFT defects like an abnormal formation of the right ventricle that are caused by an increase in oxidative stress which can lead to excessive cell death. It is indicated that the timing and duration of a hypoxic insult is crucial for the regulation of heart remodelling and tissue development (Robin, Marcillac et al. 2015).

3.2.3 The effect of gestational hypoxia on the offspring

Hypoxia during gestation has several effects on the fetal development and in the offspring. One of the earliest studies demonstrated the adverse effects of hypoxia causing ventricle septal defects in rat offspring (Lueder, Kim et al. 1995). Other studies showed that chronic fetal hypoxia is responsible for cardiomyocyte hypertrophy and myocardial hypoplasia as a compensation mechanism. An increase in apoptosis mediated through hypoxia was examined, and it was shown that apoptosis is induced via elevated caspase 3 activity and Fas mRNA resulting in supressed survival pathways (e.g. Hsp70 expression) (Bae, Xiao et al. 2003). There were also signs that the number of binucleated cardiomyocytes is increased by antenatal hypoxia, which are terminally differentiated cells that lost their ability of division (Martin, Yu et al. 1998, Bae, Xiao et al. 2003, Patterson and Zhang 2010). Overall, fetal hypoxia alters heart growth resulting in morphologic abnormalities which can impair cardiac health also in the adult.

The effects of antenatal hypoxia for the offspring are of high interest. Several studies showed that there is an intrauterine programming which predisposes to cardiovascular diseases in the adult offspring (Li, Xiao et al. 2003, Li, Bae et al. 2004, Chen, Zhang et al. 2019, Huang, Chen et al. 2019). This programming also seems to be dependent on sex, as demonstrated by the diminished recovery of male rats, which were exposed to ischemia and reperfusion injury after fetal hypoxia exposure (Xue and Zhang 2009). In male rats, myocardial infarction size and LDH release were increased compared to control group. This observation has been associated with altered programming of cardioprotective genes, namely PKCε (Xue and Zhang 2009, Patterson, Xiao et al. 2012). Several studies concluded that prenatal hypoxia is leading to a decrease in post ischemic recovery, an increase in MI, and decreased number of cardiomyocytes with a larger cell volume. Additionally, there was found an elevated caspase 3 activity and decreased levels of Hsp70 and eNOS compared to controls (Xu, Williams et al. 2006, Xue and Zhang 2009).

As already said, gestational hypoxia (10.5% oxygen from Day 15-21 in pregnant rats) results in an increased cardiac vulnerability to ischemia in the adult offspring (Patterson, Chen et al. 2010). After IRI, adult offspring exposed to gestational hypoxia showed decreased postischemic recovery (LV function) compared to controls (Li, Xiao et al. 2003).

Chronic gestational hypoxia has been associated with an increased cardiovascular risk in the offspring. Exposing sheep to chronic hypoxia in the third trimester of pregnancy (10% oxygen), the adult offspring develops high blood pressure by impairing NO dependent endothelial function. Interestingly, this effect can be prevented by treating the hypoxia exposed dam with the antioxidant vitamin C leading to an increased NO bioavailability (Brain, Allison et al. 2019). This study for example shows the link between antenatal oxidative stress and cardiovascular health in the adult.

Evidence is starting to accumulate that fetal hypoxia leads to cardiovascular programming due to epigenetic regulations. For example, antenatal hypoxia leads to hypermethylation of the PKCε promoter region which persists also in the adult offspring (Patterson, Chen et al. 2010). Besides that, gestational hypoxia also leads to programming of Hsp70 gene in the left ventricle of the adult offspring, decreasing the cardioprotecting content which is contributing to an increased susceptibility to IRI (Li, Bae et al. 2004).

3.3 Pulmonary hypertension

Pulmonary hypertension (PH) is a chronic multifactorial disease, which affects about 1% of adults (Hoeper, Ghofrani et al. 2017). It was first described over a century ago (Newman 2005), and is characterized by pulmonary vascular remodelling and endothelial dysfunction which leads to increased pulmonary vascular resistance (PVR). A chronically elevated PVR results in right ventricular remodelling and hypertrophy, which can lead to right heart failure (Humbert, Morrell et al. 2004). Until now, curative treatment is not available and molecular mechanisms still must be elucidated.

3.3.1 Clinical classification and diagnosis

PH is indeed not a full diagnosis itself but is describing a certain hemodynamic state with an elevation of the mean arterial pulmonary pressure (mPAP >25 mmHg) (Dodson, Brown et al. 2018). It is a generic term being divided into five different subgroups by the WHO classification

(Hoeper, Ghofrani et al. 2017). Table 2 shows the five subgroups of PH of the WHO classification modified after (Ryan, Thenappan et al. 2012, Hoeper, Ghofrani et al. 2017).

Pulmonary arterial hypertension (PAH) is characterized as a precapillary PH with an increased PVR, resulting in an elevation of the mPAP >25 mmHg with a normal pulmonary wedge pressure (PAWP) and PVR >250 dyn x s x cm^{-5} (Galie, Humbert et al. 2016).

Idiopathic PH is the most common subtype and is characterized by the lack of any underlying risk factor such as obesity, diabetes mellitus type 2, arterial hypertension, or ischemic heart disease (Ling, Johnson et al. 2012). Other subtypes include the connective tissue PAH and the CHD PAH which is interestingly the most common type of PAH in China due to its low operation rate of CHD (Jing, Xu et al. 2007). Meta-analysis found that female sex is a risk factor of developing PAH (Lau, Giannoulatou et al. 2017). However, male patients who are affected by PAH have a lower survival rate than women, which could be due to differences in right ventricular adaption. Overall, hormone influence and sex-dependent differences are not fully understood (Lau, Giannoulatou et al. 2017).

Table 2. WHO classification of PH (Newman 2005, Ryan, Thenappan et al. 2012, Galie, Humbert et al. 2016, Hoeper, Ghofrani et al. 2017, Dodson, Brown et al. 2018)

WHO classification of Pulmonary Hypertension		
WHO I	PAH	• Idiopathic • hereditary • Drug related • Associated with connective tissue disease/ portal hypertension/ immunodeficiency
WHO II	Derived from left heart disease	• left heart disease (LHD) • Valvular dysfunction • CHD
WHO III	Derived from lung disease/ hypoxia	• COPD • Interstitial lung disease • Alveolar hypoventilation syndrome
WHO IV	Chronic thromboembolic PH (CTEPH)	• CTEPH • Tumour or inflammation
WHO V	Derived from uncertain multifactorial mechanisms	• Haematological disease • Metabolic disorders • others

Clinically, PH shows progressive dyspnoea under physical activity and is often associated with fatigue, exhaustion and oedema. It often takes years to diagnose, as the disease is slowly progressive and is often recognized via right heart overload in the echocardiography. Diagnosis can only be made by right heart catheterization, but often, indication to this invasive procedure is not given, since there are no curative approaches to subtypes like PH derived from LV or other lung diseases (Hoeper, Ghofrani et al. 2017).

WHO I PH is mainly a diagnosis of exclusion, defined by the histological similarities you can find in these patients postmortem. Underlying causes can be hereditary disposition, but also association with drugs like amphetamines or collagen vascular disease (Ryan, Thenappan et al. 2012).

WHO II PH is caused by left heart disease (LHD). Included in LHD are valvular diseases affecting the function of the LV and CHD. In patients with chronic left heart failure, the prevalence of PH increases with the progression of functional class (FC). Due to LHD, in this

group PH develops through backwards transmission, derived from impaired LV diastolic function, mitral regurgitation and a loss of left atrial (LA) compliance (Galie, Humbert et al. 2015).

WHO III PH is often due to chronic hypoxia exposure, like living at high altitudes. This alveolar hypoxia leads to vasoconstriction primarily in the distal pulmonary arteries, and to remodelling processes over the course of time (Zhao, Mason et al. 2001).

WHO IV chronic thromboembolic pulmonary hypertension (CTEPH) is an obstructive form of PH with vessel remodelling as a consequence. It mostly occurs within two years after a thromboembolic incidence, but exact prevalence and annual incidence is unknown (Pepke-Zaba, Jansa et al. 2013).

WHO V is defined by unclear or multifactorial mechanisms, which involves haematological diseases like anaemia or metabolic disorders. In this group, also therapeutic options are different, because there is no indication for pressure regulating drugs. Here, the overall goal should be the treatment of the lung, not the decrease of mean PAP (Galie, Humbert et al. 2015).

3.3.2 Pathogenesis of pulmonary hypertension

The molecular mechanisms are complex and not completely understood. Vascular remodelling affects especially the small pulmonary arteries, which contribute to the majority of PVR. Normally, these small intraacinar arteries (<30 µm) have no smooth muscle cells in their media layer due to embryonic development (deMello, Sawyer et al. 1997). Vascular remodelling can occur due to a response to injury or a stimulus like hypoxia. To cope with an elevated intraluminal pressure, smooth muscle cells and adventitial cells are proliferating and creating a thicker vessel wall in the small intraacinar arteries. This results in a decreased lumen diameter and less flexibility in vasodilatation (Jeffery and Morrell 2002).

Besides the muscularization of small pulmonary vessels, the formation of a neointima between the endothelium and the internal elastic lamina is a sign of severe PH. This neointima formation occurs mainly in arteries <200 µm diameter (Yi, Kim et al. 2000). However, this important feature could not be recapitulated in the exposure of rodents to chronic hypoxia to induce PH, which is the most commonly used model to induce PH (Patel, Alhawaj et al. 2014). Interestingly, it could be shown, that rodents only undergo neointima formation when the

pulmonary blood flow is increased for example with pneumectomy (Okada, Tanaka et al. 1997).

The endothelium is the semi-permeable barrier between the remaining intima layer and the blood flow, preventing thrombosis and mediating a variety of metabolic functions (Stiebellehner, Belknap et al. 1998). It is exposed to increased shear-stress, altering mediators that influence vasoactive mediators such as urotensin II or endothelin 1 (Dschietzig, Richter et al. 2001). Unfortunately, there are very few studies addressing shear stress in PH. A sign of endothelial dysfunction is often seen in patients suffering from this disease. Clinically, it is evident that in situ thrombosis occurs in the small arteries of patients with PH, and that anticoagulant therapy (e.g. with warfarin) increases survival (Frank, Mlczoch et al. 1997).

3.3.3 Therapeutic options

Therapeutic approach to PH involves an intensive staging of the disease, and treatment is dependent on the underlying pathogenesis and vascular responsiveness. The initial step includes general measures such as physiotherapy, infection prevention, O_2 treatment, oral anticoagulation and further disease modifying measures. After this, it is considered whether the patient is suitable for calcium channel blocker (CCB) treatment. Depending on the responsiveness on the CCB therapy, further pharmaceutical approaches can be considered (Galie, Humbert et al. 2015).

Pharmaceutical treatment of PAH is complex and targets different aspects of PAH. The main pathways which are targeted by modern PAH treatment are endothelin 1 (ET-1), prostacyclin and nitric oxide (NO) (Dunlap and Weyer 2016).

ET-1 is known to be a potent vasoconstrictor and contributes to pulmonary artery smooth muscle cell (PASMC) proliferation. ET-1 has its effect to the receptors ET (A) and ET (B), which both have been connected to smooth muscle cell proliferation in small pulmonary arteries in PAH patients (Davie, Haleen et al. 2002).

Targeting the NO pathway, phosphodiesterase-5 (PDE-5) inhibitors as well as soluble guanylate cyclase (sGC) are therapeutic goals in PH treatment. PDE-5 inhibitors are used to maximize vasodilatation in PAH treatment and therefore decreasing the PVR. Mechanistically, cGMP is mediating the relaxation of PASMC and is hydrolysed by PDE enzymes (Rybalkin, Yan et al. 2003). Therefore, PDE-5 inhibitors contribute to vasodilatation in pulmonary arteries.

Another approach to treat PAH is made by stimulating the soluble guanylate cyclase (sGC). sGC is catalysing the generation of cGMP from GTP, also contributing to vasodilatation in the end (Stasch and Evgenov 2013). Treatment of PAH is evolving fast, and currently recommendations are to treat patients with an initial combination therapy even in milder states of the disease, as reviewed in Lau et. al (Lau, Giannoulatou et al. 2017).

3.3.4 Pulmonary hypertension in animal studies

To search for new therapeutic approaches and insights in the development of PAH, animal models are still needed. Although it is not possible to mimic the exact conditions given in human PH due to the shorter life span of experimental animals, animal studies are promising in finding new therapeutic approaches and insights.

One of the most common models to mimic PH in experimental research is hypoxia induced PH in mice. They are kept under 10% oxygen for about 21 days (Patel, Alhawaj et al. 2014, Zhang, Trautz et al. 2019). Chronic hypoxia is also known to induce PH in humans and is often derived by smoking or chronical lung diseases like COPD or interstitial lung diseases (Galie, Humbert et al. 2015).

Another model to induce PH are monocrotaline injections, often used in rats. Commonly, it is injected i.p. for 21 days with a dose of 60 mg/kg and saline i.p. injections as control group. MCT is a toxic alkaloid with a global pneumotoxicity. This leads to increased RV systolic pressure and RV hypertrophy as well as hypertrophy of muscular pulmonary arteries and interstitial lung fibrosis (Lee, Byun et al. 2005, Long, Ormiston et al. 2015).

A model which combines hypoxia and injections is the SuHx model, where Sugen 5416, a VEGFR2 antagonist is injected intraperitoneal. Afterwards, the rats are put in a hypobaric hypoxia chamber for three weeks. This causes severe PH with precapillary arterial occlusion (Taraseviciene-Stewart, Kasahara et al. 2001). This model was not only used in rats, but also in mice to develop new therapeutic approaches (Bueno-Beti, Hadri et al. 2018).

Furthermore, it is also possible to use genetic mutations to examine PH. For example, mice that are deficient in bone morphogenic protein receptor type 2 (BMPR 2) develop a mild form or predisposition of PH (Hong, Lee et al. 2008, Colvin and Yeager 2014), overexpression of interleukin 6 (IL-6) leads to PH (Steiner, Syrkina et al. 2009) and transgenic mice for fos related antigen 2 (Fra-2) show increased PASMC proliferation (Colvin and Yeager 2014).

3.4 NADPH oxidases

The family of NADPH oxidases consists of seven isoforms, named NOX 1-5 and DUOX 1 & 2. The sole function of NADPH oxidases is to generate ROS in contrast to other sources of ROS such as mitochondria, cytochrome p450 or peroxisomes which generate ROS as a metabolic by-product (Panday, Sahoo et al. 2015, Buvelot, Jaquet et al. 2019).

NADPH oxidases use NADPH as a H^+ donor to reduce oxygen to superoxide anion radicals ($O_2\cdot$). Superoxide anion radicals are then spontaneously or enzymatically converted to H_2O_2 (Buvelot, Jaquet et al. 2019).

$$NADPH + 2O_2 \rightarrow\leftarrow NADP^+ + 2O_2\cdot + H^+$$

The members of the NADPH oxidase family all have some structural similarities. NOX 1-5 have a catalytic core centre consisting out of six (DUOX1 &2 have seven) transmembrane α-helical domains. They all have a NADPH binding site at their COOH terminus, and a proximal FAD binding site. Furthermore, they have highly conserved histidines which are heme-binded in the third and fifth transmembrane domain (Bedard and Krause 2007, Buvelot, Jaquet et al. 2019).

NOX2 (also known as gp91phox) was the first discovered NADPH oxidase (Fig. 1). It was found in the plasma membrane of phagocytes, but today it is known that it is widely expressed throughout the body, including in endothelial cells, smooth muscle cells, cardiomyocytes, hepatocytes, and different types of stem cells. It consists of gp91phox/NOX2 and p22phox, forming the flavocytochrome b558. For full activation, the cytosolic subunits p40phox, p47phox, p67phox and the GTPase Rac are required (Mikhed, Gorlach et al. 2015). NOX2 reacts as the catalytic centre, while p22phox acts as a stabilizer and binds to p47phox. Resting neutrophils have the flavocytochrome b558 in the plasma membrane, while the other subunits are in the cytoplasm. Upon activation, p47phox gets phosphorylated and translocates together with the other cytosolic components to the membrane, where they associate with the flavocytochrome b558. For activation, there is also either the small GTP binding protein Rac1 or Rac2, required. When activated, Rac binds guanine triphosphate (GTP), and is transferred to the membrane together with p40phox, p47phox and p677phox, forming a fully functional NADPH oxidase. Mutations in the NADPH oxidases subunit lead to chronic granulomatous disease (CGD), resulting in a severe immunodeficiency (Buvelot, Posfay-Barbe et al. 2017). This demonstrates that NOX2 has an essential role in the immune system and is crucial in the host-defence reaction. ROS production is protective against infections by first being cell toxic

(oxidation of DNA-nucleotides, affecting protein formation) and second by being involved in phagosome pH regulation (Cabiscol, Tamarit et al. 2000).

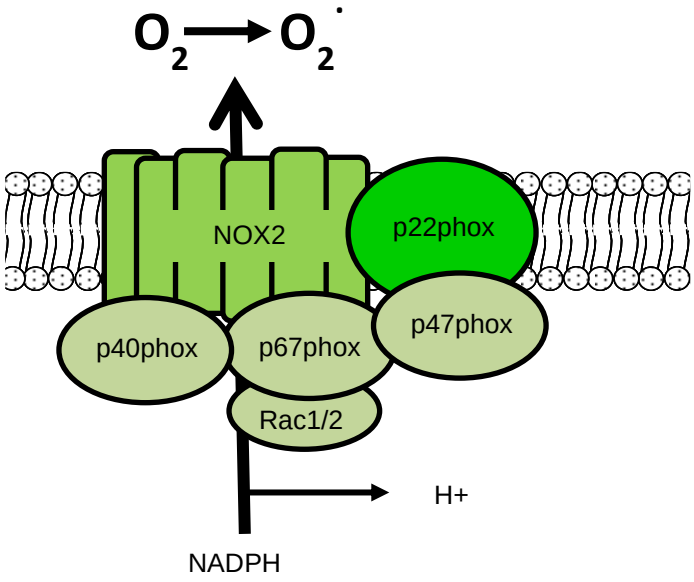

Fig. 3: Structure of NOX2 complex

The phagocyte NADPH oxidase containing NOX2 (formerly known as gp91phox) consists of NOX2 and p22phox forming the flavocytochrome b558. In order to produce ROS, the cytosolic subunits p40phox, p47phox, p67phox and Rac1/2 are required (adapted after Brenner et. al (Paik and Brenner 2011)).

The NOX1 isoform is mainly expressed in the colon epithelium, but it is also found in endothelial, smooth muscle and uterine cells (Buvelot, Jaquet et al. 2019). NOX1 is the closest relative to NOX2, sharing about 60% of their genetic sequence (Banfi, Maturana et al. 2000). Like NOX2, NOX1 is dependent on the stabilizing subunit p22phox. NOX1 is believed to play an important role in the host defence reaction in the colon, in inflammatory bowel disease and colon cancer (Szanto, Rubbia-Brandt et al. 2005). It is known that NOX1 is induced by angiotensin II, platelet derived growth factor and prostaglandin F2a, which can lead to hypertrophy of vascular smooth muscle cells due to superoxide production (Katsuyama, Fan et al. 2002).

NOX3 is mainly known as the NADPH oxidase playing a role in the inner ear. This was described due to the observation, that NOX3 deficient mice suffer from vestibular dysfunction and a head tilt (Paffenholz, Bergstrom et al. 2004). Other studies show that low NOX 3 levels

can also be found in the fetal spleen, skull, and brain. As NOX1 and 2, NOX3 is a p22phox-dependent NADPH oxidase (Bedard and Krause 2007).

NOX4 is highly expressed in the kidney (Geiszt, Kopp et al. 2000), but can also be found in a variety of tissues like smooth muscle cells (Ellmark, Dusting et al. 2005), endothelial cells (Ago, Kitazono et al. 2005) or fibroblasts (Colston, de la Rosa et al. 2005). NOX4 is also a p22phox-dependent NADPH oxidase, but interestingly it requires no obligatory cytosolic subunits like NOX1-3 (Martyn, Frederick et al. 2006). A peculiarity of NOX4 is that it can produce hydrogen peroxide (H_2O_2). A possible theory for that is, that superoxide is released into the cellular organelles and quickly mutates into hydrogen peroxide (Bedard and Krause 2007).

NOX5 is a NADPH oxidase which has been found in many tissues. Interestingly, it has not been found in rodents. Furthermore, it is not dependent on p22phox as a stabilizing subunit (Kawahara, Ritsick et al. 2005). Indeed, activation of NOX5 is Ca^{+} dependent and its N-terminus contains four calcium-binding EF hand domains (Banfi, Tirone et al. 2004).

DUOX1 and 2 were identified in thyroid glands and have an additional seventh transmembrane domain at the NH^2 terminus. Due to a N-terminal peroxidase domain they produce H_2O_2. Activation of DUOX1 and 2 does not require cytosolic subunits and can be directly activated by Ca^{2+} (De Deken, Wang et al. 2000). DUOX1 and 2 are important factors for the immune defence of the lung. They were found in ciliated cells in the airways and in type II pneumocytes, supporting the lactoperoxidase (LPO) to produce bactericidal hypothiocyanite anions (Fischer 2009).

4 Aim of the study

Fetal hypoxia has been described to negatively affect fetal growth and cardiac and pulmonary development and maturation. Furthermore, evidence is starting to accumulate that fetal hypoxia is not only detrimental to the newborn but also has persistent effects on the adult offspring in an unknown extent. Currently there is limited knowledge on the underlying mechanisms, and preventive and curative interventions to impede damage for the developing organism are lacking.

Increasing evidence points to a role of reactive oxygen species (ROS) in cardiopulmonary disorders associated with hypoxia such as pulmonary hypertension or myocardial infarction. The family of NADPH oxidases has been described to contribute to ROS generation in these disorders. However, it is not known whether NADPH oxidases are involved in the response to fetal hypoxia.

Therefore, the aim of this study is to elucidate whether NADPH oxidases play a role in the fetal and adult offspring's response to exposure to a limited period of hypoxia during pregnancy known to be important for cardiopulmonary development (E10.5-11.5).

Specifically, we hypothesize that loss of a functional NADPH oxidase

a) would affect ROS generation in the embryo and adult offspring in response to fetal hypoxia.
b) would affect fetal growth and cardiac and pulmonary development in response to fetal hypoxia.
c) would affect cardiopulmonary function in the adult offspring in response to fetal hypoxia.

To test our hypotheses, a mouse model lacking the NADPH oxidase subunit p22phox as well as embryoid bodies deficient in p22phox will be used.

5 Material and Methods

5.1 Material

5.1.1 Equipment

Device	Model	Company
Analytical balance	BP 3015	Sartorius
Autoclave (big)	KSG 116-2-ED	KSG
Autoclave (small)	KSG 25-2-3	KSG
Balance	BP 4100S	Sartorius
Centrifuge	Biofuge fresco	Heraeus
Deep-freezer (-80°C)	Hera freeze	Heraeus
Dewar	Cryolab25	Statebourne
Drying chamber	T6060	Heraeus
Freezer	Comfort	Liebherr
Fridges (various sizes)	profi line	Liebherr
Heating block	Thermomixer comfort	Eppendorf
Hypoxia chamber		Ing. Humbs
Hypoxia workbench	Ruskin workstation	I&L Biosystems
Incubator	Hera Cell	Heraeus
Incubator	CB150	Binder
Incubator Kelvitron	Histology	Heraeus
Isoflurane vaporizer	Anaesthesia	Harvard Apparatus
ISOTEC pressure transducer head	Pressure measurements	Harvard Apparatus
Laboratory dishwasher system	G7783CD Mielabor	Miele
Laminar airflow cabinet (hood)	HS15	Heraeus

Magnetic stirrer	MR3000	Heidolph
Magnetic stirrer (heating)	MR3001	Heidolph
Microscope	IX 50	Olympus
Microscope	Axiovert 25	Zeiss
Microtome HM355S	Histology	Thermo Fischer Scientific
Microwave		Severin
Neubauer improved counting chamber		Brand
Oxygen sensor	Hypoxia chambers	Graininger
PCR machine	GeneAmp PCR System 9700	Applied Biosystems/ Life Technologies
pH Electrode	InLab Expert DIN	Mettler-Toledo
pH Meter	pH 540 GLP	WTW
Photometer	Nano Drop 2000	Fisher Scientific
Platereader	Tecan Safire	Tecan
Power supplies	Power Pac 200/300/3000	Bio-Rad
Pump	CVC 2000	Vacubrand
Rodent anesthesia circuit mask		Harvard Apparatus
Roller mixer	RM5 Assistant	Karl Hecht KG
Rotator	3000	Fröbel Labortechnik
SDS-Page apparatus	Mini-Protean 3	Bio-Rad
Shaker	Duomax 1030/Polymax 1040	Heidolph
Spectrophotometer	Nano Drop	Thermo Fischer Scientific
Thermocycler	Rotor-Gene 6000	Corbett/Qiagen
Tip Sonicater	Sonopuls	Bandelin

Tissue embedding machine	Tissue embedding System AP 280-2	Thermo Fischer Scientific
Transducer Amplifier Modul-A	Pressure measurements	Harvard Apparatus
Vortex	Vortex-Genie 2	Thermo Fischer Scientific
Warming plate	Histology	Witte & Sutor GmbH
Water Bath	Grant	Memmert
Water Purifying Unit	Milli-Q Synthesis	Merck Millipore
Western blot transfer unit	Mini Protean 3	Bio-Rad

5.1.2 Chemicals

Reagents	Company
β-Glycerophosphate	Sigma-Aldrich
1-hydroxy-methoxycarbonyl-2,2,5,5-tetramethylpyrrolidine hydrochloride (CMH)	Noxygen
4’6-diamidino-2-phenylindole (DAPI)	Enzo
Acetic acid	Carl Roth
Acetone	Sigma-Aldrich
Agarose standard	Carl Roth
Amido-black solution	Sigma-Aldrich
Ammonium persulfate	Carl Roth
Bond breaker	Thermo Fischer Scientific
Bovine serum albumin (BSA)	AppliChem
Bromophenol blue	Sigma-Aldrich
$CaCl_2$	Merck
Cumaric acid	Sigma-Aldrich
DAB chromogen substrate	Dako
Desferroxamine (DES)	Sigma-Aldrich

D-Glucose	Sigma-Aldrich
Diethyldithiocarbamate (DETC)	Sigma-Aldrich
Direct Red 80	Sigma-Aldrich
Dithiothreitol (DTT)	GE Healthcare
DMSO	Sigma-Aldrich
EDTA	Carl Roth
Eosin G	Carl Roth
Ethanol	Merck
Ethanol rotipuran	Carl Roth
Ethidium bromide	Carl Roth
Formalin 37 %	Carl Roth
Glycerol	Carl Roth
Glycine	Carl Roth
HIER buffer pH 6.0	Dako, Santa Clara, USA
HIER T-EDTA buffer pH 9.0	Zytomed Systems
Hydrogen chloride	CLN
Hydrogen peroxide	Merck
Hydrogen peroxide 30%	Carl Roth
Isopropanol	CLN
KCl	Merck
KH_2PO_4	Merck
Krebs-HEPES-buffer	Thermo Fisher
Luminol	Sigma-Aldrich
Matrigel matrix	BD Bioscience
Mayer’s Hemalaun	Carl Roth
Methanol	CLN
$MgCl_2$	Metabion

NaCl	Carl Roth
NaCl 0.9 % solution	B. Braun
$NaHCO_3$	Merck
Na-HEPES	Sigma-Aldrich
Naphthol blue black	Sigma-Aldrich
NEB buffer 3	New England Biolabs
PBS Tablets	Life Technologies
PDGF	Merck
PMSF	Sigma-Aldrich
PonceauS	Carl Roth
Proteinase inhibitors mix complete	Roche
Quick-Load 100bp DNA Ladder	New England Biolabs
Rhodamine Labelled Wheat Germ Agglutinin	Biozol
Rotiphorese Gel	Carl Roth
Roti-Quant	Carl Roth
SDS	Carl Roth
Skim milk powder	Merck
Sodium acetate trihydrate	Carl Roth
Sodium chloride	Carl Roth
Sodium deoxycholate	Carl Roth
Sodium dodecyl sulphate	Carl Roth
Sodium pyrophosphate	Sigma-Aldrich
TEMED	Carl Roth
TRIS „ultra“	Carl Roth
Triton X-100	Sigma-Aldrich
Tween-20	Sigma-Aldrich
Weigert’s Hematoxylin A	Carl Roth

Weigert's Hematoxylin B	Carl Roth
X-ray fixing fluid	Tetenal
X-ray rapid developer	Tetenal
Xylene	Carl Roth
β-Mercaptoethanol	Carl Roth

5.1.3 Cell culture reagents

Media and additives	Company
Dulbecco's phosphate buffered saline solution	PAA/GE Healthcare
Fetal calf serum	PAN-Biotech
Gelatine	PAN-Biotech
L-glutamine	PAN-Biotech
Lif (Leukemia inhibitory factor)	Merck-Millipore
Lipofectamine-3000	Life Technologies
Mitomycin C	Sigma-Aldrich
NEAA (Non-essential amino acids)	Sigma-Aldrich
Penicillin/streptomycin	PAA/GE Healthcare
Sodium pyruvate	Sigma-Aldrich
Trypsin-EDTA	PAA/GE Healthcare
β-Mercaptoethanol	Carl Roth

5.1.4 Chemicals for histology stainings

HE staining	Company
Meyers Hemalaun	Carl Roth
Eosin G	Carl Roth

PAS staining	Company
Periodic Acid Solution	Carl Roth

5.1.5 Consumables Lab

Designation	Company
Cell lifter	Corning
Cell scraper	Sarstedt
Combitips “Biopure” (0,5, 1, 2,5, 5 and 10 ml)	Eppendorf
Cryovials (2ml)	Carl Roth
Dishes (6cm, 10 cm)	Sarstedt
Flasks (T25, T75)	Greiner Bio-One
Pipettes, sterile (2, 5, 10, 25 and 50 ml)	Sarstedt
Pipette tips (10, 20, 200, 1000 µl)	Gilson
Plates (6-, 12- and 96-well; sterile)	Greiner Bio-One
Reagent reservoir, sterile	Corning
Spatulas, disposable, various sizes	VWR
Tubes (1.5 and 2 ml)	Eppendorf
Tubes (15 ml)	Greiner Bio-One
Tubes (50 ml)	Corning
„PageRuler“unstained protein marker	Fisher Scientific
Aluminium foil	Carl Roth
Cell culture dishes (6 cm, 10 cm)	Sarstedt
Cell lifter	SPL Lifesciences
Cover slides 24 x 50 mm	Carl Roth
Cryoboxes	Kisker
Dako pen S2002	Dako
Entellan	Merck
Eppendorf tubes	Eppendorf
Falcons (15 ml, 50 ml)	BD Bioscience
Film “Fuji Super”, various sizes	Fischer-Sehner Medical Imaging

Gene Disc 100	Qiagen
Gene Disc heat sealing film	Qiagen
Glass capillaries	Sigma-Aldrich
Gloves (nitril)	Kimberly-Clark
Jelco 25 G disposable canula	Smiths Medical
Lab tape	Kisker
Magnet stirring bars, various sizes	Carl Roth
Microtome blades S35/ A35	VWR
Millex vacuum line protector 45µm	Merck-Millipore
Mounting medium	Dako
Multi adapter	Sarstedt
Object slides Superfrost Plus	Gerhard Menzel GmbH
Paper wicks	GE Healthcare
Paraffin	Merck
pH buffer solutions	Mettler-Toledo
Membrane filter	GE Healthcare
Power pack adapter	Bio-Rad
Sample cups	GE Healthcare
S-Monovette	Draeger
Sterile filtering unit 250ml	Merck Millipore
Strip holder cleaning solution	GE Healthcare
Syringe, sterile (2 ml, 5 ml)	B. Braun
T75 Flask	Sarstedt
Tissue Tec O.C.T. Compound	Sakura Finetek
Tweezers	Carl Roth
Vinylgloves „Rotiprotect“	Carl Roth
Whatman pergamin paper	VWR

5.1.5 Enzymes

Designation	Company
Bsl I	New England Biolabs
DNAse I	VWR Life Sciences
Taq DNA Polymerase	Qiagen

5.1.6 Kits and Ready-to-Use-Reagents

Designation	Company
“EZQ” Protein Quantitation Kit	Life Technologies
DNAse Kit	Qiagen
High-capacity cDNA Reverse Transcription Kit	Applichem/ Life technologies
Genotyping KIT	Qiagen
Perfecta SYBR Green	Quanta Biosciences

5.1.7 Antibodies

Primary Antibodies

Antibody	Company
8 oxoG (rabbit)	Abcam
DMPO (mouse)	Abcam
Hif1-α (rabbit)	Abcam
Ki67 (mouse)	Abcam
p22phox (rabbit)	Santa Cruz
α-smc (mouse)	Dako
β-Actin (goat)	Santa Cruz

Secondary Antibodies

Secondary antibodies were used in a standard dilution of 1:250 in blocking solution.

Antibody	Company
Mouse (594 nm = red)	Invitrogen
Mouse (488 nm = green)	Invitrogen
Rabbit (488 nm = green)	Invitrogen

5.1.8 Primers

5.1.8.1 Primers for qPCR

Target Tissue	Target Gene	Forward ‘5	Reverse ‘5
Mouse	Brachyury	GCT CTC CAA CCT ATG CGG AC	GGT GTG TAA TGT GCA GGG GA
Mouse	cTnT	AGC CCA CAT GCC TGC TTA AA	TCT CGG CTC TCC CTC TGA AC
Mouse	Hnf1	GAG CAA AGA GGC CCT GAT CC	ATG GGT CCT CCT GAA GAA GTG
Mouse	Hsp70	CGA GGA GGT GGA TTA GAG GC	AGC CCA CGT GCA ATA CAA AA
Mouse	Nkx2.5	ATT TTA CCC GGG AGC CTA CG	CAG CGC GCA CAG CTC TTT TT
Mouse	Nox1	AGC TTG GGT GAA AGC CAT CC	TCC ACT TCC AAG ACT CAG GG
Mouse	Nox2	TTT CTC AGG GGT TCC AGT GC	CAA TTG TGT GGA TGG CGG TG
Mouse	Nox4	TGT TGC ATG TTT CAG GTG GT	TAC TGG CCA GGT CTG CTT
Mouse	Oct4	TGT GGA CCT CAG GTT GGA CT	GCT TTC ATG TCC TGG GAC TCC T
Mouse	Otx2	GAG AGC GGA ACC TTC CTC AG	GAC GGA ACT TAC AGCC CGC AT

Mouse	p22phox	TGG CCT GAT TCT CAT CAC TG	TCC AGC AGA CAG ATG AGC AC
Mouse	SP-A	TCT GCA AAC AAT GGG AGT CCT	GAA GCC CCA TCC AGG TAG TG
Mouse	SP-B	GGC CTC ACA CTC AGG ACT TC	CCT GGG ACA CAG CCA CAG
Mouse	SP-C	TAT GAC TAC CAG CGG CTC CT	TCT CCC GGA AGA ATC GGA CT
Mouse	α-MHC	GGA GGC TGA GGA ACA ATC CA	GTC ATT CCA CAG CAT CGG GA
Mouse	β-actin	GCC TTA CCC CAT GCC ATC AT	AGG GCG AGG TAA CAC AGT TT
Mouse	β-MHC	CTA CAG GCC TGG GCT TAC CT	TCT CCT TCT AGA CTT CCG CT

5.1.8.2 Primers for genotyping

Target Tissue	Target Gene	Forward ‘5	Reverse ‘5
Mouse	*Cyba*	CAG-ATG-CCC-ACT-GAC-TGC-TA	CGA-GCC-ACA-GTA-CAG-CTT-CA

5.1.9 Software for image and data analysis

The following software was used for data analysis and image analysis.

Software	Company
GraphPad Prism	GraphPad Software
HAEMODYN	Harvard Apparatus
ImageScope	Leica Biosystems
R	http://www.R-project.org (R-Development-Core-Team 2006)
REST analysis	http://rest.gene-quantification.info (Pfaffl, Horgan et al. 2002), Qiagen
IX Series Software	Olympus
ZEN core Software	ZEISS

5.2 Methods

5.2.1 Animal experiments

5.2.1.1 Mouse lines

Mice harbouring a point mutation in the *cyba* gene (nmf333 mice) resulting in a consecutive loss of p22phox (Nakano, Longo-Guess et al. 2008) were obtained from Jackson Laboratories, Bar Harbor, MN (A.B6 *Tyr*$^{+}$-*cyba*^{nmf333}/J). Due to a point mutation from T to C there is a change in the amino acid sequence, replacing tyrosine with histidine (Fig. 4). This chemically induced mutation Y121H is located on exon 5 of the *cyba* gene on the distal telomere of chromosome 8. The mutation can be found in a predicted transmembrane helix of the protein and leads to loss of p22phox protein (Nakano, Longo-Guess et al. 2008). All mice were of a genetic C57BL/6J background. In all experiments, wildtype littermates were used as controls. All animal experiments were approved by the government of Oberbayern (AZ 55.2-1-54-2532-165-2017).

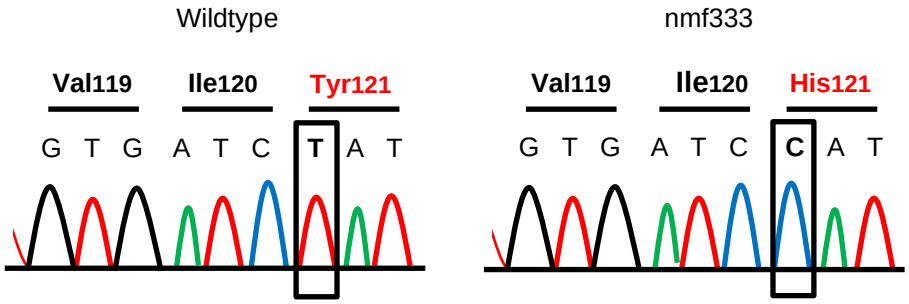

Fig. 4: nmf333 mice show Y121H mutation

Point mutation in the *cyba* gene in the nmf333 mice resulting in a consecutive loss of p22phox protein. The base exchange of thymine with cytosine leads to a change in the amino acid sequence from tyrosine 121 to histidine 121 in exon 5 of the *cyba* gene on chromosome 8. This base exchange is caused by the alkylation of thymine and a mispair with guanine during replication. In the next replication, this will then lead to a change in the amino acid sequence (cytosine instead of thymine) and therefore to a loss of p22phox protein. Adapted after Nakano et. al (Nakano, Longo-Guess et al. 2008).

Previous results published by our group were proving that the point mutation in the *cyba* gene leads to a decrease in p22phox stability underlying the loss of p22phox protein (Zhang, Trautz et al. 2019).

5.2.1.2 Mouse housing

All mice were kept under controlled pathogen free conditions in a certified animal facility under the supervision of a veterinarian. Food and water were provided ad libitum. For mating, a male and a female mouse were put together in one cage and controlled every morning for the visibility of a vaginal plug. Mated females were checked every morning at 7am for the presence of a vaginal plug. If positive, the day was defined as E 0.5. Female mice were separated from males and kept under controlled conditions. The duration of the pregnancy was between 18.5 and 21 days. The pubs were separated from their mother after three to four weeks and ear marking was performed. Since there was no difference between sex in preliminary experiments, both sexes were used.

5.2.1.3 Experimental animal model

Mice were mated and E0.5 was verified with vaginal plug check. At E10.5, mice were exposed to 10% oxygen for 24 hours in a normobaric hypoxia chamber. In Group A, mice were sacrificed immediately after hypoxia at E11.5 through cervical dislocation and embryos were dissected and analysed. In Group B, mice were kept under normoxic conditions from E11.5 until E17.5,

when the embryos were dissected and analysed. In Group C, mice gave birth to their litter, which was kept under normoxic conditions until the age of eight to nine weeks. Then, the offspring mice underwent 21 days of hypoxia (10 % oxygen) to induce PH or were kept under normoxic conditions for another three weeks (Fig. 5).

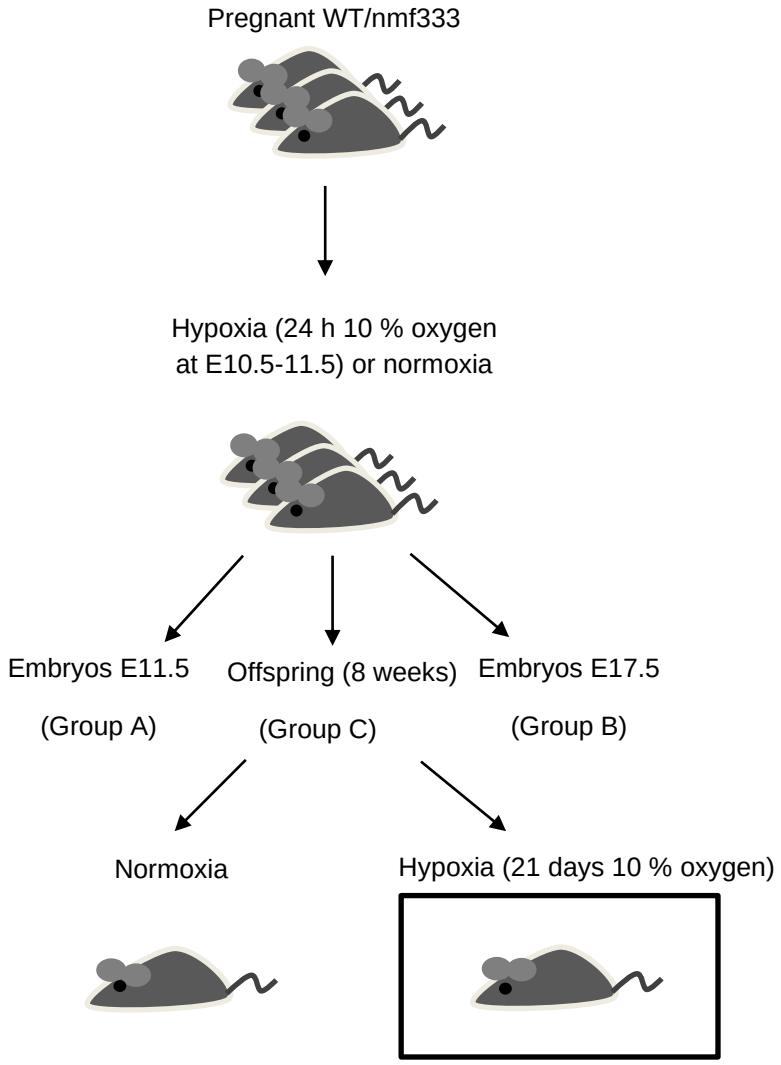

Fig. 5: Animal model

Pregnant wildtype (WT) or nmf333 mice were exposed to 10% oxygen for 24 h from E10.5 – E11.5 in a normobaric chamber or kept under normoxic conditions. Group A: Embryos were analysed at E11.5. Group B: Embryos were analysed at E17.5. Group C: Dams were allowed to deliver, the offspring was kept under normoxic conditions until 8-9 weeks of age, then either kept under normoxia or exposed to 10% oxygen for 21 days in a normobaric chamber.

5.2.1.4 Collection of embryos and organs

Mice were sacrificed through cervical dislocation and fixed for dissection of embryos and organs. An abdominal incision was made, and the thoracic cave was opened. Mice were flushed with PBS through injection into the left ventricle. The heart was separated into right and left ventricle, the left lung lobe was taken for histology, the right lung for molecular analysis. The uterus was dissected in whole and washed in PBS. The embryos were dissected, then the placenta was taken and stored separately. At E11.5, the whole embryo was taken, at E17.5, heart and lungs were separated for molecular analysis. For histology, the whole embryo was embedded. For ensuring an adequate fixation, an abdominal incision was made to allow the PFA solution to penetrate the complete tissue.

Organs for molecular analysis were frozen immediately after dissection in liquid nitrogen and stored at -80°C. For paraffin embedding, organs were put in 4% PFA for 48 hours.

For embedding, organs were dehydrated and carefully embedded in paraffin. Embedded organs were stored at 4°C. Embryos were cut in 2 µm slices and placed on a slide.

5.2.1.5 Hypoxia exposure

Adult mice at an age of 8 - 9 weeks were kept for 21 days under 10% oxygen in a normobaric chamber. Pregnant dams were kept under hypoxic conditions at 10% oxygen from E 10.5-11.5. Food and water were provided ad libitum. The oxygen concentration of each hypoxia chamber was continuously monitored via an oxygen sensor, while permanent air circulation was ensured via a ventilator. Furthermore, the air circulated through a soda lime cylinder to bind excessive CO_2. Humidity was also at a controlled level of 65-75%. Mice were assessed daily for signs of stress and discomfort according to our score sheet. Hypoxia was interrupted for about 10 minutes once a week to change cages, food, and water.

5.2.1.6 Haemodynamic measurements

Mice were anesthetized with isoflurane in a separate chamber with 5% of isoflurane gas concentration and high air flow (4 l/min). When mice were sedated, they were placed on a warming mat with an isoflurane mask. Reflexes were checked every 30 seconds to ensure proper anaesthesia. Mice were shaved as little as possible but as much as needed. For haemodynamic measurements a tip catheter pressure transducer head (IOSTEC) attached to a 25G syringe and connected to Transducer Amplifier was used and pressure data were recorded with the HAEMODYN software as described previously (Zhang, Trautz et al. 2019). The skin was punctured with the cannula between two rips in a horizontal line at the height of

the ventricles. After collecting the pressure data mice were sacrificed immediately under anaesthesia through cervical dislocation, organs were collected as described above.

5.2.1.7 RNA isolation

For RNA isolation the Total RNA peqGOLD kit was used in accordance with the manufacturer's manual. Briefly, tissue was put in lysis buffer and homogenised with ultrasound. Samples were always kept on ice. After homogenisation, lysate was further cleared, mixed with 70% EtOH and loaded on a RNA binding column. DNAse removal was performed with an on-column DNAse digest for 15 minutes included within the kit. Then, several washing steps were performed, and RNA was diluted in RNAse free water. RNA concentration was measured using the Nanodrop spectrophotometer.

5.2.1.8 cDNA synthesis

For cDNA synthesis the High-Capacity cDNA Reverse Transcription Kit was used in accordance to the manufacturer's protocol. RNA concentration was measured using Nanodrop spectrophotometer, and 1 µg of RNA was added to RNAse free water. Mastermix was prepared with 10x RT buffer, 10x dNTPs, H_2O, RT random primers and the enzyme. For negative control, the same Mastermix was used without the enzyme. Then, reverse transcriptase PCR program was performed (25°C for 10 min, 37°C for 120 min, 85°C for 5 min, 4°C forever), and the resulting cDNA was kept at -20°C.

5.2.1.9 qPCR

After cDNA synthesis, cDNA was diluted in water (1:20) for qPCR. The PerfeCTa SYBR Green mix and the Rotor Gene 6000 system were used for qPCR. In each tube, a total volume of 10 µl was used (2 µl diluted cDNA, 5 µl PerfeCTa, 0.1 µl primer forward, 0.1 µl primer reverse and 2.8 µl of H_2O). Each sample was run in three to get technical triplicates of the target gene expression. For negative control, one sample of the negative cDNA control was used for each sample with a blank water sample. The qPCR program consisted out of the following steps: Denaturation (95°C for 0.5 min), then 30-50 cycles of denaturation (95°C for 2 seconds), extension (60°C for 20 seconds) and holding (55°C for 30 seconds) and then melting (1°C increase every 5 seconds) to confirm the amplification point. Analysis was performed using the Rotor-Gene 6000 software followed by REST analysis software to calculate the fold change regulation based on the ΔCT method.

5.2.1.10 DNA isolation

For genotyping, the One-Step Genotyping kit was used. A mouse tissue sample was placed in a 1.5 ml tube. 100 µl of fresh Buffer L with 2 µl of Protease plus was prepared for each sample. The protease mixture was added to each tube and incubated at 55°C for 30 minutes. After the digestion process, the tubes were incubated for 5 minutes at 95°C to inactivate protease. The tissue lysate was used as PCR template and stored at -20°C.

5.2.1.11 PCR

After the DNA was isolated, genotyping was performed (example results seen in Fig.6). For nmf333 genotyping a PCR followed by enzymatic digestion using Bsl I was performed with a total reaction volume of 25 µl, containing 2 µl of DNA, H_2O (18.5 µl), complete PCR buffer 10x with $MgCl_2$ (2.5 µl), dNTPs (10 mM, 0.25 µl), DMSO, Taq-Polymerase (5 u/µl, 1.0 µl) and primers (nmf333-FW 5'-CAG ATG CCC ACT GAC TGC TA and nmf333-RV 5'-CGA GCC ACA GTA CAG CTT CA, each 0.25 µl). PCR was performed for 5 min at 94°C for denaturation, followed by 40 cycles of denaturation (94°C for 0,5 min), annealing (59°C for 1 min) and extension (72°C for 1 min). Then, extension was performed at 72°C for another 7 minutes, followed by incubation at 4°C until the samples were taken for further processing. The PCR product was digested with Bsl I enzyme. Digestion was performed for 2 h at 55°C with a total volume of 20 µl (15 µl PCR product, 2 µl CutSmart Buffer, 2.5 µl H_2O, 0.5 µl Bsl I. Then, the digestion mix was applied on a 3% agarose gel and electrophoresis was done. Due to the point mutation of the nmf333 mice, an additional Bsl I digestion site was inserted into the genome. As a consequence, homozygote nmf333 mice show a 162 bp band after digestion instead of the 202 bp of the wildtype animals. Results: nmf333 -/-: 162 and 89 bp, nmf333 +/-: 202, 162, 89 bp, nmf333 +/+: 202 and 89 bp.

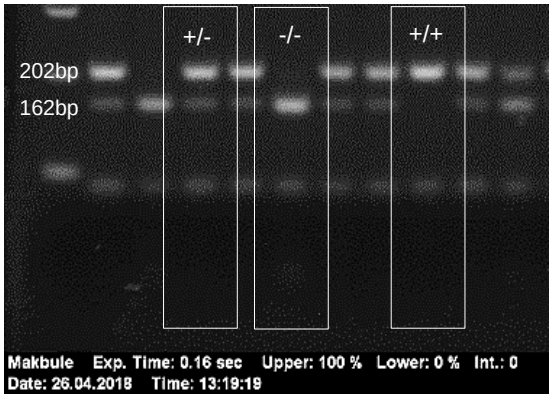

Fig. 6: Genotyping of nmf333 mice

Ear tissue samples of all mice were genotyped via agarose gel electrophoresis to visualize the *cyba* gene mutation characterizing the nmf333 mouse strain. In the picture of the gel electrophoresis, three bands at 202 bp, 162 bp and 89 bp are visible in heterozygous mice (+/-), 162 bp and 89 bp bands are visible only in homozygous nmf333 mice (-/-) with the Y121H point mutation, and the bands at 202 bp and 89 bp are visible in wildtype mice (+/+).

5.2.1.12 Preparation of histological slides

Tissue samples were fixated in 4% PFA solution for 48 hours at room temperature. Afterwards, dehydration was performed using a dehydration machine. Then, the dehydrated samples were embedded in molten paraffin and left on a cooling plate to harden. Afterwards, samples were stored at 4°C. After hardening, the paraffin embedded samples were sectioned at a thickness of 2 µm using a rotary microtome. Slices were carefully placed on a glass slide for further experiments.

5.2.1.13 Haematoxylin-Eosin staining

Slides were incubated for at least 1 hour at 60° C to melt paraffin. Then slides were exposed to an alcoholic row (2x5 minutes xylene, 2x3 minutes 100% EtOH, 2x3 minutes 96% EtOH, 3 minutes 70% EtOH). Afterwards slides were washed for 2x3 minutes in demineralized water. Then slides were stained for 15 minutes with Mayer's Hämalaun. Hämalaun was discarded and slides were washed in demineralized water until the water remained clear. Slides were put in blueing solution for 1 minute and then stained for 3 minutes with Eosin. After washing with demineralized water, slides were exposed to a reverse alcoholic row (1 minute 70% EtOH, 2x1 minute 96% EtOH, 2x1 minute 100% EtOH, 2x1 minutes Xylene). Slides were carefully covered with Entellan and a cover slip and stored in the dark.

5.2.1.14 Wheat germ agglutinin staining

To assess whether transient fetal hypoxia induces hypertrophy of cardiomyocytes especially in the right ventricle, wheat germ agglutinin staining was performed. Slides were incubated for at least 1 hour at 60°C to melt paraffin. Then, the slides were exposed to an alcoholic row (2x5 minutes xylene, 2x3 minutes 100% EtOH, 2x3 minutes 96% EtOH, 3 minutes 70% EtOH, 2x3 minutes demineralized water). Afterwards, slides were washed in Triton buffer (0.05% Triton X 100 in PBS) and incubated for 1 hour in blocking buffer (1% BSA in PBS and 0.05% Triton X 100) to block unspecific fluorophore binding sites. Samples were circled with a DAKO pen and incubated with WGA staining solution (1:500 in blocking buffer) for 1 hour at 37°C in the dark. Then slides were washed 3x2 minutes in Triton buffer and stained with DAPI (1:10.000) for 1 minute. Finally, slides were washed for 3x2 minutes in PBS, covered with DAKO mounting medium and a cover slide and stored in the dark at 4°C.

5.2.1.15 8-hydroxy-desoxyguanine staining

8-hydroxy-desoxyguanine (8oxodG) is a well-known mutagenic lesion generated under oxidative stress. To visualize oxidative DNA damage, immunofluorescence staining was performed with an antibody raised against 8oxodG. Slides were incubated for at least 1 hour at 60°C to melt paraffin. Then, the slides were exposed to an alcoholic row (2x5 minutes xylene, 2x3 minutes 100% EtOH, 2x3 minutes 96% EtOH, 3 minutes 70% EtOH, 2x3 minutes demineralized water). Blocking solution was made with 5% goat serum in PBS and slides were incubated for 2 hours in a humid chamber. Afterwards, the primary antibody (1:200 in 0.2% Triton X 100) was applied and slides were incubated over night at 4°C. The next day, slides were washed in PBS, 0.2% Triton X 100 and PBS (each 5 minutes). The secondary antibody (AlexaFluor 488 goat anti-mouse, 1:200 in PBS) was applied for 2 hours in the dark at room temperature. Slides were washed with PBS for 3x2 minutes. DAPI was added (1:10.000 dilution) for 1 minute at room temperature. Slides were washed again with PBS 3x2 minutes, covered with DAKO mounting medium and a cover slide and stored at 4°C in the dark. For evaluation, relative nuclear staining intensity was compared in between the experimental groups, as higher levels of oxidative damage leads to an accumulation of 8oxodG.

5.2.1.16 α-smooth muscle actin staining

α-smooth muscle actin is expressed in smooth muscle cells. This marker was used to visualize small vessels which undergo muscularization in lung tissue. For staining, slides were incubated at 60°C for a minimum of 1 hour and deparaffinated as described in 4.2.1.15. Antigen retrieval buffer was used with a pH of 9. Unspecific binding sites were blocked with 5% BSA for 30

minutes in PBS and the primary antibody (1:100) was incubated at 4°C overnight. The next day, slides were washed, incubated with the secondary antibody (AlexaFluor 594 nm 1:200 in PBS) and DAPI and coversliped with DAKO mounting medium as described above. For evaluation, the count of small vessels (<30 µm, 30-60 µm, >60 µm) was compared per high power field (0.55 mm^2) in between the experimental groups. A minimum of four high power fields (0.55 mm^2) per sample was evaluated.

5.2.1.17 PAS staining

PAS staining was performed to assess if transient fetal hypoxia leads to an impaired lung development, as PAS positive pneumocytes II are still storing mucopolysaccharides, which is negatively correlated with the ability to produce surfactant (Wang, Tan et al. 2020). Slides were incubated at 60°C and deparaffinated as described above for the HE staining procedure in 4.2.1.13. Slides were immersed in Periodic Acid Ready to use solution for 15 minutes and rinsed for four times in distilled water. Then, slides were immersed in Schiff's solution for 35 minutes and rinsed with hot running tap water and distilled water. Counterstaining was done for 2 minutes with Haematoxylin. Slides were rinsed again with tap water, dehydrated through an alcoholic row as described above, mounted with Entellan and coversliped in the end.

5.2.1.18 Measurement of superoxide levels

To measure ROS production (superoxide) in mouse and cell samples, electron paramagnetic resonance (EPR) was used. Our experiments were performed with the Bruker E-scan (Zhang, Trautz et al. 2019). The underlying technique can detect unpaired electrons in the superoxide molecule with spectroscopy. CMH is used as a spin trap and is oxidized by superoxide, becoming a radical itself, but with a much longer half-time, which is suitable for detection. EPR temperature controller was set on 37°C. Krebs-Hepes-buffer (KHB, 99 mM NaCl, 4.69 mM KCl, 2.5 mM $CaCl_2$, 1.2 mM $MgSO_4$, 25 mM $NaHCO_3$, 1.03 mM KH_2PO_4, 5.6 mM D-glucose, 20 mM Na-HEPES) was thawed over night at 4°C. CMH, DES and DETC were freshly thawed from -80°C on ice before the measurements. Embryos were dissected, and the embryo was put directly into 100 µl of KHB buffer and kept on ice. KHB buffer was aspirated and 100 µl of KHB buffer + 25 µM DES + 5 µM DETC (1000:1) were added to the embryo. Then the embryo was macerated with a scissor until the solution appeared homogenized. 10 µl of CMH was added and 50 µl of the solution was measured in a capillary. The capillary was placed in a resonator containing a gas mixture (1% O_2, 5% CO_2, 94% N_2). EPR settings were defined as centre field at 3455 G, sweep width of 10 G, frequency of 9.7690 GHs. The measurements were recorded for 10 minutes. By linear regression of the measurement points, production rate was calculated. The relative production rates were normalized against embryonic mass.

Negative control was measured with KHB buffer with detergents (DES and DETC) and CMH. Positive control was measured with xanthine (1 µM) and xanthine oxidase (5 U, each 5 µl). Furthermore, EPR measurements were performed with ROS inhibitors to prove that the origin of the embryonic ROS production are NADPH oxidases. By adding the NOX inhibitors, the signal given by the superoxide production should be decreased in case the superoxide was generated by NADPH oxidases. GKT137831 (2 mM stock solution, dilution 1:1000) was used as a specific inhibitor for NOX1 and 4 (Murphy-Marshman, Quensel et al. 2017), whereas gp91 ds-tat (2.5 mM stock solution, dilution 1:500) was used as an inhibitor for NOX2 (Khayrullina, Bermudez et al. 2015). As a reference group, embryos were placed in KHB buffer with scrambled gp91 ds-tat, in KHB + GKT137831 for NOX1 and NOX4 and in KHB + gp91ds-tat (2.5 mM 1:500) for NOX2. Measurements were performed as described above.

EPR measurements with cells were performed as described above. In the beginning the medium was aspirated and the cells were washed two times with KHB buffer. Then cells were collected and measured as described before.

5.2.2 Cell culture

5.2.2.1 Culture of murine embryonic stem cells

R1 murine embryonic stem cells (mESC provided by Prof. Moretti's AG) were used for the following experiments. mESC were cultured on a feeder cell layer (MEFs) on gelatine coated 10 cm dishes. R1 mESC were grown in Dulbecco's modified Eagle's medium (DMEM; Invitrogen, Karlsruhe, Germany) containing 4.5 g/L glucose, supplemented with 20% fetal calf serum (PAN-Biotech), and 100 U/mL penicillin, 100 µg/mL streptomycin (PAA Laboratories), 0.1 mM β-Mercaptoethanol, 0.1 mM pyruvate, 0.1mM non-essential amino acids (NEAA) and maintained at 37°C under an atmosphere of 5% CO_2. Additionally, Lif (Leukemia inhibitory factor, 10 µg/ml) was added freshly to the medium to prevent mESC from spontaneous differentiation. Stem cells were used up to passage 50.

To passage the stem cells, medium was aspirated, and the dish was washed with PBS. Afterwards each 10 cm dish was treated with 5 ml trypsin to detach mESC and the feeder cells. The dish was incubated for about 10 minutes at 37°C. Trypsin was inactivated with 5 ml medium, the cell suspension was aspirated and centrifuged at 200 g for 5 minutes. The supernatant was discarded, and the cells were resuspended with fresh stem cell medium. For

passaging, mESC were seeded on a new gelatine coated dish with inactivated MEF feeder cells.

For experiments where only mESC were required, the mESC were separated from the MEF feeder cells. The cells were incubated for 30 minutes on an uncoated dish to separate feeder cells from mESC. After 30 minutes, feeder cells are attached to the dish while the mESC are still in floating in the stem cell medium. After separation, the mESC were collected for further experiments.

For seeding the cells, the separated mESC were counted and seeded at a density of 500.000 cells/ 6cm dish on gelatine. The next day, mESC were exposed for 24 hours to hypoxia (0.1% O_2).

5.2.2.2 Isolation of mouse embryonic fibroblasts

MEFs (mouse embryonic fibroblasts) were isolated from pregnant C57 BL/6J mice at E 13.5-14.5. Embryos were harvested as described before. Embryos were transferred into a new dish with PBS and blood was carefully removed. The embryo was decapitated, and the red tissue which is consisting out of the heart and liver was removed carefully with a forceps. The remaining embryo was placed in 0.25% trypsin-EDTA. Then the embryo was macerated with scissors into pieces of 1-2 mm. The solution was pipetted up and down and the dish was placed in a 37°C incubator for 10 minutes. Afterwards the solution was pipetted up and down for several times and again incubated for about 10 minutes. Cell suspension was transferred to a 50 ml tube and 20 ml of ESC medium was added to inactivate the trypsin. Then the suspension was incubated for 5 minutes at room temperature to allow the bigger parts to settle down. The supernatant was transferred to T75 flasks (each flask received the volume of cell suspension equivalent to 3 embryos). ESC culture medium was added. The following morning, medium was changed and splitted as needed. MEFs were splitted until passage 6 and then inactivated for 2 hours with mitomycin C (10 µg/ml). Afterwards MEFs did not proliferate anymore and were used as a feeder cell layer for mESC. Cells were trypsinated as described and cryoconserved using ESC culture medium supplemented with 10% DMSO at a density of $1x10^7$ cells per ml.

5.2.2.3 Embryoid bodies

To differentiate mESC to cardiomyocytes, the hanging drop method was used (Behringer, Gertsenstein et al. 2016). Separated mESC were counted and a solution of 50.000 cells/µl was used. Drops had a volume of 20 µl with 1000 cells/ drop. Drops were placed on the top of a 10

cm dish, which was filled with PBS to prevent drying of the hanging drops (as seen in Figure 7). After 4 days of incubation (day of seeding was counted as day 0) embryoid bodies were collected and seeded on gelatine coated 6 cm dishes. Embryoid bodies started to beat around day 8. Hypoxia (24 hours, 0.1% O_2) was performed on day 1, 4 and 7.

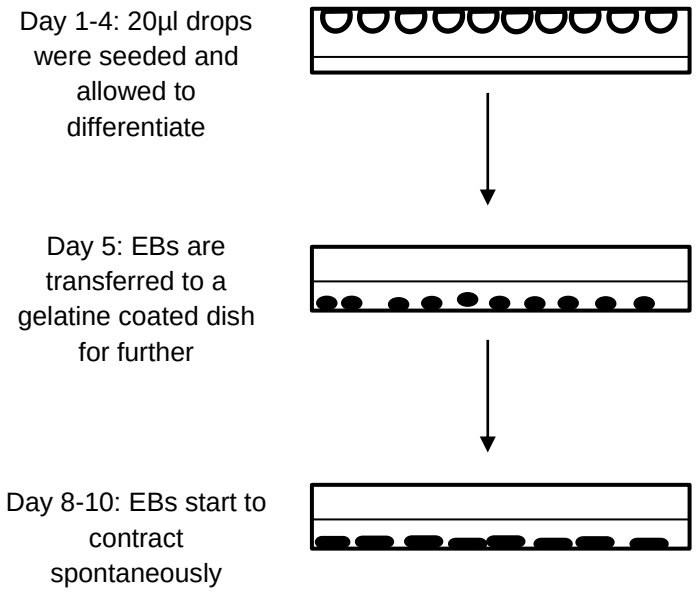

Fig. 7: Hanging Drop Method

R1 mESC were applied on the top of a 10 cm dish in 20 µl drops, each containing 1000 cells. Top was turned and placed on the dish containing PBS to humidify the drops. After 4 days, EBs were collected carefully with a pipette and transferred to a gelatine coated dish for further differentiation. Medium was changed every two days. Around day 8-10 the EBs start to contract spontaneously.

5.2.2.4 Lentivirus production

HEK 293FT cells were used for production of shctr and shp22 virus. HEK 293FT cells were seeded on 10 cm dishes with DMEM medium (without L-glutamine, 4.5 g/l glucose, 10% FCS, 1% penicillin/streptomycin). When they reach about 80 - 90% confluency, the Trans-IT Lenti transfection reagent (Sigma-Aldrich) was applied to the cells. The transfection reagent was mixed with 3 ml serum free DMEM medium, 9 µl of ViraPower Packaging Mix, 3 µl of pLenti-based plasmid DNA (shGFP, sh288), 36 µl of Lipofectamine 3000 and 24 µl of P3000. The transfection reagent was incubated for 25 minutes at room temperature and then applied to the HEK 293FT cells. The following day, medium was changed. 48 hours post-transfection,

the cell supernatant was collected and centrifuged with 3000 rpm at 4°C for 5 minutes to pellet cell debris. The medium containing the formed lentivirus particles was frozen at -80°C or stem cells were transduced directly with the virus (1 ml virus containing supernatant). For transduction, the lentivirus was added to a 10 cm mESC dish and incubated for 48 hours. Afterwards, the transduced mESC were washed 4 times and the medium was changed. Then, Zeocin (500 µg/ml) was applied to eliminate untransduced cells. Medium with Zeocin was changed after 24 hours.

5.2.2.5 Colorimetric bromodeoxyuridine ELISA

For measuring proliferation, a colorimetric bromodeoxyuridine (BrdU) ELISA assay was used (Abcam). BrdU is a modified thymidine analogue which is incorporated into the DNA during synthesis and can be detected by specific antibodies thus acting as a proliferation marker. Stem cells were separated from MEFs as described above and seeded on 96 well plates (5000 cells/well). BrdU ELISA was performed in accordance with the manufacturer's protocol.10 µl of BrdU labelling reagent (stock solution diluted 1:100 with sterile culture medium resulting in a concentration of 100 µM) was added to each well containing mESC in 100 µl stem cell medium. Cells were exposed to either 1% oxygen or 0.1% oxygen for 24 hours. After hypoxia, the medium was aspirated carefully, and the cells were fixed by adding 150 µl of FixDenat solution and incubated for 2 hours at room temperature. Afterwards, FixDenat was discarded and 100 µl of the Anti-BrdU-POD solution (Anti-BrdU-POD stock solution 1:100 with antibody dilution solution) per well was added and incubated for 2 hours at room temperature. Then, wells were washed 3-5 times with 200 µl of diluted washing buffer (washing buffer concentrate diluted 1:10 with distilled water) and dried at the end. 100 µl of the substrate solution was added and incubated until a green-blue colour developed which took approximately 5 to 30 minutes. Absorbance was measured with the Tecan absorbance reader at an absorbance wavelength of 450 nm and a reference wavelength of 690 nm.

5.2.2.6 Alamar Blue assay

Stem cells were seeded on 96 well plates as described in BrdU assay. 10 µl of Alamar Blue was added to each well. After hypoxia exposure (24 hours, 1% and 0.1% oxygen), the absorbance was measured with the Tecan absorbance reader at a wavelength of 492 and 560 nm.

5.2.2.7 DMPO/ actinin staining

Embryoid bodies at differentiation day 7 were seeded on gelatinized ibidi 8-well slides (10 EBs per well). DMPO (50 mM) was added to the stem cell medium, and cells were incubated at

hypoxic (0.1% oxygen) or normoxic conditions for 24 hours. After hypoxia, EBs were fixed for 10 min with 4% PFA and washed with PBS. Then, EBs were permeabilized with 0.1% Triton-X-100 in PBS and unspecific binding sites were blocked with 5% BSA in PBS for 1 hour. Afterwards, the primary antibody anti-DMPO and anti-actinin as a counterstain for cardiomyocytes were applied over night at 4°C (DMPO anti-rabbit 1:200 in 1% BSA, α-actinin anti-mouse 1:200 in 1% BSA). The next day, EBs were washed three times with PBS and the secondary antibodies (AlexaFluor anti-mouse 594 nm 1:250 in 1% BSA in PBS for anti-actinin, AlexaFluor anti-mouse 488nm 1:250 in 1% BSA in PBS for anti-DMPO) were applied for 1 hour in the dark. Then, EBs were washed again with PBS and nuclear DAPI staining (1:5000 in PBS for 1 minute) was performed. Afterwards, EBs were washed in PBS for two times 2 minutes each. Finally, EBs were mounted with fluorescence medium and stored at 4°C in the dark.

5.3 Statistical analysis

All values shown were calculated as the mean value with standard error. To evaluate statistical significance, an unpaired two-sided student`s t-test of the mean value was performed for the comparison of two groups. To compare more than two groups an analysis of variance (ANOVA) followed by Tukey's test to compare the different groups was performed. A p-value <0.05 was considered as significant. All statistics were performed with GraphPad Prism.

6 Results

6.1 The effect of transient fetal hypoxia on the embryo at E11.5

6.1.1 Fetal growth and cardiac maturation

Wildtype (WT) pregnant dams were exposed to hypoxia for 24 h in a normobaric hypoxia chamber at 10% oxygen. The time point for hypoxia was defined from E10.5 to E11.5 since this is a sensitive time in cardiac development: at E10.5 cardiac looping should be finished and septation of atria and ventricles is beginning (Krishnan, Samtani et al. 2014). Previous studies showed that this period during development is sensitive to hypoxia (Ream, Ray et al. 2008).

WT embryos at E11.5 which were exposed to transient fetal hypoxia showed a decrease in total embryonic mass (Fig. 8 A) and crown to rump length (Fig. 8 B). To test the impact of p22phox on the embryonic response towards hypoxia, pregnant nmf333 dams were exposed to hypoxia as described above. In contrast to WT embryos, nmf333 embryos did not show a decrease in body mass. Similarly, crown to rump length was not affected by the loss of p22phox protein neither under normoxia nor after hypoxia. Similar findings were subsequently obtained in the lab (Yishi Qin, unpublished data). These findings suggest that nmf333 embryos are protected against hypoxia induced growth retardation.

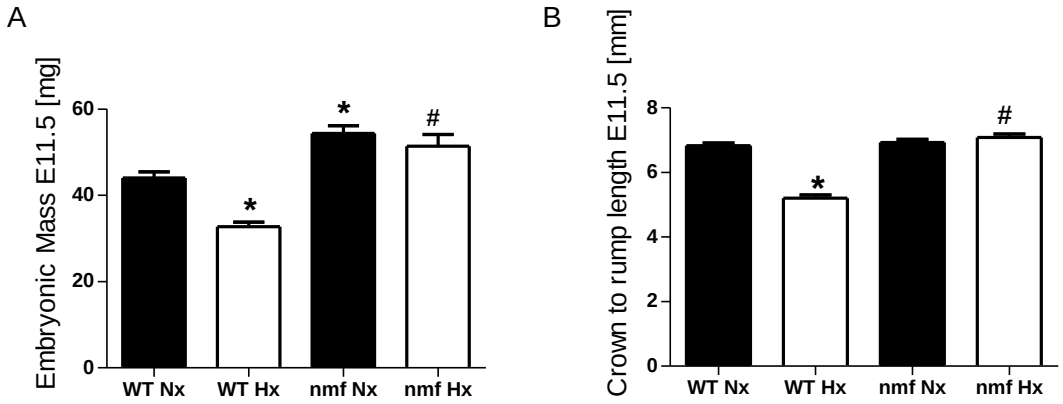

Fig. 8: Fetal hypoxia leads to growth retardation of wildtype embryos at E11.5

Pregnant wildtype (WT) or nmf333 mice (nmf) were exposed to hypoxia (10% oxygen) or normoxia for 24 h from E10.5 to E11.5. Afterwards, embryos were dissected at E11.5 and total embryonic mass (A) and crown to rump length (B) were measured (A: n=15-55, *p<0.05 WT Hx vs. WT Nx, nmf Nx vs. WT Hx, #p<0.05 nmf Hx vs. WT Hx, SEM; B: n=15-55, *p<0.05 WT Hx vs. WT Nx, #p<0.05 nmf Hx vs. WT Hx, SEM).

To examine the morphological differences of the embryonic heart between the different groups, hearts of embryos were sectioned in a sagittal axis on the level of the OFT and atrioventricular cushions (Fig. 9 A). Histology revealed no morphological malformations in the embryos analysed. Nevertheless, the ventricle was enlarged in WT embryos exposed to hypoxia (Fig. 9 B). To assess the density of the myocardium which should be progressing in this sensitive stage of cardiac development, nuclei were counted in the ventricular area. Compared to normoxic WT embryos the relative number of nuclei in the myocardium was decreased in WT hypoxic embryos, but not in nmf333 embryos exposed to hypoxia (Fig. 9 C).

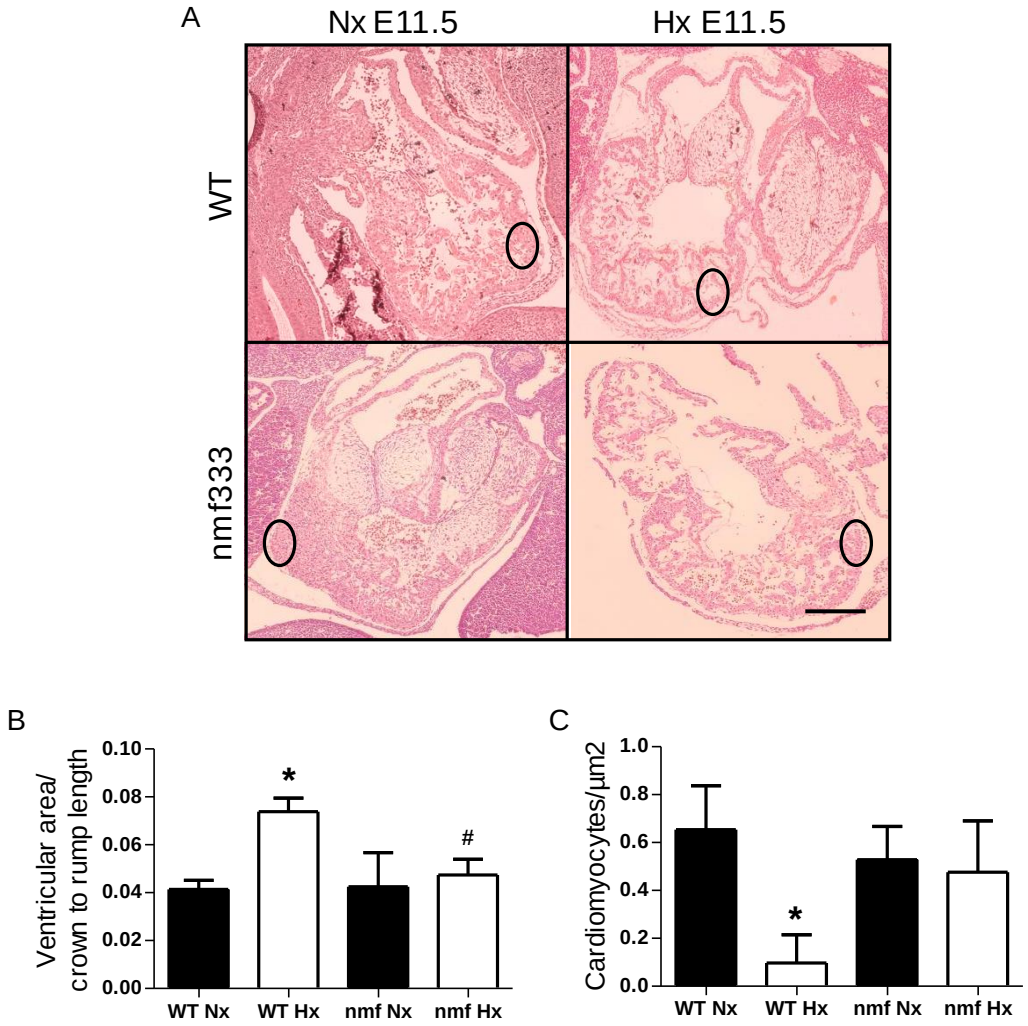

Fig. 9: Fetal hypoxia leads to myocardial thinning in wildtype embryos at E11.5

A: Pregnant wildtype (WT) or nmf333 (nmf) mice were exposed to 24 h hypoxia (10% oxygen) from E10.5 until E11.5. Afterwards, embryos were dissected, embedded in toto and cut through the area of the atrioventricular cushions in sagittal axis to ensure comparability between embryos before HE staining. Circles show examples of different myocardial density. B: Comparison of ventricular area to crown to rump length of the embryo (n=3, *p<0.05 WT Hx vs. WT Nx, #p<0.05 nmf Hx vs. WT Hx, SEM) C: Evaluation of the number of cardiomyocytes per µm^2. For the analysis, the number of cardiomyocytes was counted in the primitive ventricular area and divided through the total area of the primitive ventricle (n=3, *p<0.05 WT Nx vs. WT Hx, SEM). All analyses were performed with Image Scope software (Leica Biosystems). Scale bar = 400 µm.

To test whether fetal hypoxia would affect cardiac maturation, mRNA levels of the cardiac maturation markers α- and β-MHC and cTnT were determined. Fetal hypoxia decreased mRNA levels of the cardiac differentiation markers α-MHC (Fig. 10 A) and cTNT (Fig. 10 B) (known to be primarily expressed in adult cardiomyocytes), in WT embryos but not in nmf333 embryos. The mRNA levels of β-MHC (known to be primarily expressed in embryonic cardiomyocytes) remained unchanged (Fig. 10 C). Furthermore, mRNA levels of the stress marker Hsp70 were increased after transient gestational hypoxia in WT embryos but not in nmf333 embryos (Fig. 10 C).

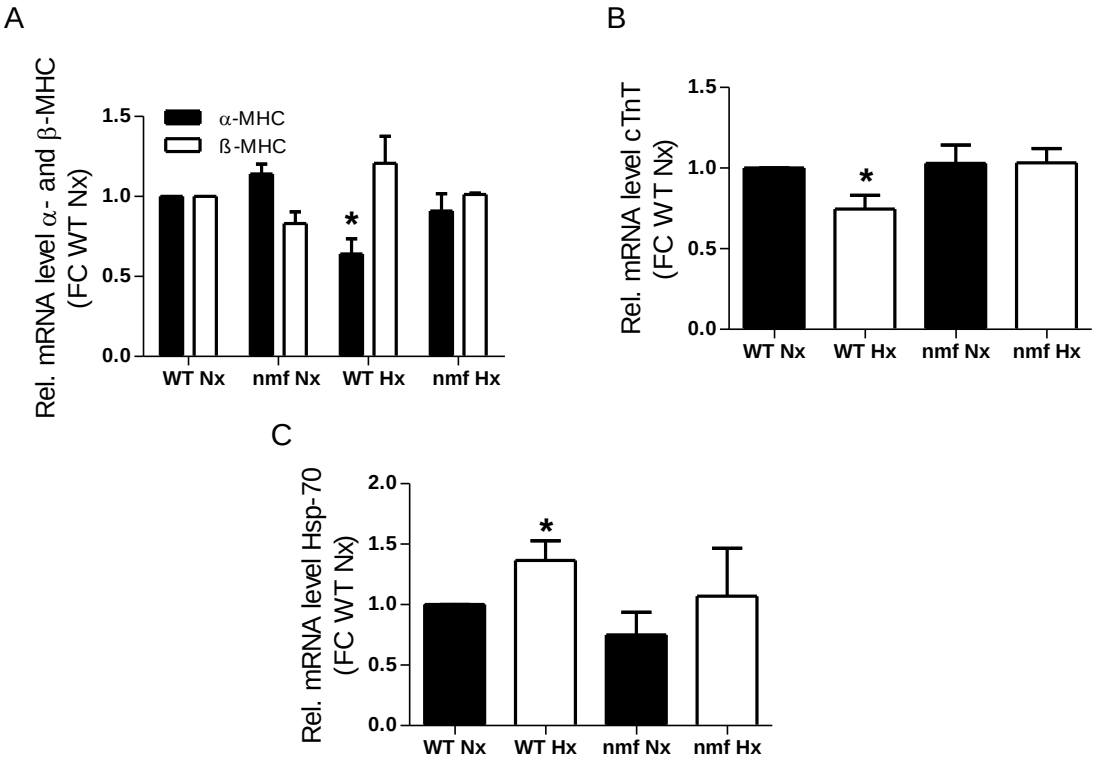

Fig. 10: Fetal hypoxia modulates expression of cardiac maturation and stress markers in embryos at E11.5

Pregnant wildtype (WT) or nmf333 (nmf) mice were exposed to 24 h of hypoxia (10% oxygen) from E10.5 until E11.5. Afterwards embryos were dissected and RNA was isolated for qPCR analysis. A: mRNA levels of α- and β-MHC (n=3, *p<0.05 WT Hx vs. WT Nx, SEM). B: mRNA levels of cTnT (n=3, *p<0.05 WT Hx vs. WT Nx, SEM). C: mRNA levels of Hsp70 as a marker for cardiac differentiation (n=3, ns, SEM).

6.1.2 NADPH oxidases and reactive oxygen species

To evaluate the involvement of NADPH oxidases in the fetal response to hypoxia, expression of NOX1 (Fig. 11 A), NOX2 (Fig. 11 B) and NOX4 (Fig. 11 C) was determined by qPCR. The expression of all subunits was upregulated after transient fetal hypoxia in WT embryos while it did not change significantly after transient fetal hypoxia in nmf333 embryos. Similar findings were subsequently obtained by others in the lab (Yishi Qin et. al, unpublished data).

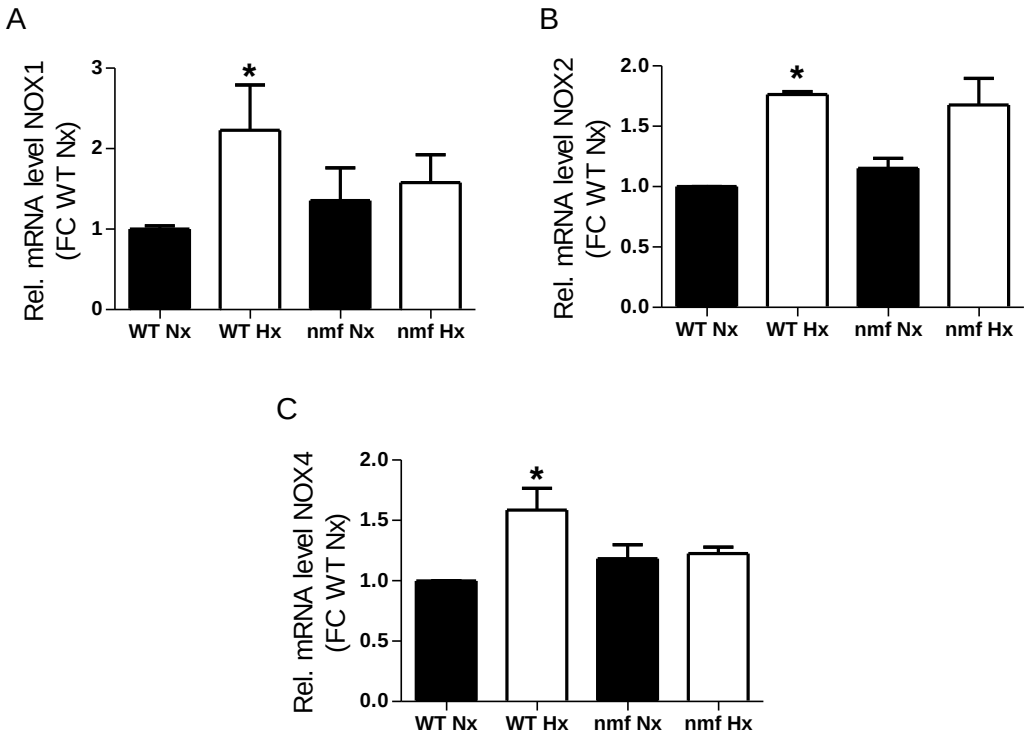

Fig. 11: Fetal hypoxia leads to elevated NOX1, NOX2 and NOX4 mRNA levels in wildtype, but not in nmf333 embryos at E11.5

Pregnant wildtype (WT) and nmf333 (nmf) mice were exposed to 24 h hypoxia (10% oxygen) from E10.5 until E11.5. Afterwards, embryos were dissected and RNA was isolated for qPCR analysis. A: mRNA levels of NOX1 (n=3, *p<0.05 WT Hx vs. WT Nx, SEM). B: mRNA levels of NOX2 (n=3, *p<0.05 WT Hx vs. WT Nx, SEM). C: mRNA levels of NOX4 after 24 h hypoxia (n=3, *p<0.05 WT Hx vs. WT Nx, SEM).

To test whether transient fetal hypoxia would also increase ROS levels dependent on NADPH oxidases, EPR measurements were performed to measure superoxide generation after hypoxia exposure at E11.5. The embryos were isolated and macerated under reoxygenated conditions. Fig. 12 A shows that transient fetal hypoxia increased superoxide production in WT embryos, but not in nmf333 embryos. To verify, that the superoxide production is derived from

NADPH oxidases, EPR measurements were performed with NADPH oxidase inhibitors. Therefore, embryos were incubated with GKT137831 as a NOX1 and NOX4 inhibitor (Murphy-Marshman, Quensel et al. 2017) and the peptide gp91 ds-tat as a NOX2 inhibitor (Khayrullina, Bermudez et al. 2015). Scrambled gp91 ds-tat was used as control for both inhibitors. Indeed, both inhibitors diminished superoxide generation after transient fetal hypoxia in WT embryos whereas superoxide generation in nmf333 embryos remained unaffected (Fig. 12 B).

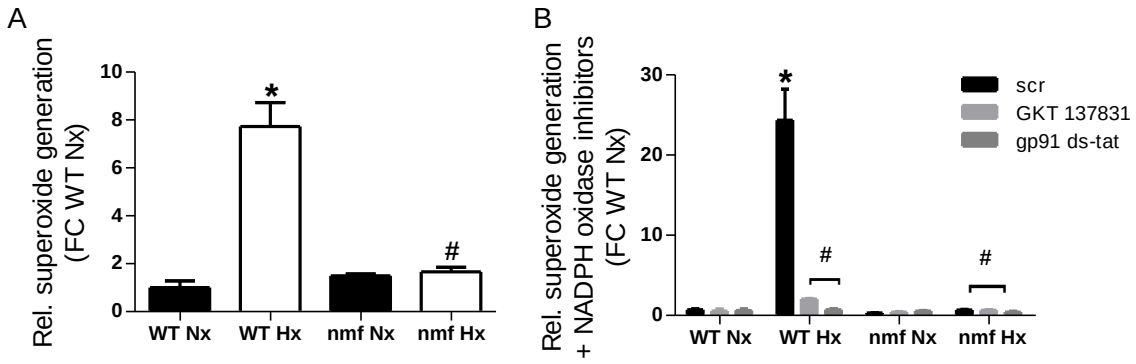

Fig. 12: Fetal hypoxia leads to NADPH oxidase dependent superoxide generation in wildtype embryos at E11.5

Pregnant wildtype (WT) or nmf333 (nmf) mice were exposed to 24 h hypoxia (10% oxygen) from E10.5 until E11.5. A: Embryos were dissected and directly macerated for EPR measurements under reoxygenated conditions using CMH. Relative fold change (FC) to normoxic wildtype embryos is shown. (n=5-6, *p<0.05 WT Hx vs. WT Nx, #p<0.05 nmf Hx vs. WT Hx, SEM). B: After dissection, embryos were incubated for 15 minutes with the NADPH oxidase inhibitors GKT137831 (NOX1/4 inhibitor, 2 mM 1:1000), gp91 ds-tat (NOX2 inhibitor, 2.5 mM 1:500) or scrambled gp91 ds-tat (2.5 mM 1:500 as a control. (n=3, *p<0.05 WT Hx vs. WT Nx scr, #p<0.05 nmf Hx vs. WT Hx GKT, nmf Hx vs. WT Hx ds-tat, nmf Hx vs. WT Hx scr, SEM).

To test whether fetal hypoxia causes oxidative DNA damage, 8-oxoG staining was performed in E11.5 embryos. Following exposure to hypoxia, the embryo was dissected in reoxygenated conditions and embedded in toto. 8-oxoG staining was significantly enhanced in WT embryos exposed to transient fetal hypoxia, whereas this effect was not seen in hypoxic nmf333 embryos (Fig. 13 A, B). Similar findings were subsequently obtained by others in the lab (Yishi Qin, unpublished data). Overall, transient fetal hypoxia increased ROS production by NADPH oxidases dependent on p22phox.

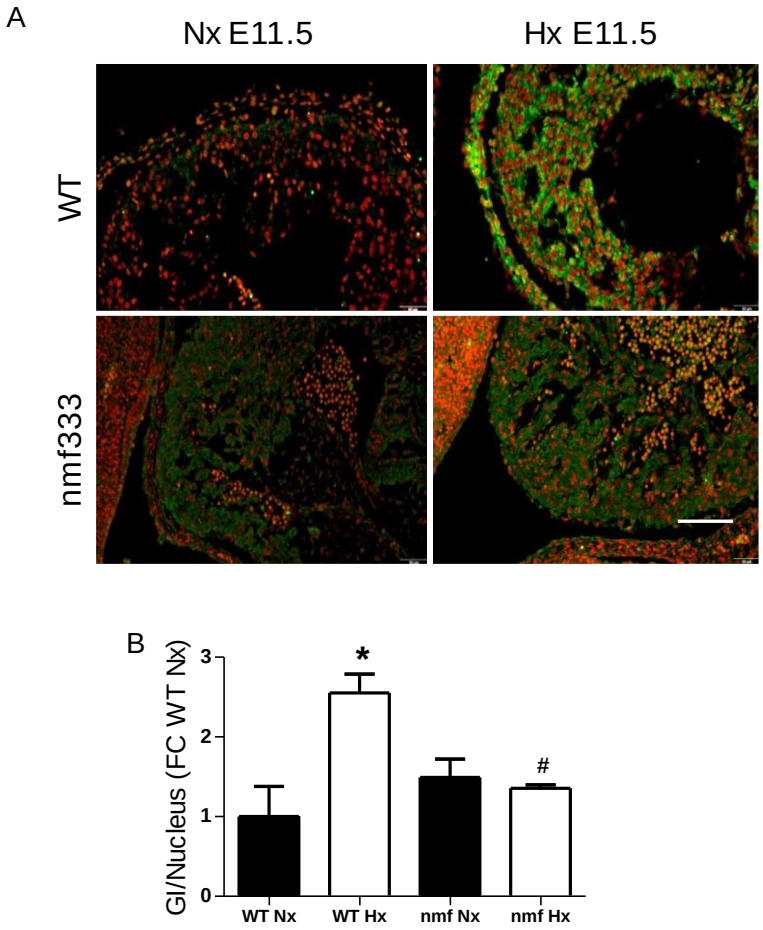

Fig. 13: Fetal hypoxia promotes signs of oxidative DNA damage in the wildtype embryo, but not in the nmf333 embryo at E11.5

Pregnant wildtype (WT) or nmf333 (nmf) mice were exposed to 24 h hypoxia (10% oxygen) from E10.5 until E11.5. Embryos were embedded and immunohistochemistry was performed with an 8-oxodG antibody A: 8-oxodG staining (8-hydroxy-deoxyguanosine) in E11.5 hearts (red = DAPI, green = 8-oxodG, scale bar = 50 µm) B: Quantitative analysis of 8-oxodG staining; grey value intensity (GI) per nucleus (n=3, *p<0.05 WT Nx vs. WT Hx, #p<0.05 WT Hx vs. nmf Hx, SEM).

6.2 The effect of transient fetal hypoxia on the embryo at E17.5

6.2.1 Growth at E17.5

To explore whether transient fetal hypoxia at E10.5 to E11.5 would also have prolonged effects on the developing fetus, embryos were analysed at E17.5 following a period of 6 days under normoxia. Similar to the situation at E11.5, the mass and crown to rump lengths of wildtype embryos exposed to transient fetal hypoxia were lower than those of normoxic WT embryos while this effect was not observed in nmf333 embryos exposed to fetal hypoxia (Fig. 14 A/B).

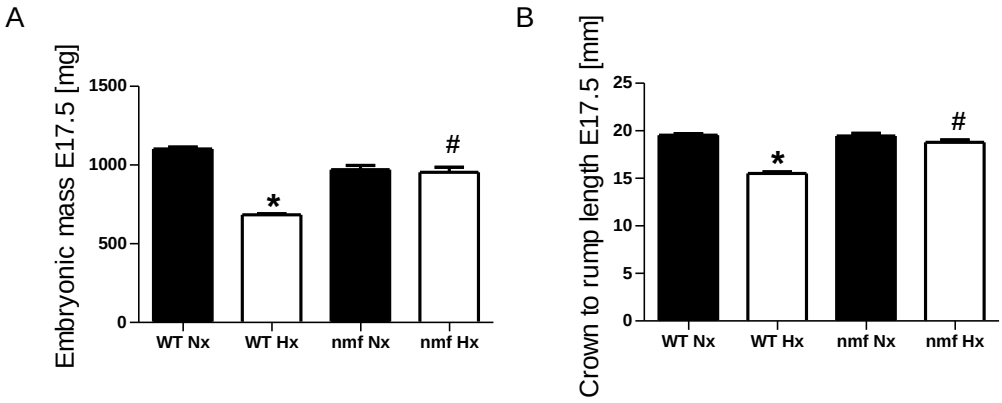

Fig. 14: Transient fetal hypoxia leads to persistent growth retardation until E17.5

Pregnant wildtype (WT) or nmf333 (nmf) mice were exposed to 24 h hypoxia (10% oxygen) from E10.5 until E11.5. Afterwards, pregnant dams were kept under normoxic conditions until the dissection of the embryos at E17.5, when embryonic mass (A) and crown to rump length (B) was assessed (n=21-35, *p<0.05 WT Hx vs. WT Nx, #p<0.05 nmf Hx vs. WT Hx, SEM).

6.2.2 Oxidative DNA damage and cardiac maturation

To evaluate whether oxidative DNA damage after transient fetal hypoxia would persist until E17.5, 8-oxodG staining was performed in the heart (Fig. 15 A). Hypoxic WT embryos still showed increased levels of cardiac oxidative DNA damage at E17.5, similar to the situation of E11.5 embryos (Fig. 15 A and B). Again, the hearts of nmf333 embryos at E17.5 were not affected by transient fetal hypoxia at E10.5 for 24 h.

To assess cardiac maturation, mRNA expression levels of α- and β-MHC were analysed (Fig.15 C). α-MHC levels were decreased in hypoxic WT embryos but increased in normoxic and hypoxic nmf333 embryos. β-MHC levels were not changed.

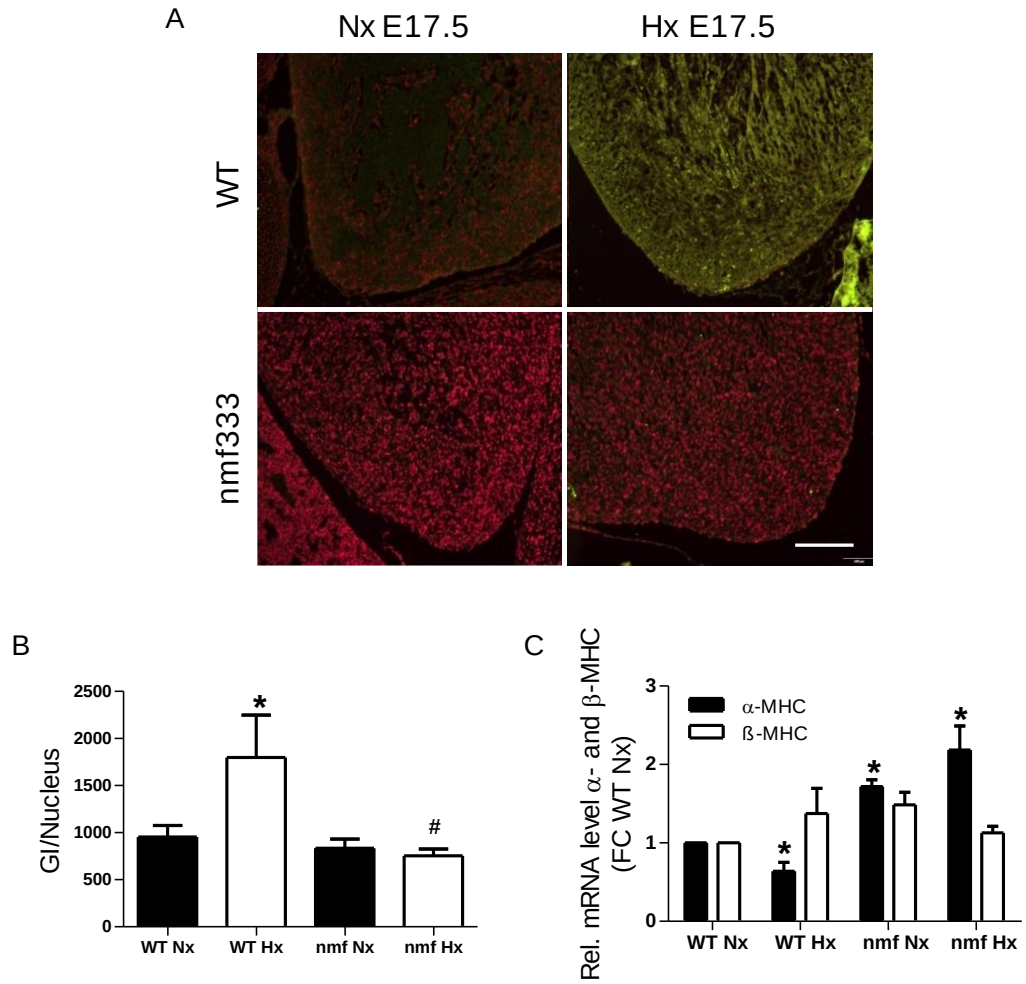

Fig. 15: Transient fetal hypoxia promotes oxidative DNA damage at E17.5 dependent on p22phox

Pregnant wildtype (WT) or nmf333 (nmf) mice were exposed to 24 h hypoxia (10% oxygen) from E10.5 until E11.5. Afterwards, pregnant dams were kept under normoxic conditions until the dissection of the embryos at E17.5. Embryos were embedded and immunohistochemistry was performed. A: 8-oxodG staining (8-hydroxy-deoxyguanosine) in E17.5 hearts (red = DAPI, green = 8-oxodG, scale bar = 200 µm). B: Quantitative analysis of 8-oxodG GI (grey value intensity) per nucleus (n=3, *p<0.05 WT Hx vs. WT Nx, #p<0.05 nmf Hx vs. WT Hx, SEM). C: mRNA levels of α- and β-MHC in E17.5 embryos. Data are shown as fold change (FC) to normoxic wildtype embryonic hearts (WT Nx) (n=3, *p<0.05 WT Hx vs. WT Nx, nmf Nx vs. WT Nx, nmf Hx vs. WT Nx, #p<0.05 nmf Hx vs. WT Hx, SEM).

Taken together, transient fetal hypoxia from E 10.5-11.5 followed by reoxygenation resulted in persistent oxidative stress and impaired α-MHC expression in the embryonic heart. On the other hand, nmf333 embryos did not show signs of oxidative stress or developmental delay after transient fetal hypoxia.

6.2.3 Lung development

To test whether fetal hypoxia affects lung development and maturation, lungs of E17.5 embryos were analysed for signs of maturation. HE staining was performed to explore general morphology (Fig. 16 A). Lungs from hypoxic WT embryos showed signs of delayed lung maturation as manifested for example by disorganized cells and less aerated areas with fully developed acini, which are surrounded by dense mesenchyme (Fig. 16 A). In comparison, nmf333 mice did not show these impairments. Thus, while the WT normoxic embryos and nmf333 embryos were showing signs of the canalicular stage where bronchioles are produced and the cuboidal epithelium is formed correlating with their gestational age and even signs of the saccular stage with fully developed bronchioli, the WT embryos exposed to transient fetal hypoxia showed less fully developed acini and bronchioles with aerated areas and dense mesenchyme.

To assess the functionality of the pneumocytes type II, glycogen storage was evaluated since it is known that glycogen storage negatively correlates with the ability to produce surfactant (Meyerholz, DeGraaff et al. 2006, Wang, Tan et al. 2020). Glycogen storage was visualized by PAS staining. Differentiation between pneumocytes type II which are already able to produce surfactant at E17.5, and pneumocytes type I was done via morphology criteria (pneumocytes type II are smaller and cubical compared to type I being oval shaped). Compared to normoxic WT embryos, lungs from hypoxic WT embryos showed a higher rate of PAS positive cells which do not yet produce surfactant, while this was not the case in lungs from hypoxic nmf333 embryos (Fig. 16 B). In line, determination of mRNA levels of surfactant proteins A-C via qPCR analysis showed that lungs from hypoxic E17.5 WT embryos had decreased surfactant protein mRNA levels. However, lungs from hypoxic nmf333 embryos showed higher levels of surfactant protein A-C mRNA than those from normoxic WT and nmf333 embryos (Fig. 16 C).

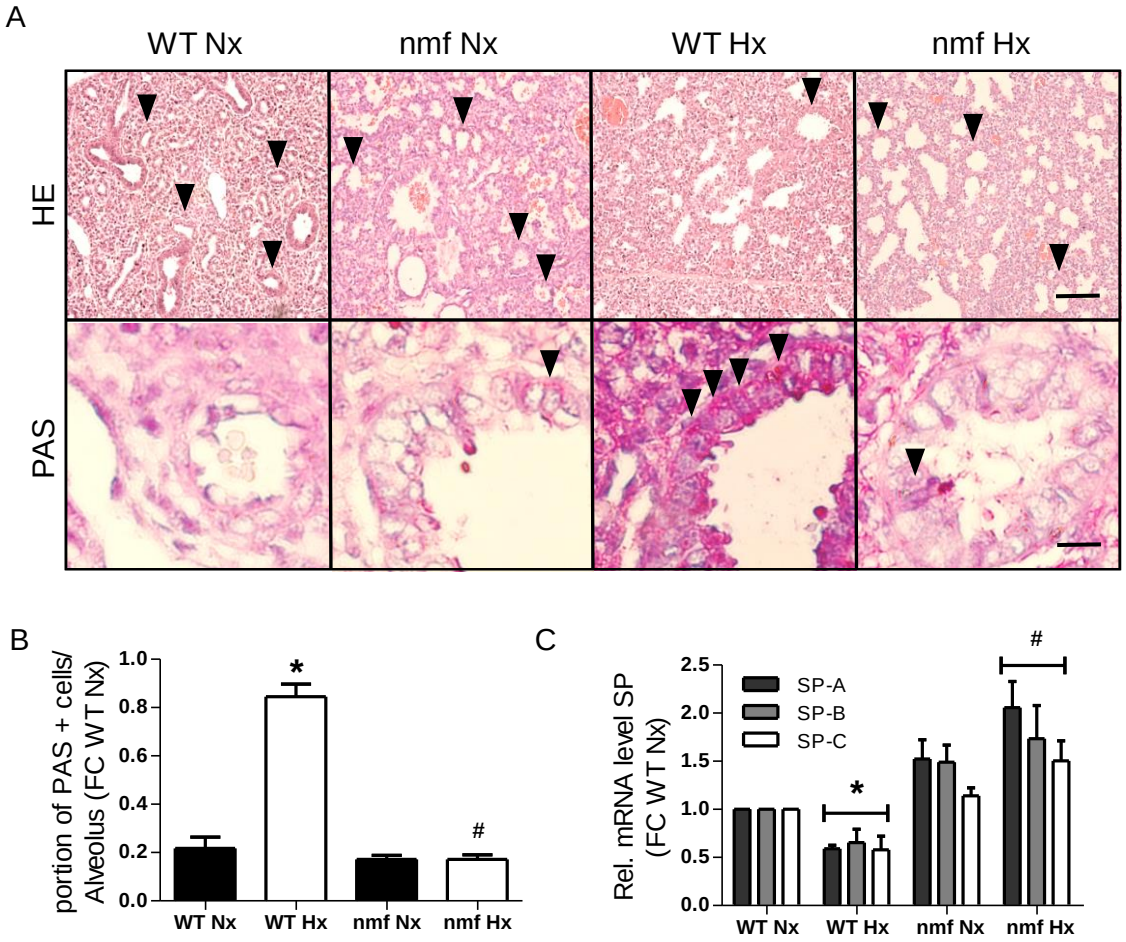

Fig. 16: Transient fetal hypoxia delays lung development dependent on p22phox

Pregnant wildtype (WT) or nmf333 (nmf) mice were exposed to 24 h hypoxia (10% oxygen, Hx) from E10.5 until E11.5. Afterwards, pregnant dams were kept under normoxic conditions (Nx) until the dissection of the embryos at E17.5. Embryos were embedded and histologically analysed. A: Upper row: Lung tissue sections were stained with HE (Scale bar = 40 µm). Arrows point to fully developed alveoli. Lower row: Lung sections were stained with PAS to show mucopolysaccharide containing cells. Arrows point to PAS positive cells (Scale bar = 5 µm). B: Quantitative analysis of PAS positive cells: 10 alveoli were counted and the ratio between PAS positive cells / total number of cells in one alveolus was evaluated (n=3, *p<0.05 WT Hx vs. WT Nx, #p<0.05 nmf Hx vs. WT Hx, SEM). C: mRNA levels of surfactant protein A-C. Data are shown as fold change (FC) to normoxic wildtype embryos (WT Nx) (n=3, *p<0.05 WT Hx vs. WT Nx, #p<0.05 nmf Hx vs. WT Hx, SEM).

6.3 The effect of transient fetal hypoxia on the adult offspring

To test whether transient fetal hypoxia affects the susceptibility of the cardiopulmonary system of the adult offspring towards chronic hypoxia, WT and nmf333 mice exposed to 10% oxygen from E10.5-11.5 were kept under normoxic conditions until they were 8 weeks old and were then exposed to chronic hypoxia for 3 weeks (10% oxygen) or remained under normoxia. In comparison, mice derived from normoxic pregnancies were exposed to chronic hypoxia at 8 weeks age for 3 weeks or remained under normoxia. Thus, a total of 8 different subgroups was analysed as described in Table 3.

Table 3: *Experimental protocol for the different groups of adult offspring.*

Experimental groups of adult offspring	Protocol
NxNx	Fetal normoxia, adult normoxia (Control)
NxHx	Fetal normoxia, adult chronic hypoxia for 3 weeks at 10% oxygen
HxNx	Transient fetal hypoxia, adult normoxia
HxHx	Transient fetal hypoxia, adult chronic hypoxia for 3 weeks at 10% oxygen

6.3.1 Body mass of the adult offspring

First, the consequences of transient fetal hypoxia on body mass were examined. WT mice but not nmf333 mice exposed to transient fetal hypoxia showed reduced body mass in adulthood (Fig. 17). Similar findings were subsequently obtained by others in the lab (Yishi Qin, unpublished data). Similarly, WT mice, but not nmf333 mice, exposed to chronic hypoxia only in adulthood also showed a lower body mass than normoxic controls (Fig. 17). Exposure to hypoxia in adulthood following transient fetal hypoxia decreased body mass in WT and nmf333 mice (Fig. 17).

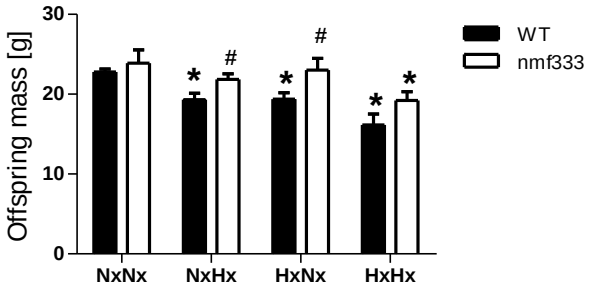

Fig. 17: Transient fetal hypoxia promotes persistent mass restriction in the adult offspring dependent on p22phox

Pregnant wildtype (WT) or nmf333 (nmf) mice were exposed to 24 h hypoxia (10% oxygen) from E10.5 until E11.5. Afterwards, pregnant dams were kept under normoxic conditions and offspring was born. Offspring at an age of 8 weeks was either exposed to 21 days of hypoxia (NxHx, HxHx) or kept at normoxic conditions (NxNx, HxNx). Mice were sacrificed at 11 weeks and total body mass was analysed (n=6, *p<0.05 WT NxHx/ HxNx/ HxHx/ nmf HxHx vs. WT NxNx, #p<0.05 nmf NxHx vs. WT NxHx, nmf HxNx vs. WT HxNx, SEM). NxNx= control group, NxHx= fetal normoxia, adult hypoxia 21 days 10 % oxygen, HxNx= fetal hypoxia 24 h E10.5-11.5 10% oxygen, adult normoxia, HxHx= fetal hypoxia 24 h E10.5-11.5 10% oxygen, adult hypoxia 21 days 10% oxygen.

6.3.2 The effect of transient fetal hypoxia on the adult lung

Next, mRNA levels of NADPH oxidases NOX1, NOX2 and NOX4 were measured in adult offspring lungs. NOX1 mRNA levels were not significantly altered by transient fetal or adult hypoxia in WT and nmf333 lungs (Fig. 18 A). NOX2 mRNA levels were significantly upregulated in lungs from WT mice exposed to hypoxia (HxNx, NxHx, HxHx) while they remained unchanged in nmf333 mice (Fig. 18 B). NOX4 mRNA levels were only increased in lungs from WT HxHx adult offspring (Fig. 18 C).

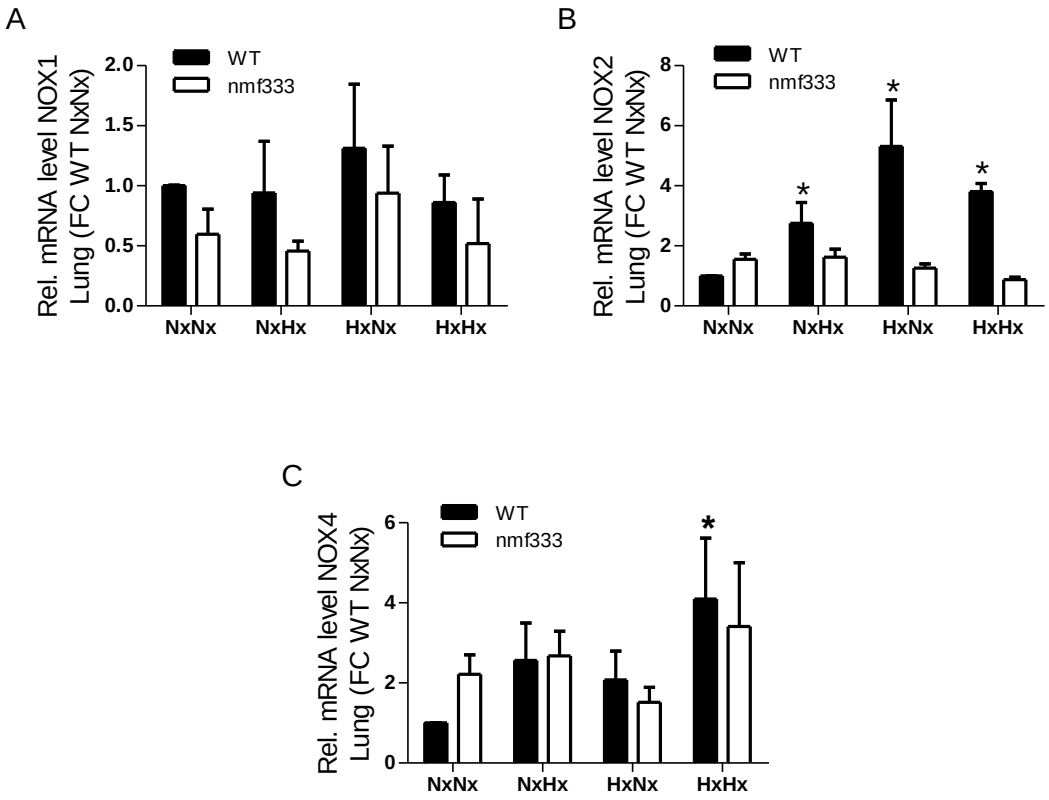

Fig. 18: Transient fetal hypoxia leads to elevated mRNA levels of NOX subunits in lungs from adult offspring dependent on p22phox

Pregnant wildtype (WT) or nmf333 (nmf) mice were exposed to 24 h hypoxia (10% oxygen) from E10.5 until E11.5. Afterwards, pregnant dams were kept under normoxic conditions until offspring was born. Adult offspring mice (8 weeks old) were either exposed to another 21 days of hypoxia (NxHx, HxHx) or kept at normoxic conditions (NxNx, HxNx). A: mRNA expression levels of NOX1 in lungs of adult offspring mice at 11 weeks (n=3, ns, SEM). B: mRNA expression levels of NOX2 in lungs of adult offspring mice at 11 weeks (n=3, *p<0.05 WT NxHx/ HxNx/ HxHx vs. WT NxNx, SEM). C: mRNA levels of NOX4 in lungs of adult offspring mice at 11 weeks (n=3, *p<0.05 WT HxHx vs. WT NxNx, SEM).

Next, lung tissues of adult offspring mice were analysed for surfactant protein (SP) mRNA expression. SP-A mRNA levels were significantly decreased in WT offspring mice exposed to transient fetal hypoxia (HxNx) or in mice exposed to hypoxia only in adulthood (NxHx), although they were not decreased in HxHx mice (Fig. 19 A). SP-B and SP-C mRNA levels were not affected by hypoxia. Moreover, SP mRNA levels were not affected by hypoxia in nmf333 mice (Fig 19 B).

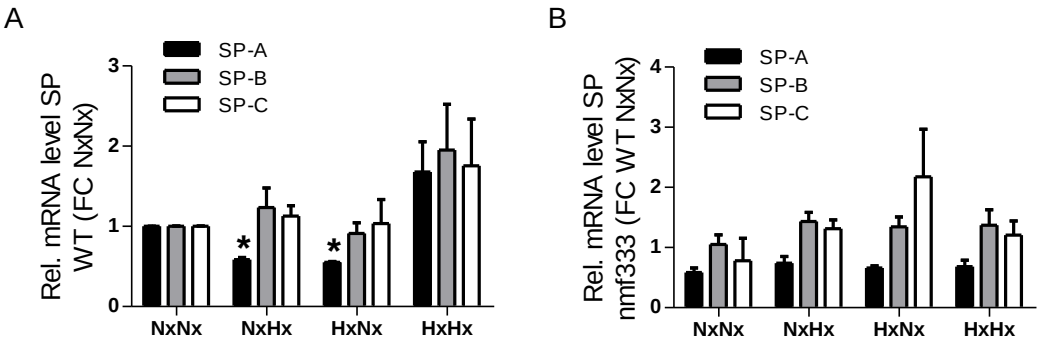

Fig. 19: Transient fetal hypoxia leads to decreased surfactant protein-A levels in adult offspring lungs dependent on p22phox

Pregnant wildtype (WT) or nmf333 (nmf) mice were exposed to 24 h hypoxia (10% oxygen) from E10.5 until E11.5. Afterwards, pregnant dams were kept under normoxic conditions until offspring was born. Adult offspring mice (8 weeks old) were either exposed to another 21 days of hypoxia to induce PH (NxHx, HxHx) or kept at normoxic conditions (NxNx, HxNx). A: mRNA levels of SP A-C in WT adult offspring mice lungs at 11 weeks (n=3, *p<0.05 WT NxHx/HxNx SP-A vs. WT NxNx SP-A, SEM). B: mRNA levels of SP A-C in nmf333 adult offspring mice lungs at 11 weeks (n=3, ns, SEM).

6.3.3 Transient fetal hypoxia leads to signs of pulmonary vascular remodelling

Pulmonary hypertension is characterized by increased vascular resistance in small lung vessels. As a chronic reaction, muscularization of small vessels (<30 µm) can be seen in the lung. To visualize pulmonary vascular remodelling, adult offspring lungs were stained for α-smooth muscle cell actin (Fig. 20 A). The number of small muscularized vessels was increased in lungs from WT mice exposed to transient fetal hypoxia and/or adult hypoxia while it remained unchanged in lungs from nmf333 mice (Fig. 20 B). In contrast, the number of larger vessels remained unchanged between the different genotypes and treatments (Fig. 20 C, D).

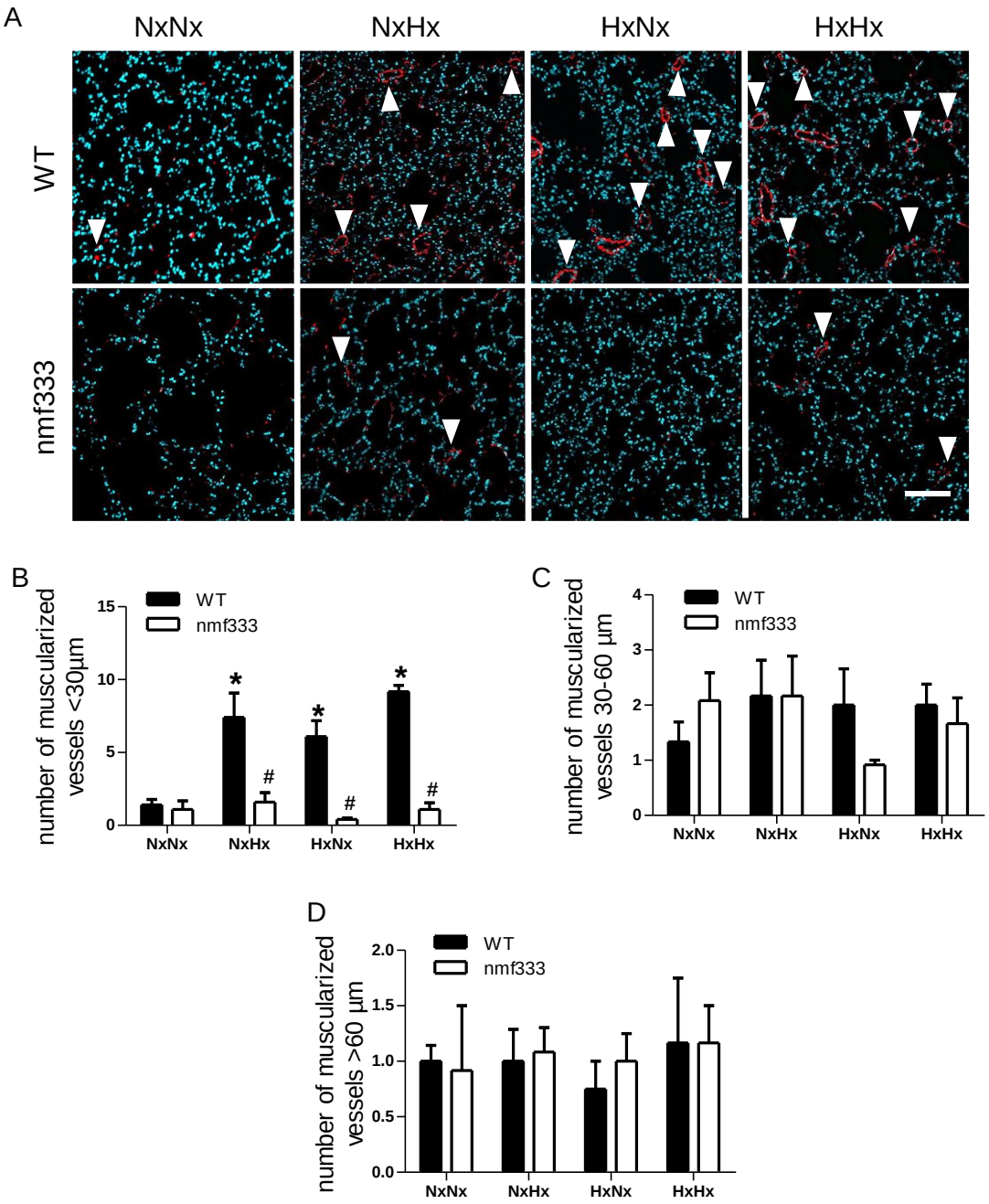

Fig. 20: Transient fetal hypoxia leads to muscularized small vessels in the adult lung

Pregnant wildtype (WT) or nmf333 (nmf) mice were exposed to 24 h hypoxia (10% oxygen) from E10.5 until E11.5. Afterwards, pregnant dams were kept under normoxic conditions until offspring was born. Offspring at an age of 8 weeks was either exposed to another 21 days of hypoxia (NxHx, HxHx) or kept at normoxic conditions (NxNx, HxNx). Lungs were stained with an antibody against alpha-smooth muscle cell actin (α-smc). A: α-smc staining (red= α-smc, blue= DAPI) of adult offspring lungs (arrows pointing at small vessels <30µm, scale bar = 50µm). B: Quantitative analysis of α-smc staining of vessels <30 µm (n=3, *p<0.05 WT NxNx vs. WT NxHx/ WT HxNx/ WT HxHx, #p<0.05 WT NxHx vs. nmf333 NxHx, WT HxNx vs. nmf333 HxNx, WT HxHx vs. nmf333 HxHx, SEM). C: Quantitative analysis of α-smc staining of vessels between 30 and 60 µm (n=3, ns, SEM). D: Quantitative analysis of α-smc staining of vessels >60µm (n=3, ns, SEM).

Furthermore, total alveolar septal thickness was measured as a sign of lung remodelling (Fig. 21 A). Exposure to transient fetal hypoxia and/or adult hypoxia resulted in increased alveolar septal thickness in WT mice but not in nmf333 mice (Fig. 21 B).

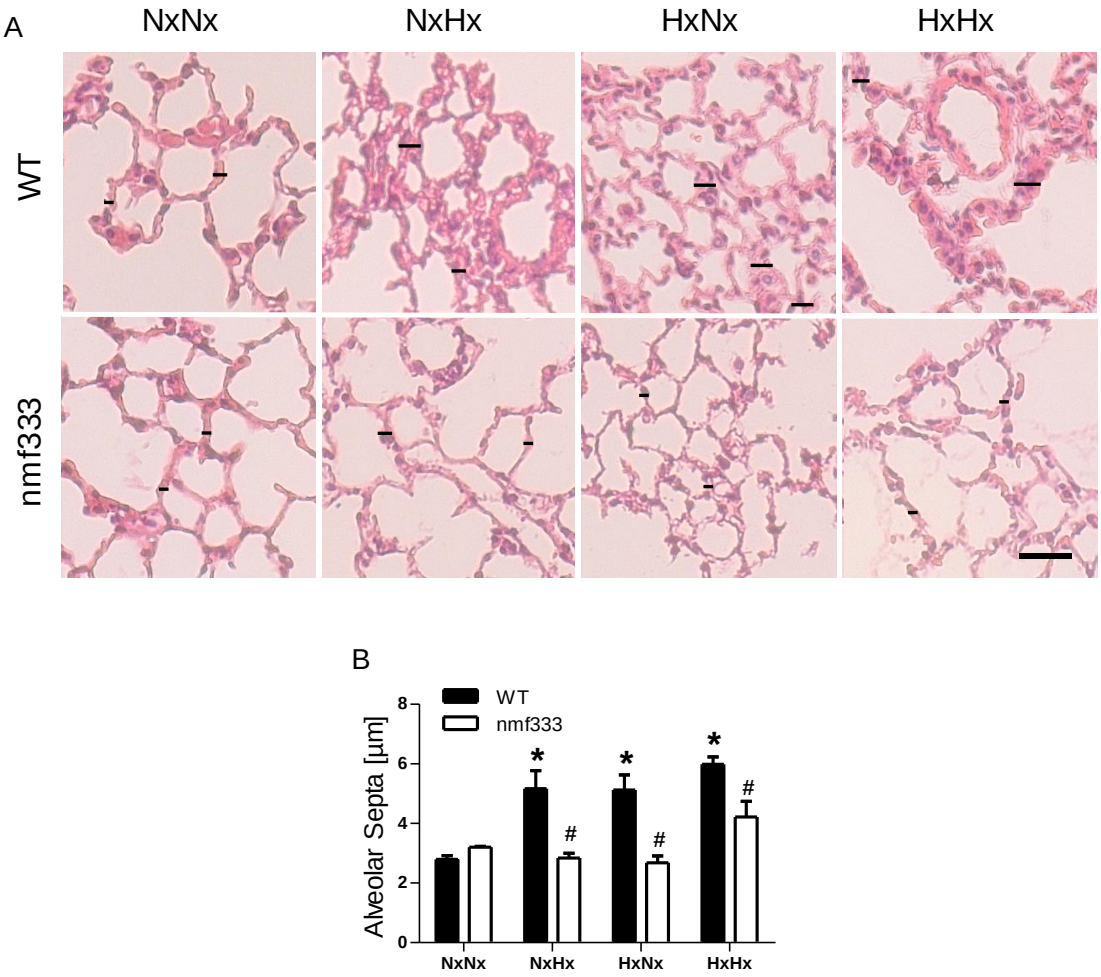

Fig. 21: Transient fetal hypoxia increases diameter of alveolar septa in the adult lung

Pregnant wildtype (WT) or nmf333 (nmf) mice were exposed to 24 h hypoxia (10% oxygen) from E10.5 until E11.5. Afterwards, pregnant dams were kept under normoxic conditions until offspring was born. Adult offspring mice (8 weeks old) were either exposed to another 21 days of hypoxia (NxHx, HxHx) or kept at normoxic conditions (NxNx, HxNx). Lungs were stained with haematoxylin & eosin (HE). Alveolar septal thickness was analysed with the Image Scope software, measuring the diameter of 50 alveolar septa per sample. A: HE staining of adult lungs. Black bars indicate diameters of alveolar septa. B: Diameters of alveolar septa as a marker of remodeling were determined. Scale bar = 10µm (n=3, *p<0.05 WT NxNx vs. WT NxHx/ WT HxNx/ WT HxHx, #p<0.05 WT NxHx vs. nmf333 NxHx, WT HxNx vs. nmf333 HxNx, WT HxHx vs. nmf333 HxHx, SEM).

6.3.4 Transient fetal hypoxia leads to increased right ventricular pressure and remodelling

As we saw signs of pulmonary vascular remodelling and increased muscularization of small vessels in the WT adult offspring exposed to transient fetal hypoxia as indication for the development of pulmonary hypertension, we also investigated the adult heart.

First, LV and RV systolic and diastolic pressure values were measured and mean pressure values were calculated (Fig. 22). Transient fetal hypoxia and/or adult hypoxia elevated RV mean pressure in WT mice, but not in nmf333 mice (Fig. 22 A). Interestingly, the LV pressure was not significantly different among the groups (Fig. 22 B).

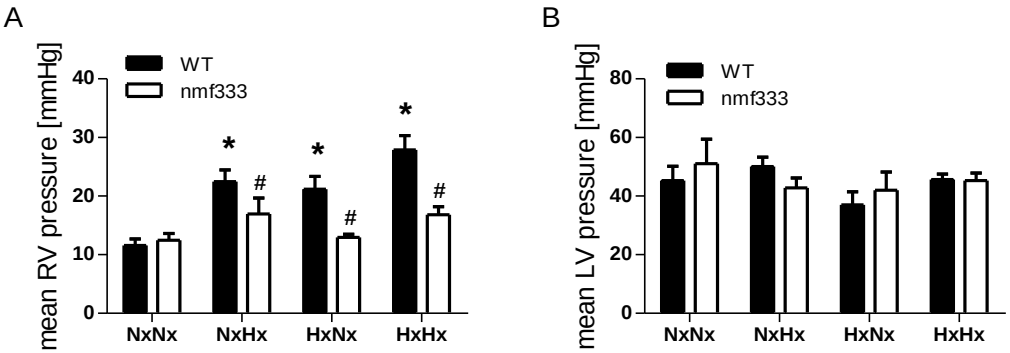

Fig. 22: Transient fetal hypoxia promotes elevated right ventricular pressure in adult mice

Pregnant wildtype (WT) or nmf333 (nmf) mice were exposed to 24 h hypoxia (10% oxygen) from E10.5 until E11.5. Afterwards, pregnant dams were kept under normoxic conditions until offspring was born. Adult offspring mice (8 weeks old) were either exposed to another 21 days of hypoxia (NxHx, HxHx) or kept at normoxic conditions (NxNx, HxNx). A: Right ventricular (RV) pressure was measured by a transthoracic approach. Mean RV pressure values are displayed (n=6, *p<0.05 WT NxHx/ HxNx/ HxHx vs. WT NxNx, #p<0.05 nmf NxHx vs. WT NxHx, nmf HxNx vs. WT HxNx, nmf HxHx vs. WT HxHx, SEM). B: Left ventricular (LV) pressure was measured. Mean LV pressure values are displayed.

To analyse RV hypertrophy, Fulton index (RV mass/ LV + septum mass, Fig. 23 B) and RV mass/ body mass ratio were determined (Fig. 23 A). Transient fetal hypoxia and/or adult hypoxia resulted in the development of RV hypertrophy in WT mice, but not in nmf333 mice.

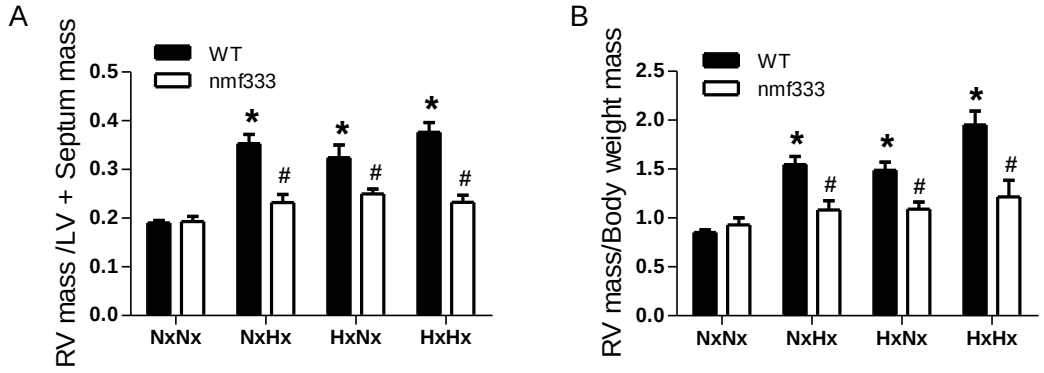

Fig. 23: Transient fetal hypoxia leads to increased right ventricular hypertrophy indices in the adult offspring

Pregnant wildtype (WT) or nmf333 (nmf) mice were exposed to 24 h hypoxia (10% oxygen) from E10.5 until E11.5. Afterwards, pregnant dams were kept under normoxic conditions until offspring was born. Adult offspring mice (8 weeks old) were either exposed to another 21 days of hypoxia (NxHx, HxHx) or kept at normoxic conditions (NxNx, HxNx). A: Fulton Index (RV to LV+ septum ratio) was analysed in adult offspring mice at 11 weeks (n=6-15, *p<0.05 WT NxHx/ WT HxNx/ WT HxHx vs. WT NxNx, #p<0.05 nmf NxHx vs. WT NxHx, nmf HxNx vs. WT HxNx, nmf HxHx vs. WT HxHx, SEM). B: RV/ Body weight index was evaluated in adult offspring mice at 11 weeks (n=6-15, *p<0.05 WT NxHx/ WT HxNx/ WT HxHx vs. WT NxNx, #p<0.05 nmf NxHx vs. WT NxHx, nmf HxNx vs. WT HxNx, nmf HxHx vs. WT HxHx, SEM).

The ratio of LV + septum mass/body mass was not affected by hypoxia in WT and nmf333 mice (Fig. 24).

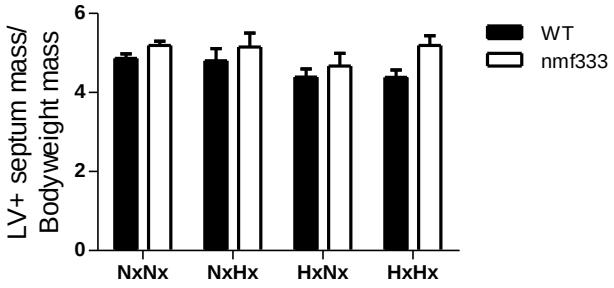

Fig. 24: Transient fetal hypoxia does not lead to increased left ventricular hypertrophy indices

Pregnant wildtype (WT) or nmf333 (nmf) mice were exposed to 24 h hypoxia (10% oxygen) from E10.5 until E11.5. Afterwards, pregnant dams were kept under normoxic conditions until the adult offspring mice (8 weeks old) were either exposed to another 21 days of hypoxia (NxHx, HxHx) or kept at normoxic conditions (NxNx, HxNx). Left ventricle (LV) + septum mass/ Body mass index was evaluated in adult offspring mice at 11 weeks (n=6-15, ns, SEM).

Next, cardiomyocyte size was determined in the RV by WGA staining (Fig. 25 A). Transient fetal hypoxia and/or adult hypoxia increased the size of RV cardiomyocytes in WT mice, but not in nmf333 mice (Fig. 25 B).

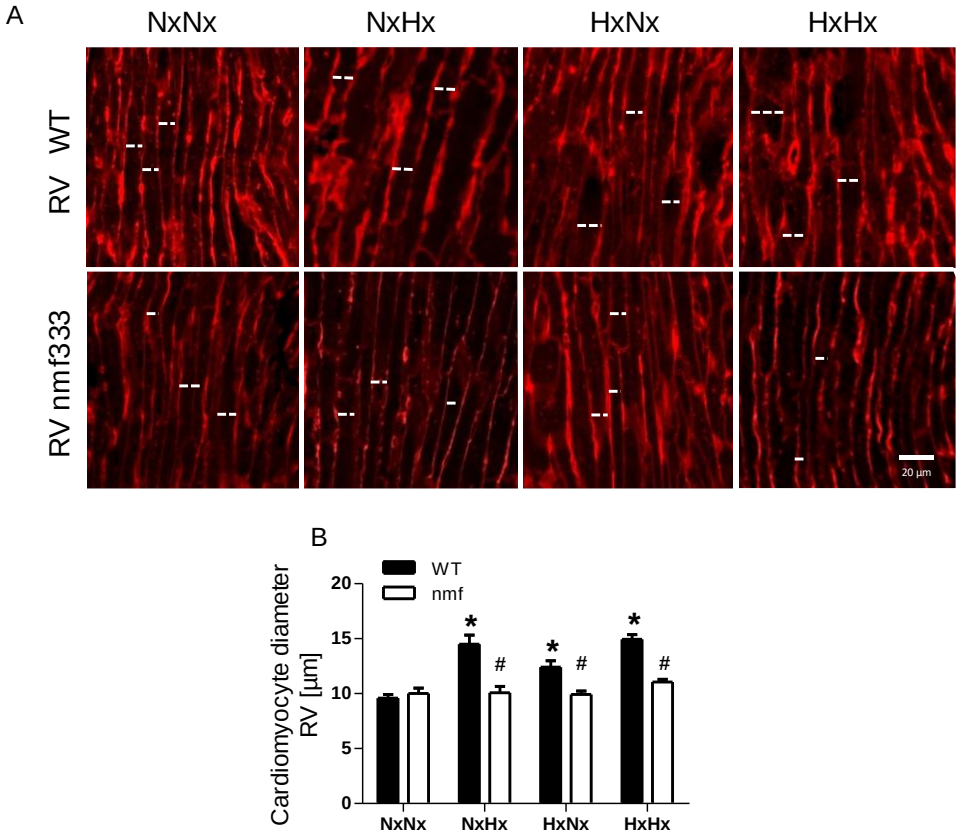

Fig. 25: Transient fetal hypoxia leads to increased right ventricular cardiomyocyte diameter

Pregnant wildtype (WT) or nmf333 (nmf) mice were exposed to 24 h of hypoxia (10% oxygen) from E10.5 until E11.5. Afterwards, pregnant dams were kept under normoxic conditions until the adult offspring mice (8 weeks old) were either exposed to another 21 days of hypoxia (NxHx, HxHx) or kept at normoxic conditions (NxNx, HxNx). Right ventricular (RV) sections were stained with wheat germ agglutinin (WGA). A: WGA staining of right ventricular (RV) cardiomyocytes is shown. B: Quantitative analysis of WGA staining in RV cardiomyocyte cells (n=3 *p<0.05 WT NxHx/ WT HxNx/ WT HxHx vs. WT NxNx, #p<0.05 nmf NxHx vs. WT NxHx, nmf HxNx vs. WT HxNx, nmf HxHx vs. WT HxHx, SEM).

Next, α- and β-MHC mRNA levels were measured in the RV (Fig. 26), taking β-MHC as a remodelling parameter. Whereas α-MHC levels were unaffected (Fig. 26 A), β-MHC mRNA levels were significantly increased in WT HxNx and WT HxHx groups, but not in nmf333 HxNx or HxHx mice (Fig.26 B).

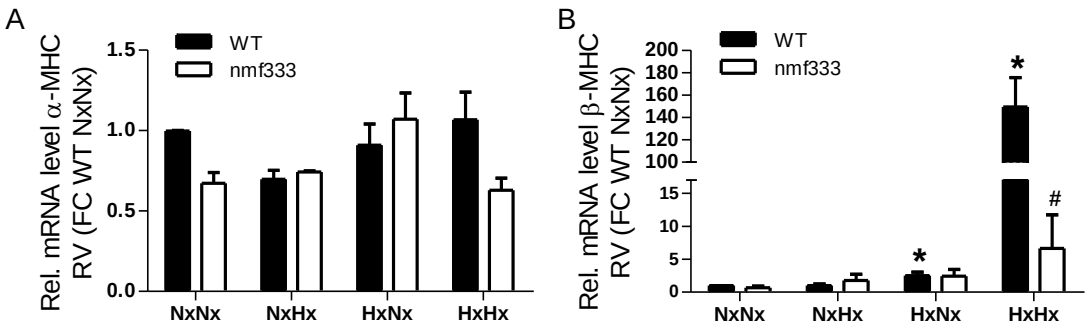

Fig. 26: Transient fetal hypoxia leads to elevated β-MHC mRNA levels in the right ventricle of adult offspring

Pregnant wildtype (WT) or nmf333 (nmf) mice were exposed to 24 h hypoxia (10% oxygen) from E10.5 until E11.5. Afterwards, pregnant dams were kept under normoxic conditions until offspring was born. The adult offspring mice (8 weeks old) were either exposed to another 21 days of hypoxia (NxHx, HxHx) or kept at normoxic conditions (NxNx, HxNx). Expression of α-MHC and β-MHC in the right ventricle (RV) was determined by qPCR. A: mRNA levels of α-MHC in the RV of adult offspring mice at 11 weeks (n=3, ns, SEM). B: mRNA expression level of β-MHC in RV of adult offspring mice at 11 weeks (n=3, *p<0.05 WT HxNx and WT HxHx vs. WT NxNx, #p<0.05 nmf333 HxHx vs. WT HxHx, SEM).

α- and β-MHC mRNA levels in the LV of adult offspring were not different between WT and nmf333 mice and were not affected by transient fetal and/or adult hypoxia (Fig. 27).

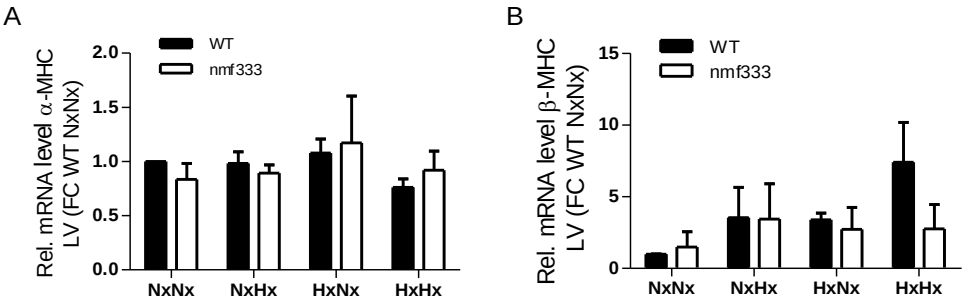

Fig. 27: Transient fetal hypoxia does not affect α- and β-MHC mRNA levels in the left ventricle

Pregnant wildtype (WT) or nmf333 (nmf) mice were exposed to 24 h hypoxia (10% oxygen) from E10.5 until E11.5. Afterwards, pregnant dams were kept under normoxic conditions until offspring was born. Adult offspring mice (8 weeks old) were either exposed to another 21 days of hypoxia (NxHx, HxHx) or kept at normoxic conditions (NxNx, HxNx). Expression of α-MHC and β-MHC in the left ventricle (LV) was determined by qPCR. A: mRNA levels of α-MHC in the left ventricle (LV) of adult offspring mice at 11 weeks (n=2-3). B: mRNA levels of β-MHC in LV of adult offspring mice at 11 weeks (n=2-3, ns).

6.3.5 Transient fetal hypoxia leads to persistent oxidative stress

To evaluate the levels of oxidative DNA damage in the adult RV, 8-oxodG staining was performed (Fig. 28 A). Quantitative analysis showed that 8-oxodG staining was increased in hearts from WT mice exposed to transient fetal hypoxia alone or in conjunction with adult hypoxia, but not in the RV from WT mice only exposed to adult hypoxia (Fig. 28 B). RV from nmf333 mice did not show oxidative DNA damage.

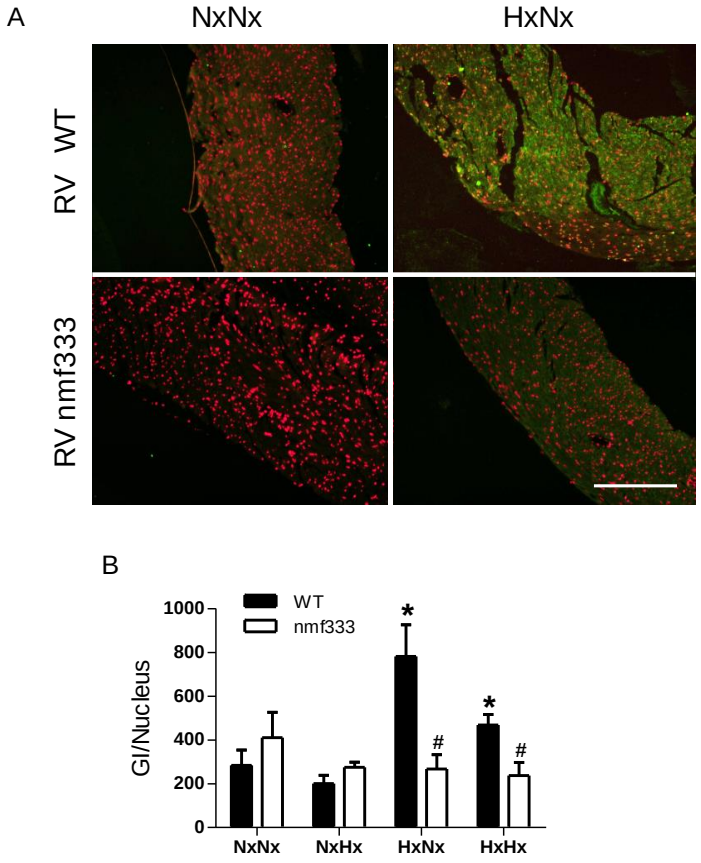

Fig. 28: Transient fetal hypoxia promotes oxidative DNA damage in adult offspring right ventricle dependent on p22phox

Pregnant wildtype (WT) or nmf333 (nmf) mice were exposed to 24 h hypoxia (10% oxygen) from E10.5 until E11.5. Afterwards, pregnant dams were kept under normoxic conditions until offspring was born. Adult offspring mice (8 weeks old) were either exposed to another 21 days of hypoxia (NxHx, HxHx) or kept at normoxic conditions (NxNx, HxNx). Right ventricles (RV) were stained with 8-hydroxy-deoxyguanosine (8-OHdG). A: 8-OHdG staining in the RV of adult offspring (red = DAPI, green = 8-OHdG, scale bar = 200 µm). B: Quantitative analysis of 8-OHdG grey value intensity (GI) per nucleus (n=3, *p<0.05 WT HxNx/HxHx vs. WT NxNx, #p<0.05 nmf HxNx vs. WT HxNx and nmf HxHx vs. WT HxHx, SEM).

In line, mRNA levels of NOX1, NOX2 and NOX4 tended to be increased in the RV from WT mice exposed to transient fetal hypoxia alone or in conjunction with adult hypoxia, although this effect only reached significance for NOX2 levels in the HxNx group and for NOX4 in the HxNx and HxHx groups (Fig. 29)

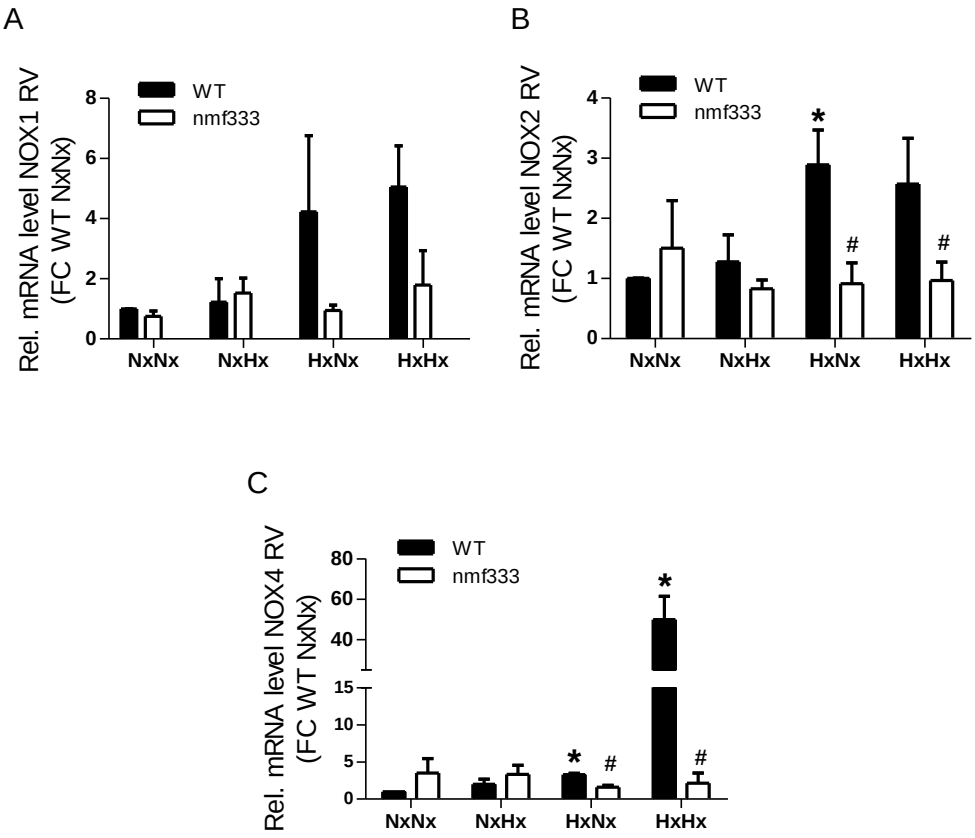

Fig. 29: Transient fetal hypoxia leads to elevated NOX1, NOX2 and NOX4 mRNA levels in the right ventricle of adult offspring dependent on p22phox

Pregnant wildtype (WT) or nmf333 (nmf) mice were exposed to 24 h of hypoxia (10% oxygen) from E10.5 until E11.5. Afterwards, pregnant dams were kept under normoxic conditions until offspring was born. Adult offspring mice (8 weeks old) were either exposed to another 21 days of hypoxia (NxHx, HxHx) or kept at normoxic conditions (NxNx, HxNx). mRNA levels of NOX1, NOX2 and NOX4 were determined by qPCR in the right ventricle (RV). A: mRNA levels of NOX1 in the right ventricle (RV) of adult offspring mice at 11 weeks (n=3, ns, SEM). B: mRNA levels of NOX2 in RV of adult offspring mice at 11 weeks (n=3, *p<0.05 WT HxNx vs. WT NxNx, #p<0.05 nmf HxNx vs. WT HxNx and nmf HxHx vs. WT HxHx, SEM). C: mRNA levels of NOX4 in RV of adult offspring mice at 11 weeks (n=3, *p<0.05 WT HxNx/ WT HxHx vs. WT NxNx, #p<0.05 nmf HxNx vs. WT HxNx and nmf HxHx vs. WT HxHx, SEM).

Conclusively, p22phox mRNA levels were increased in the RV from WT mice exposed to transient fetal hypoxia while they remained unchanged in the RV from nmf333 mice (Fig. 30).

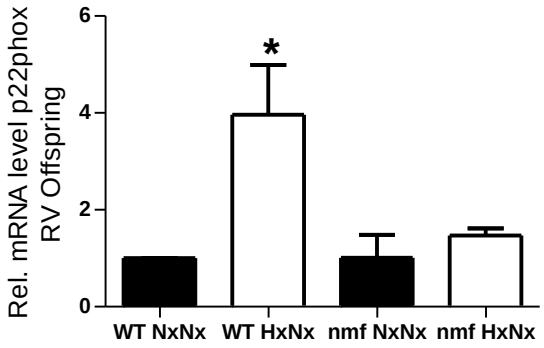

Fig. 30: Transient fetal hypoxia leads to elevated p22phox mRNA levels in the right ventricle

Pregnant wildtype (WT) or nmf333 (nmf) mice were exposed to 24 h hypoxia (10% oxygen) from E10.5 until E11.5. Afterwards, pregnant dams were kept under normoxic conditions until offspring was born. Adult offspring mice (8 weeks old) were either exposed to another 21 days of hypoxia (NxHx, HxHx) or kept at normoxic conditions (NxNx, HxNx). mRNA levels of p22phox in the right ventricle (RV) of adult offspring mice were determined by qPCR. (n=3, n=2 nmf HxNx, *p<0.05 WT HxNx vs. WT NxNx, SEM).

In contrast, mRNA levels of NOX1, NOX2 and NOX4 remained unchanged in all groups in the LV (Fig. 31)

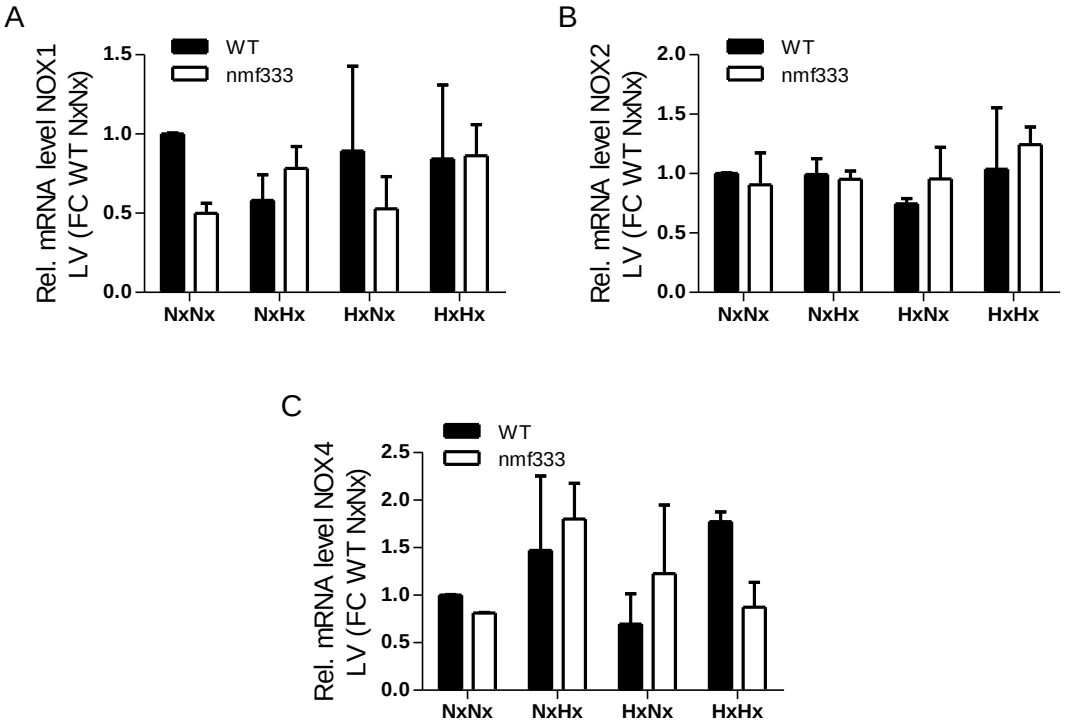

Fig. 31: Transient fetal hypoxia does not lead to elevated NADPH oxidase mRNA levels in the left ventricle

Pregnant wildtype (WT) or nmf333 (nmf) mice were exposed to 24 h hypoxia (10% oxygen) from E10.5 until E11.5. Afterwards, pregnant dams were kept under normoxic conditions until offspring was born. The adult offspring mice (8 weeks old) were either exposed to another 21 days of hypoxia (NxHx, HxHx) or kept at normoxic conditions (NxNx, HxNx). NOX1, NOX2 and NOX4 mRNA levels in the left ventricle (LV) were determined by qPCR. A: mRNA levels of NOX1 in the LV of adult offspring mice at 11 weeks (n=3, ns, SEM). B: mRNA levels of NOX2 in the LV of adult offspring mice at 11 weeks (n=3, ns, SEM). C: mRNA levels of NOX4 in LV of adult offspring mice at 11 weeks (n=3, ns, SEM).

6.4 The effect of hypoxia on embryoid bodies

6.4.1 Effects on ROS generation

To validate the results observed in the in vivo experiments, in vitro experiments were performed with R1 mESC transduced with a lentiviral vector expressing shp22 (shp22). Compared to wildtype mESC, mESC transduced with the shp22 vector showed decreased p22phox mRNA levels (Fig. 32).

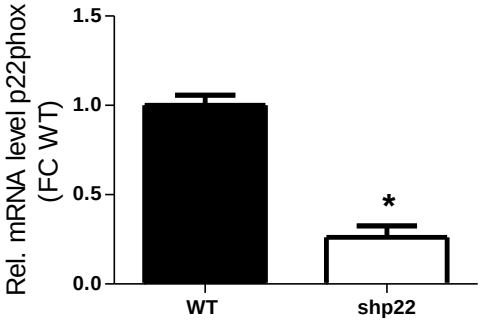

Fig. 32: Lentiviral knockdown of p22phox leads to a decrease of p22phox mRNA in murine embryonic stem cells

R1 mESC were transduced with a lentiviral vector coding for shp22. RNA was isolated and p22phox RNA levels were measured by qPCR (n=3, *p<0.05 shp22 vs. WT, SEM).

To assess whether mock transduction using a lentiviral construct expressing shGFP as a control vector (shCtr) would affect ROS production, superoxide generation was determined in mESC expressing shGFP as a control vector and WT mESC using EPR under normoxic conditions and after exposure to 0.1% oxygen for 24 h (Fig. 33 A). Measurements were performed in normoxia under reoxygenated conditions. Although increased levels of ROS were observed after hypoxia, no differences could be observed between WT mESC and shGFP expressing mESC. Next, metabolic activity using Alamar Blue assay (Fig. 33 B) and proliferation using BrdU incorporation (Fig. 33 C) were measured. Hypoxia increased metabolic activity in both cell lines, while BrdU incorporation was similar in all conditions tested. As there was no difference in the phenotype between WT and control-transduced cells, we used in the following experiments WT mESC as control cells.

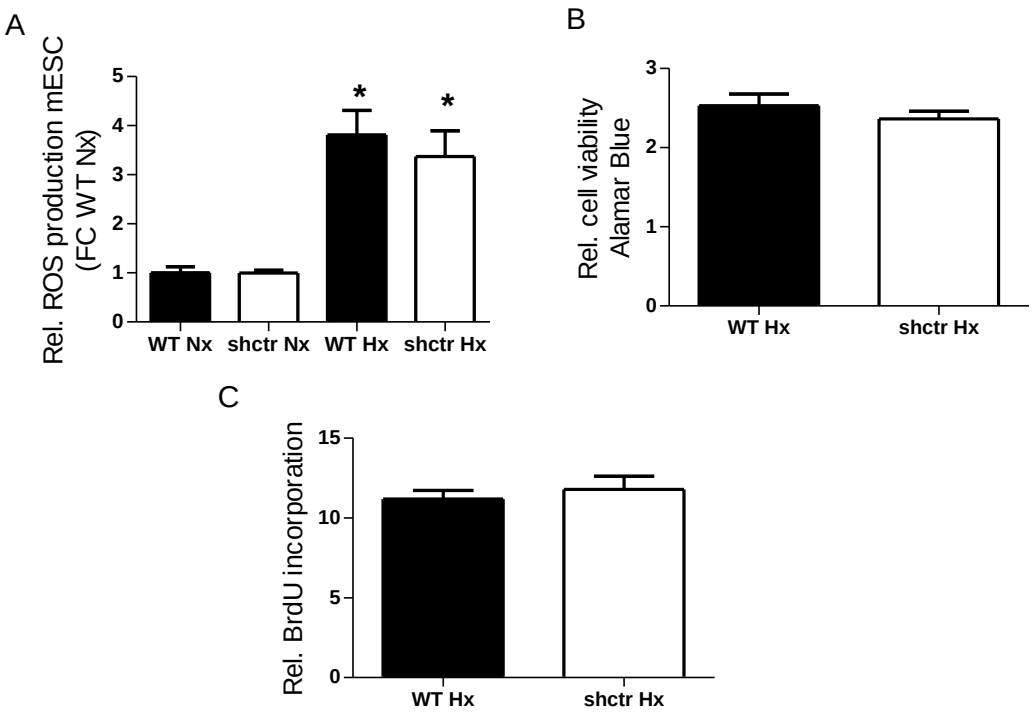

Fig. 33: Comparison between wildtype and shctr murine embryonic stem cells

Murine embryonic stem cells (mESC) either transduced with a lentiviral vector expressing shGFP (shctr) or wildtype (WT) mESC were exposed to 24 h hypoxia (0.1% oxygen). A: Superoxide generation was measured via electron magnetic resonance (EPR) using the spin trap CMH. EPR measurements were performed under reoxygenated conditions (n=3, *p<0.05, WT Hx and shctr Hx vs. WT Nx, SEM). B: Cell viability was analysed by AlamarBlue with mESC transfected with a control lentivirus (shctr) or WT and exposed to hypoxia for 24 h (0.1 % oxygen, n=3, ns, SEM). C: Proliferation was analysed by BrdU incorporation ELISA (n=3-12, ns, SEM).

Next, the differential influence of 1.0% and 0.1% oxygen for 24 h on metabolic activity and proliferation was determined using Alamar Blue assay and BrdU incorporation (Fig. 34). Whereas exposure to 1.0% oxygen for 24 h had no effect on metabolic activity or proliferation (Fig. 34 A, B), exposure to 0.1% oxygen for 24 h decreased metabolic and proliferation activity of WT mESC whereas shp22 expressing mESC were not affected (Fig. 34 C and D).

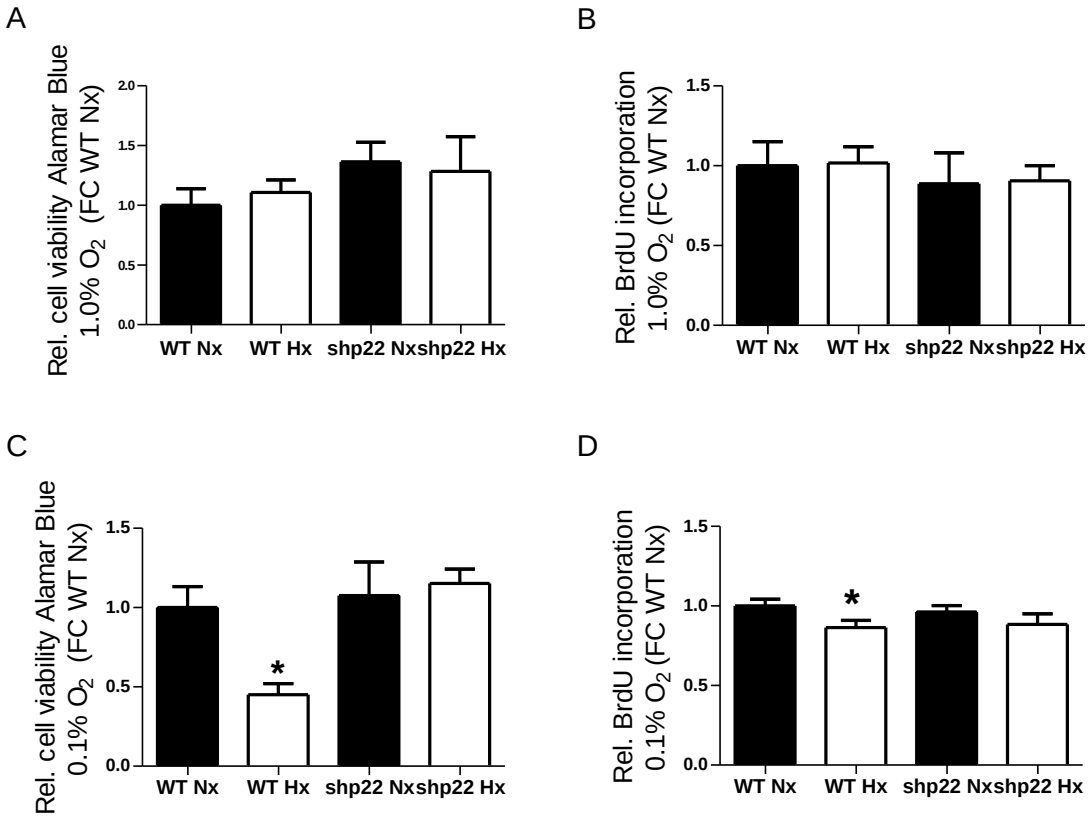

Fig. 34: Depletion of p22phox leads to decreased metabolic activity and proliferation at 0.1% but not at 1% oxygen in murine embryonic stem cells

Murine embryonic stem cells (mESC) transduced with a lentiviral vector coding for shp22phox (shp22) or control mESC (WT) were exposed to either 1% (A/B) or 0.1% (C/D) oxygen for 24 h. A/C) Metabolic activity was analysed by AlamarBlue. Rel. absorbance values are shown. B/D) Proliferation was assessed by BrdU incorporation ELISA. Rel. absorbance values are shown (n=6-9, ns, SEM).

Therefore, we chose 0.1% oxygen for a period of 24 hours as our experimental conditions. Subsequent EPR measurements showed that the increase in ROS production following exposure to 0.1% oxygen observed in WT mESC was significantly lower in p22phox-deficient mESCs (Fig. 35 A).

We next measured ROS levels by EPR in EBs at day 4 of differentiation. This is the first day after transfer of the EBs from the hanging drops to cell dishes and the first day of solid EB formation. While ROS generation in p22phox-deficient EBs did not differ from normoxic WT EBs, hypoxic WT EBs showed a tendency towards higher ROS levels although this trend did not reach significance (Fig. 35 B).

As on day 8 of differentiation a visible contraction of cardiomyocytes can be seen for the first time, EBs were exposed to hypoxia for 24 h starting on day 7. ROS levels were significantly elevated in control EBs following hypoxia while this response was blunted in p22phox-deficient EBs (Fig. 35 C). Similar results were subsequently obtained by others in the lab (Yishi Qin, unpublished results). Similarly, pre-treating EBs with GKT137831, an inhibitor of NOX1 and NOX4, or gp91ds-tat which inhibits NOX2 prevented hypoxia-induced ROS generation (Fig 35 C). Moreover, addition of these inhibitors to p22phox-deficient EBs did not affect ROS production under normoxia, but further reduced ROS production following hypoxia (Fig 35 C).

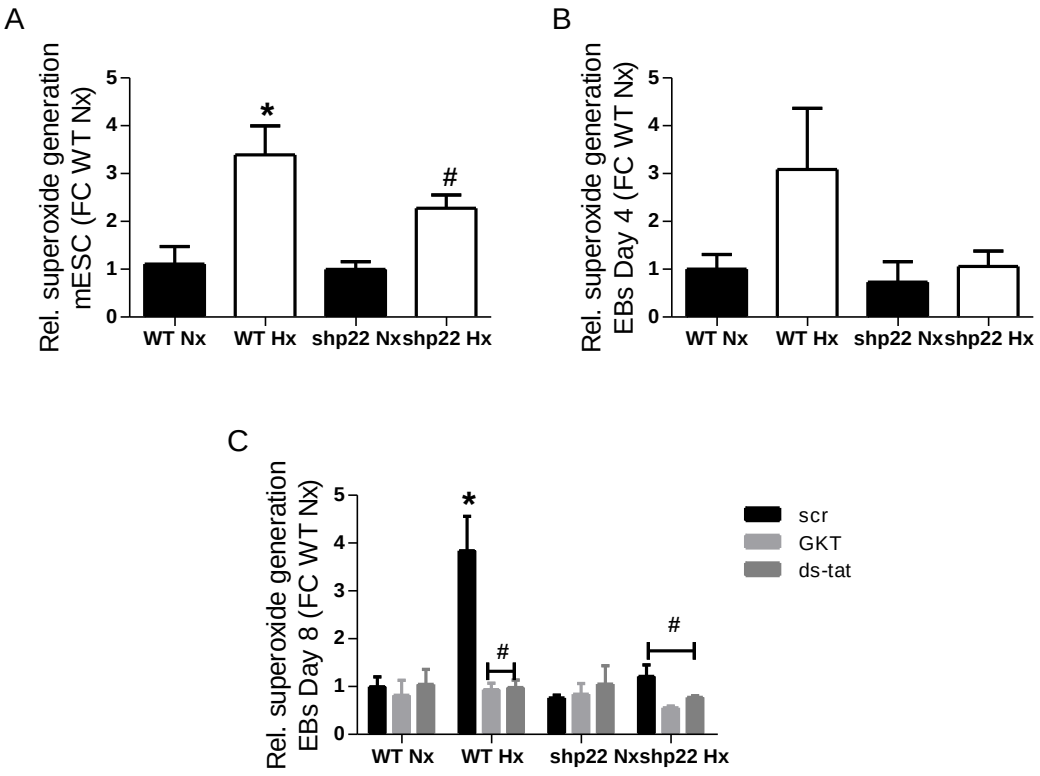

Fig. 35: Relative superoxide generation of murine embryonic stem cells and embryoid bodies dependent on p22phox

A: Undifferentiated R1 wildtype (WT) murine embryonic stem cells (mESC) and mESC transduced with a lentiviral vector encoding shp22phox were exposed to normoxia or hypoxia (24 h at 0.1% oxygen). EPR measurements were performed under reoxygenated conditions after hypoxia exposure. Rel. superoxide generation is displayed (n=5-6, *p<0.05 WT Hx vs. WT Nx, #p<0.05 shp22 Hx vs. WT Hx, SEM). B: Relative superoxide generation of EBs at days 3-4 of differentiation with the hanging drop method were exposed to hypoxia for 24 h at 0.1% oxygen. Rel. superoxide generation was measured by EPR (n=3, SEM). C: After hypoxia exposure from day 7-8 for 24 h at 0.1% oxygen, NADPH oxidase inhibitors GKT 137831 (2 mM 1:1000, GKT, specific for NOX1 and 4) and gp91ds-tat (2.5 mM 1:500, ds-tat, specific inhibitor of NOX2), or scrambled gp91ds-tat (2.5 mM 1:500, scr) as control were added to the harvested EBs. Relative superoxide generation of EBs at day 8 of differentiation was measured by EPR 15 min after hypoxia under reoxygenated conditions (n=3, *p<0.05 WT Hx scr vs. WT Nx scr, #p<0.05 WT Hx GKT/ds-tat vs. WT Hx scr and shp22 Hx scr/ GKT/ ds-tat vs. WT Hx scr, SEM).

Oxidative stress was further visualized in EBs at day 8 by immuno-spin trapping of DMPO (Ramirez, Gomez-Mejiba et al. 2007). ROS-induced DMPO adducts were significantly increased in WT EBs but not in p22phox-deficient EBs after exposure to hypoxia (Fig. 36). Similar findings were obtained by others in the lab (Yishi Qin, unpublished results).

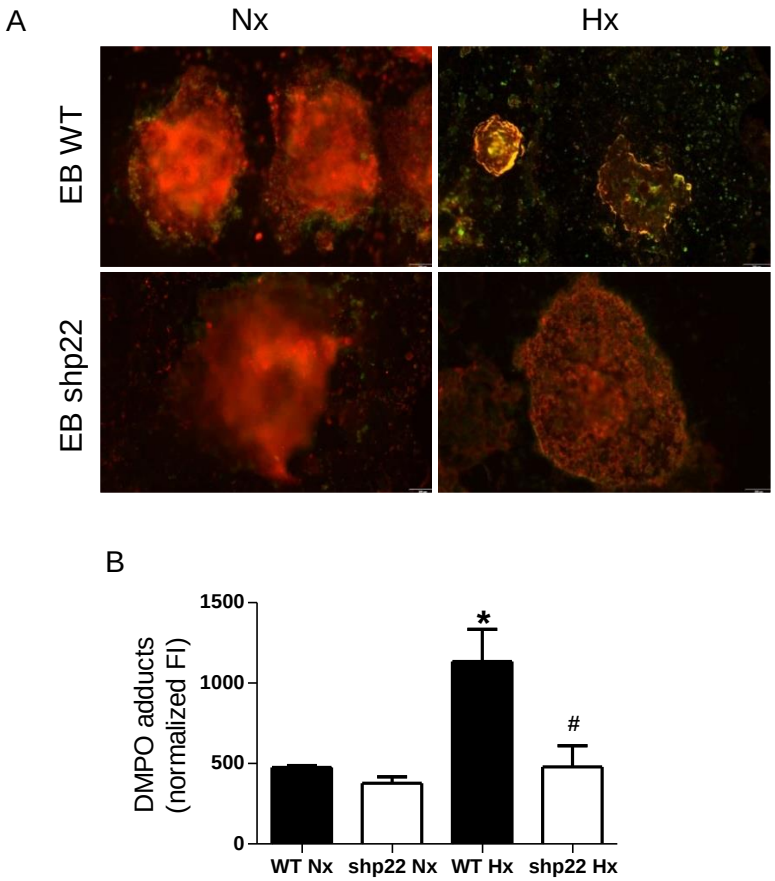

Fig. 36: DMPO adduct formation is dependent on p22phox expression in embryoid bodies

Wildtype (WT) R1 murine embryonic stem cells (mESC), or mESC depleted of p22phox (shp22), were differentiated into embryoid bodies (EBs) using the hanging drop method. EBs were exposed to 24 h of hypoxia (0.1 % oxygen) at day 8 of differentiation. Before hypoxia, DMPO (50 mM) was added to the stem cell medium. After hypoxia, EBs were analysed via immunochemistry for forming of DMPO adducts. A: DMPO adduct formation (green) and α-actinin (red) staining. B: Quantitative analysis of DMPO staining. Fluorescence intensity normalized to total area of EBs (n=3, *p<0.05 WT Hx vs. WT Nx, #p<0.05 shp22 Hx vs. WT Hx, SEM).

Next, we tested whether hypoxia also affects NADPH oxidase expression levels in EBs at day 8. Indeed, p22phox mRNA levels were significantly elevated in hypoxic WT EBs. As expected, transduction of EBs with the lentiviral construct expressing shp22phox reduced p22phox mRNA levels under normoxic conditions and prevented upregulation of p22phox mRNA levels by hypoxia (Fig. 37).

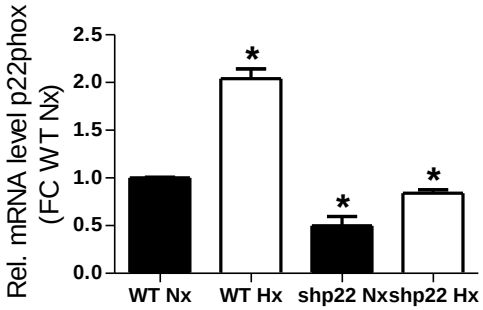

Fig. 37: mRNA levels of p22phox are dependent on hypoxia in embryoid bodies

Wildtype (WT) R1 murine embryonic stem cells (mESC), or mESC depleted of p22phox (shp22), were differentiated into embryoid bodies (EBs) using the hanging drop method. EBs were exposed to 24 h of hypoxia (0.1% oxygen) from day 7 to 8 of differentiation. After hypoxia, EBs were harvested immediately and RNA was isolated for qPCR analysis. p22phox mRNA levels were assessed. Data shown as relative foldchange (FC) compared to normoxic wildtype EBs (WT Nx) (n=3, *p<0.05 shp22 Nx/ shp22 Hx vs. WT Nx, SEM).

6.4.2 Effects on differentiation

To investigate whether hypoxia and p22phox affect differentiation of EBs, expression of different germ layer markers was measured using qPCR (Fig. 38). Expression of the pluripotency marker Oct4 (Matthai, Horvat et al. 2006) was not regulated by hypoxia in wildtype embryoid bodies at all, while it was lower in shp22phox embryoid bodies (Fig. 38 A).

The mesodermal differentiation marker Brachyury which is involved in the formation of cardiomyocytes, was significantly downregulated by hypoxia in WT EBs, but not in p22phox deficient EBs (Fig. 38 B).

Otx2, an endodermal differentiation factor was not significantly regulated at all (Fig. 38 C), while Hnf-1, an ectodermal differentiation factor showed a significant decrease in shp22phox embryoid bodies after hypoxia exposure (Fig. 38 D).

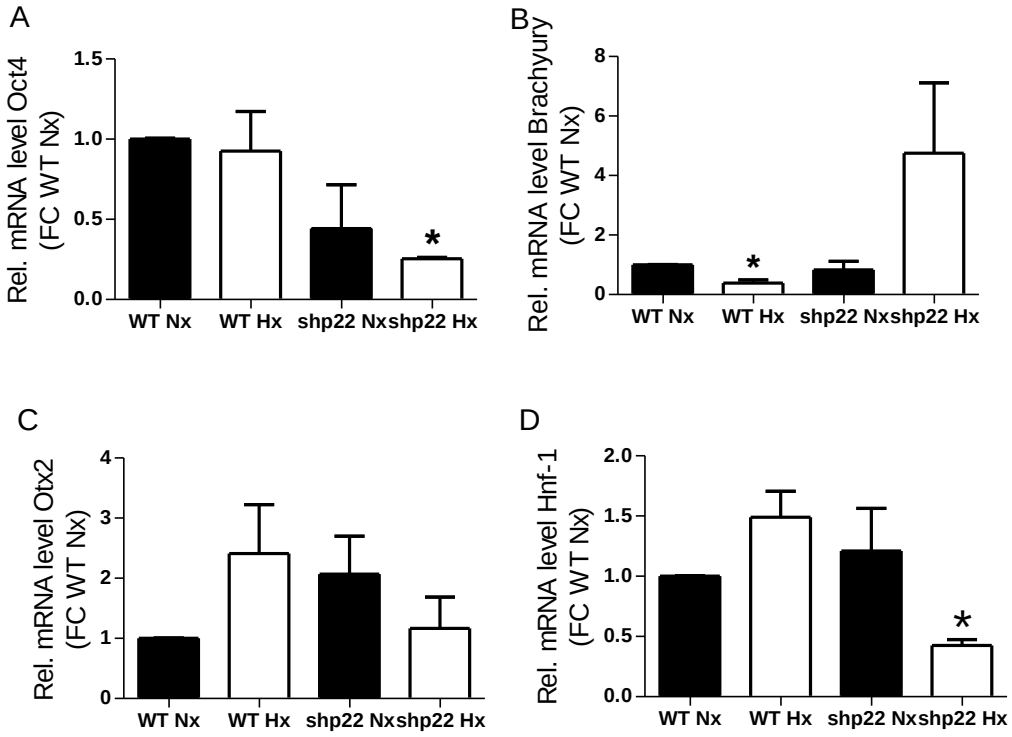

Fig. 38 mRNA expression of differentiation factors in embryoid bodies dependent on p22phox

Wildtype (WT) R1 murine embryonic stem cells (mESC), or mESC depleted of p22phox (shp22), were differentiated into embryoid bodies (EBs) using the hanging drop method. EBs were exposed to 24 h of hypoxia (0.1% oxygen) from day 7-8 of differentiation. After hypoxia, EBs were harvested immediately and RNA was isolated for qPCR analysis. A: mRNA levels of Oct 4 as a pluripotency factor in EBs (n=3, WT Nx vs. shp22 Hx, SEM). B: mRNA levels of Brachyury (n=3, *p<0.05 WT Hx vs. WT Nx, SEM). C: mRNA levels of Otx2 as an endodermal differentiation factor (n=3, ns, SEM). D: mRNA levels of Hnf-1 as an ectodermal differentiation factor in EBs (n=3, *p<0.05 shp22 Hx vs. WT Nx, SEM).

Next, mRNA levels of cardiac differentiation factors were assessed (Fig. 39). Nkx2.5 mRNA levels were decreased in hypoxic WT EBs but were increased in p22phox-deficient EBs in particular following exposure to hypoxia (Fig. 39 A). Similar data were subsequently obtained in the lab (Yishi Qin et. al, unpublished results). Similarly, β-MHC mRNA levels were downregulated in hypoxic WT EBs but not in p22phox-deficient EBs (Fig. 39 B). Hypoxia and deficiency of p22phox tended to increase α-MHC mRNA levels although this trend did not reach significance (Fig. 39 C).

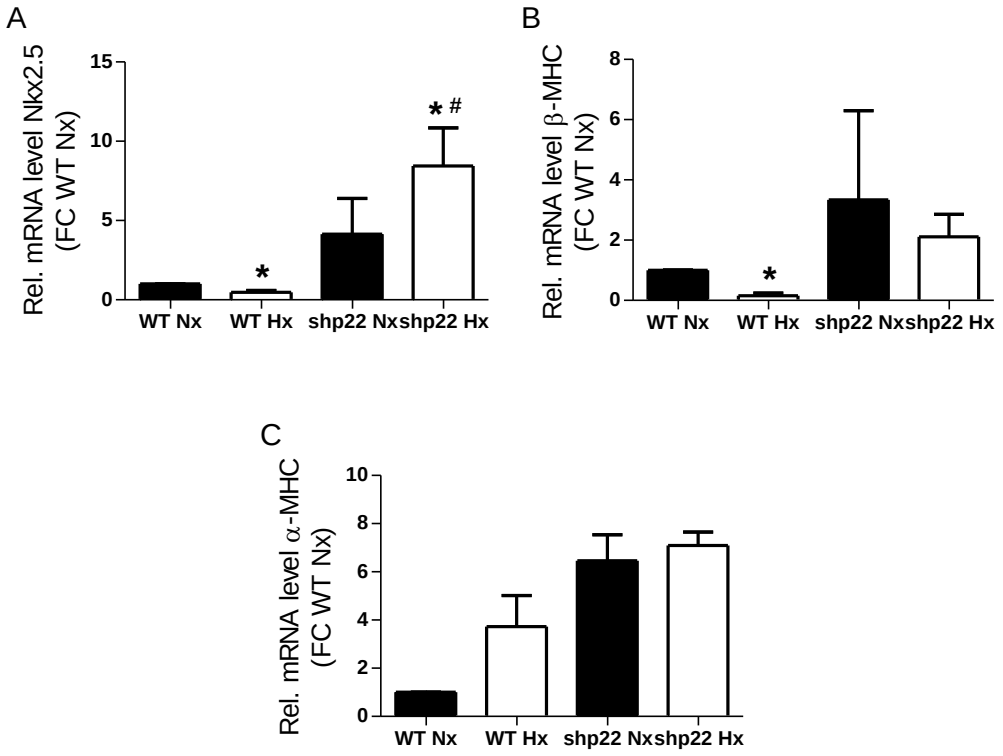

Fig. 39: Cardiac differentiation factors in embryoid bodies at day 8 dependent on p22phox

Wildtype (WT) R1 murine embryonic stem cells (mESC), or mESC depleted of p22phox (shp22), were differentiated into embryoid bodies (EBs) using the hanging drop method. EBs were exposed to 24 h of hypoxia (0.1% oxygen) from day 7-8 of differentiation. After hypoxia, EBs were harvested immediately and RNA was isolated for qPCR analysis. A: mRNA levels of Nkx2.5 (n=3, *p<0.05 WT Hx/ shp22 Hx vs. WT Nx, #p<0.05 shp22 Hx vs. WT Hx, SEM). B: mRNA levels of β-MHC (n=3, *p<0.05 WT Hx vs. WT Nx, SEM). C: mRNA levels of α-MHC in EBs (n=2-3).

7 Discussion

The main finding of this study was that p22phox-dependent NADPH oxidases are involved in the fetal and adult offspring cardiopulmonary response to fetal hypoxia. Specifically, we found that:

a) p22phox contributed to persistent ROS generation and oxidative DNA damage in the embryo and in the adult offspring in response to fetal hypoxia as well as in hypoxic embryoid bodies.
b) p22phox promoted persistent IUGR and decreased body mass in adulthood induced by fetal hypoxia.
c) p22phox promoted delayed cardiac maturation in mouse embryos induced by fetal hypoxia and in hypoxic embryoid bodies.
d) p22phox promoted delayed lung maturation and surfactant production in E17.5 embryos induced by fetal hypoxia.
e) p22phox promoted the development of pulmonary hypertension in adulthood in response to fetal hypoxia.

7.1 Transient fetal hypoxia leads to ROS derived from NADPH oxidases

To evaluate a potential role of NADPH oxidases in the response to fetal hypoxia we determined whether ROS formation and NADPH oxidases are regulated by hypoxia in embryoid bodies as a model system for cardiac differentiation as well as in the embryo and adult offspring cardiopulmonary system following fetal hypoxia.

Exposure to hypoxia has been previously shown to be followed by increased levels of ROS in different cell types. In line, exposure to 0.1% oxygen for 24 h resulted in a clear increase in ROS levels in mESC and EBs. Importantly, our in vivo data also showed that fetal hypoxia from E10.5 to E11.5 increased ROS levels in the embryo at E11.5.

Oxidative stress after different periods of fetal hypoxia was reported by several studies during the last decades (Patterson, Xiao et al. 2012, Kim, Kim et al. 2022, Smith, Swiderska et al. 2022). In isolated fetal rat hearts and H9C2 cells, an embryonic rat cardiomyoblast cell line, hypoxia increased ROS production which was diminished by the ROS scavengers N-acetylcysteine and tempol (Patterson, Xiao et al. 2012). Increased ROS generation in the fetal

heart after hypoxia has been reported in several species (Patterson, Xiao et al. 2012, Giussani, Niu et al. 2014, Kane, Hansell et al. 2014, Frasch, Herry et al. 2020). Furthermore, enhanced ROS production was not only found in the embryo, but also in the human placenta, plasma and umbilical cord of humans affected by intrauterine growth restriction (Agarwal, Aponte-Mellado et al. 2012).

Consecutively, increased oxidative DNA damage indicated by staining with 8-oxodG, a commonly used biomarker to measure and quantify oxidative stress (Martinet, Knaapen et al. 2002, Di Minno, Turnu et al. 2016), was observed in WT E11.5 embryos directly after fetal hypoxia exposure, and this effect was still observed in E17.5 embryo hearts and even in the adult offspring heart. Increased oxidative DNA damage was observed in the newborn after birth complications such as asphyxia (Millan, Pinero-Ramos et al. 2018). In pregnant diabetic women, chronic fetal hypoxia elevated levels of 8-oxodG in the amniotic fluid (Escobar, Teramo et al. 2013).

While fetal ROS generation has been suggested in some studies to be derived from mitochondria (Patterson, Xiao et al. 2012, Smith, Swiderska et al. 2022), our data clearly point to the involvement of NADPH oxidases since NADPH oxidase inhibitors diminished ROS levels in hypoxic WT embryos. In line, ROS levels and oxidative DNA damage were low in hypoxic nmf333 embryos lacking p22phox-dependent NADPH oxidases. In support, ROS generation following hypoxia was diminished in EBs treated with inhibitors of NADPH oxidases or depleted of the NADPH oxidase subunit p22phox. Interestingly, inhibitors of NADPH oxidases further decreased ROS levels in p22phox-deficient EBs pointing to either insufficient depletion of NADPH oxidases by shp22phox or additional, NADPH oxidase independent effects of the inhibitors.

Moreover, mRNA levels of p22phox, NOX1 and NOX2 were significantly upregulated in WT EBs after hypoxia but not in p22phox-deficient EBs. Importantly, mRNA levels of NOX1, NOX2, and NOX4 were increased in WT embryos following fetal hypoxia but not in nmf333 embryos.

In line, previous studies showed that hypoxia increases p22phox protein levels in vascular cells as well as in the adult lung (Zhang, Trautz et al. 2019). Upregulation of NOX1, NOX2 and NOX4 by hypoxia has also been previously reported in pulmonary artery smooth muscle cells (Diebold, Petry et al. 2010, Ghouleh, Sahoo et al. 2017).

Moreover, p22phox mRNA has been described to be already expressed at E5.5 (Baehner, Millar-Groff et al. 1999), although its function in early development has not been addressed. However, NADPH oxidases have been considered to be important sources of ROS in stem

cells (Maraldi, Angeloni et al. 2021) and have also been found in EBs differentiated to the cardiac lineage (Li, Stouffs et al. 2006).

These findings strongly indicate that upregulation of NADPH oxidases by fetal hypoxia results in increased ROS generation in the embryo as well as in hypoxic EBs leading to oxidative DNA damage persisting even into the adult heart. Further studies have to show which mechanisms underlie the sustained increase in ROS levels and upregulation of NADPH oxidases from fetal life into adulthood following fetal hypoxia.

7.2 Transient fetal hypoxia leads to persistent IUGR dependent on p22phox

Our study further showed that 24 h of hypoxia from E10.5-11.5 leads to a 25.7% reduction in embryonic mass in WT embryos at E11.5. This reduction in mass even became more severe at E17.5 with a 38% reduction in embryonic mass of WT embryos after hypoxia exposure at E10.5. In contrast, the nmf333 embryos did not suffer from statistically significant intrauterine growth restriction. Moreover, reduced body mass in response to fetal hypoxia persisted into adulthood, as adult WT mice still had a decreased body mass of 15.8% at an age of 11 weeks compared to normoxic WT mice. The effect was neither seen in fetal nor adult nmf333 offspring. These results suggest that fetal hypoxia induces IUGR with persisting effects on body mass even in adulthood which are promoted by NADPH oxidases.

Gestational hypoxia has been previously shown to lead to IUGR in rodents and humans (Keyes, Armaza et al. 2003, Mehta and Mehta 2008, Giussani, Bennet et al. 2016). Several studies in humans, mostly observing pregnancies in high altitude (Keyes, Armaza et al. 2003) or pregnancies at a high risk of gestational hypoxia because of preeclampsia (Kovo, Schreiber et al. 2015) showed intrauterine growth restriction. Observational studies in humans showed that mothers living in Tibet or Bolivia and used to staying at high altitudes develop an elevated uterine artery blood flow and are therefore partially protected against IUGR associated with high altitude (Moore, Zamudio et al. 2001, Keyes, Armaza et al. 2003, Moore 2003).

In experimental studies, there is a wide variety of protocols published differing in levels and duration of hypoxia. For example, exposure to 10% oxygen from E14-17.5 showed a mass reduction of 28% in addition to a decrease in the fronto-occipital diameters as a further parameter for growth restriction in preterm born mice (Gortner, Hilgendorff et al. 2005). While exposure to hypoxia for 12 h from E11.5-12.5 at an oxygen level of 8% did not lead to a

significant mass reduction, exposure to these conditions for 24 h resulted in a 26% reduction of body mass similar to our results (Ream, Ray et al. 2008). Similarly, while exposure to 10% oxygen from E10.5-18.5 led to a 36% reduction in the offspring mass at birth (Rueda-Clausen, Stanley et al. 2014), exposure to 12% oxygen from E14.5 until delivery led to a body mass reduction of only 12% of the newborn pups. These findings suggest that the time of onset of hypoxia, the duration of hypoxia and the amount of oxygen supplied affects the degree of IUGR in the offspring.

While hypoxia exposure from E10.5-18.5 at 10% oxygen significantly reduced the number of viable pups (Rueda-Clausen, Stanley et al. 2014), litter sizes did not differ significantly in pregnant mice exposed to 12% oxygen at E14.5 of pregnancy (Walton, Singh et al. 2016). Similarly, we could not observe significant differences in litter sizes between normoxic and hypoxic pregnancies.

Other studies show that male and female pups show decreased body mass 1 week after birth. Interestingly, at week 16, the male offspring showed a significant increase in body weight compared to the female indicating a higher risk of developing cardiometabolic diseases (Badran, Yassin et al. 2019). While these studies supported our observation of intrauterine growth restriction, our study shows a persistent decrease in body mass in male and female offspring in line with other studies (Walton, Singh et al. 2016) who could not observe gender differences.

It is noteworthy that most published studies investigated longer periods of hypoxia during pregnancy, however, our study showed that already a 24 h exposure to 10% oxygen was sufficient to lead to a mass reduction in the embryo with lasting effects into adulthood, indicating that this quite short event is sufficient to induce a permanent reduction in body mass. One could speculate that longer exposures trigger a more mature hypoxic adaptation which allows the embryo to partially compensate the IUGR.

Our study further showed that nmf333 embryos exposed to 24 h hypoxia did not suffer from intrauterine growth restriction. Similarly, adult nmf333 offspring from hypoxic pregnancies did not show decreased body mass compared to offspring from normoxic pregnancies. These results suggest that ROS derived from NADPH oxidases contribute to persistent IUGR induced by gestational hypoxia. In support of our study, IUGR has been associated with an increase in NOX2 expression in the placenta, which was connected to aberrant placental angiogenesis (Hu, Wu et al. 2021).

In fact, IUGR has been frequently associated with oxidative stress (Rashid, Bansal et al. 2018). Increased markers of oxidative stress have been found in cord blood of newborns with IUGR (Maisonneuve, Delvin et al. 2015) or in small for gestational age neonates (Gupta, Narang et al. 2004, Saker, Soulimane Mokhtari et al. 2008). Pregnancies which are complicated by preeclampsia, often leading to IUGR, have been associated with increased ROS production (Formanowicz, Malinska et al. 2019). In support of our study, treatment of mothers with IUGR pregnancies with antioxidants ameliorated not only the levels of oxidative stress markers but also of IUGR (Karowicz-Bilinska, Suzin et al. 2002), although other studies did not show effects of antioxidant treatments (Villar, Purwar et al. 2009).

As antioxidants usually do not exhibit the same efficiency in humans than in rodents for (Giussani 2021), more specific approaches are needed to suppress ROS production as for example inhibitors of NADPH oxidases. Further studies have to show whether NADPH oxidase inhibitors currently in the developmental pipeline (Elbatreek, Mucke et al. 2021) might be effective in preventing IUGR in response to hypoxic pregnancy complications.

7.3 Transient fetal hypoxia impairs cardiac development and maturation dependent on p22phox

To address the impact of fetal hypoxia on cardiopulmonary development, pregnant dams were exposed for 24 h to 10% oxygen at E10.5-11.5. This period of development represents a vulnerable phase in heart and lung development as the vascular connection between the lung bud and the developing heart evolves together with cardiac looping and the beginning of atrial and interventricular septation and early outflow tract formation (Krishnan, Samtani et al. 2014).

Morphological analysis of the WT embryonic heart showed that fetal hypoxia results in thinning of the myocardium and a decreased number of cardiomyocytes/cm^2 although the absolute area of the ventricle was enlarged pointing to decreased proliferative activity of myocardial cells. These effects were not observed in nmf333 embryos following fetal hypoxia. Accordingly, we observed that depletion of p22phox decreased proliferation of mESC by hypoxia.

Similar to our findings it was shown that exposure of embryos to 8% oxygen from E11.5 to E12.5 induced myocardial thinning as a result of reduced proliferation of cardiac cells. However, no evidence for increased apoptosis could be observed in this study (Ream, Ray et al. 2008). But as already said in the introduction, it was also shown that prenatal hypoxia can

increase proapoptotic pathways (Bae, Xiao et al. 2003, Patterson and Zhang 2010). Conclusively to this finding, in our study mRNA levels of Hsp70 were enhanced in hypoxic WT embryos, but not in nmf333 embryos. Thus, further studies have to show whether apoptosis contributes to myocardial thinning and to clarify the role of NADPH oxidases.

While these findings support the notion that increased ROS induced by fetal hypoxia would negatively affect proliferative responses of heart cells other studies indicated that a certain level of ROS enhanced proliferation of neonatal cardiomyocytes (Sauer, Rahimi et al. 2000, Buggisch, Ateghang et al. 2007). Moreover, silencing Nox1 in mESC resulted in decreased vasculogenesis in EB formation (Bekhite, Muller et al. 2016).

It was further suggested that fetal hypobaric hypoxia would result in thinning of myofibrils and a disarray of muscle fibers due to fetal hypobaric hypoxia in rats, a response which was significantly counteracted by short time reoxygenation (Shati, Zaki et al. 2022). Further studies have to show whether such a response is also present in our experimental setting.

Our observation that the ventricular area is enlarged in response to fetal hypoxia in WT but not in nmf333 embryos might be related to decreased contractility of the heart in WT embryos exposed to hypoxia. Studies in drosophila exposed to hypoxia (1% O_2 for 18 hours) showed that heart rate and contractility were suppressed (Pearson 2015). In support, it has been shown that chronic fetal hypoxia negatively affects cardiac pacemaker cell development which might contribute to fetal heart rate variability as a parameter of disrupted fetal wellbeing (Frasch and Giussani 2020, Frasch, Herry et al. 2020).

Although it is known that ROS are involved in various physiological processes in the myocardium (Perjes, Kubin et al. 2012), pharmacological inhibition of ROS production by NOX2 and NOX4 was found beneficial for contractile recovery after ischemia reperfusion (Szekeres, Walum et al. 2021). These findings support the notion that under conditions of low oxygen availability NADPH oxidases might promote cardiac dysfunction and reduce contractility which can be ameliorated by decreasing NADPH oxidase-dependent ROS generation as is the case in nmf333 mice.

Our results further showed that hypoxia exposure decreased levels of the cardiac maturation markers α-MHC and cTnT at E11.5. cTnT is a cardiomyocyte specific marker at this stage of development. It is first expressed at E7.0, and specifically expressed in the heart until E13.5 (Wang, Reiter et al. 2001) where it indicates successfully differentiated cardiomyocytes (Bin, Sheng et al. 2006). Also the expression of α-MHC as a sarcomeric protein indicates the presence of contracting and thus differentiated cardiomyocytes (Forough, Scarcello et al.

2011). Thus, the observed decrease of both cTnT and α-MHC in the post-hypoxic WT embryos suggests a delayed or otherwise disturbed differentiation and function of cardiomyocytes in WT embryos exposed to fetal hypoxia. Comparable to our in vivo results, hypoxia exposure of the neonate rat decreased levels of α-MHC (Razeghi, Essop et al. 2003).

In contrast, cardiac differentiation markers were not reduced in hypoxic nmf333 embryos further supporting the notion that increased NADPH oxidase dependent ROS generation in hypoxic embryos delays cardiac maturation and function.

This notion is further supported by studies in WT EBs where hypoxia decreased the expression of the cardiomyocyte differentiation marker Nkx2.5 and the mesodermal differentiation marker Brachyury (Chen, Kuo et al. 2010). Conclusively, hypoxic EBs deficient in p22phox were not affected.

In support, it has been previously shown that exposure to hypoxia (5% O_2) suppresses the expression of Brachyury in differentiating iPSCs (Shimomura, Inoue et al. 2022). In line, Brachyury and cTnT levels were decreased in mESC by hypoxia (1% O_2) during differentiation (Lee, Yoo et al. 2021).

Nkx2.5 is also known as an early marker of cardiogenesis besides α-MHC and β-MHC. Exposure of pregnant mice to 12% oxygen for 72 h from E15 to E18 prevented further differentiation of cardiomyocytes ex vivo under 1% oxygen but enhanced the number of Nkx2.5 positive cells (Meng, Zhang et al. 2020). In contrast, and similar to our observations, hypoxia from E10.5 to E12.5 reduced Nkx2.5 levels in fetal hearts (Ducsay, Goyal et al. 2018). While the reasons for these conflicting data are not clear, Nkx2.5 knock out mice were developmentally arrested around E10.5 because of delayed cardiac differentiation (Terada, Warren et al. 2011, Egea, Fabregat et al. 2018) thus supporting the idea that decreased Nkx2.5 expression by fetal hypoxia might contribute to delayed cardiac development.

Our study further indicates that the delay in cardiomyocyte differentiation by fetal hypoxia was mediated by p22phox-dependent NADPH oxidases, as we did not observe downregulation of cTnT and α-MHC in embryos from hypoxia exposed nmf333 mice. In line, depletion of p22phox by siRNA in EBs prevented downregulation of Nkx2.5, Brachyury and β-MHC. These findings further support the notion that ROS derived from p22phox-dependent NADPH oxidases promote the hypoxia-induced delay in cardiomyocyte differentiation and maturation.

While hypoxic conditions are physiological in utero, these findings indicate that even transient periods of non-physiological hypoxia during pregnancy might allow by induction of NADPH

oxidases an increased ROS generation leading to detrimental effects on embryonic maturation.

In contrast, under normoxic conditions, low amounts of ROS derived from NADPH oxidases have been reported to play a crucial role in embryonic cell differentiation (Ding, Liang et al. 2008, Bartsch, Bekhite et al. 2011, Bekhite, Muller et al. 2016, Kim, Kim et al. 2022). ROS have also been described to be important for EB formation (Sauer, Rahimi et al. 2000). Induction of NOX1 or NOX4 promoted the initiation of cardiovascular differentiation (Sauer, Ruhe et al. 2008) while NOX4 knock out iPSC lines were delayed in differentiation (Kim, Kim et al. 2022). A significant inhibition of cardiomyogenesis was seen by Bartsch et. al, caused by the downregulation of NOX4 by short hairpin RNA (shRNA) which abolished the stimulation of β-MHC and MLC2v gene expression (Bartsch, Bekhite et al. 2011). Suppression of cardiogenesis could also be seen by the application of ROS scavengers to mESC (Li, Stouffs et al. 2006).

In contrast, in our study depletion of p22phox or treatment with antioxidants did not affect cardiac maturation in EBs under normoxic conditions. Furthermore, we did not observe a difference in cardiac differentiation between WT and nmf333 embryos under normoxic conditions. While the reasons for these conflicting data are not known to date, they might relate to different experimental conditions and species related differences.

7.4 Transient fetal hypoxia impairs lung maturation dependent on p22phox

Our studies further showed that transient fetal hypoxia also affected lung development. In fact, we saw significant structural differences in the lungs between WT normoxic and hypoxic embryos. WT normoxic embryos showed the typical histology of the canalicular stage with bronchioles and partially formed air sacs and alveolar ducts. WT embryos exposed to transient fetal hypoxia did not progress in the same way and still were in the pseudoglandular stage defined by epithelial tubes surrounded by thick mesenchyme. They showed disorganized cells in the lung and a lower amount of fully developed acini. However, lungs from nmf333 E17.5 embryos exposed to fetal hypoxia were not different to normoxic WT lungs suggesting that ROS derived from NADPH oxidases delay lung maturation in response to fetal hypoxia (Ten Have-Opbroek 1991, deMello, Sawyer et al. 1997, Hislop 2005, Roy, Rahmani et al. 2011).

Moreover, alveolar septae were thickened in the adult lung from offspring exposed to fetal hypoxia, and an increased amount of small muscularized pulmonary vessels indicating pulmonary hypertension was observed. In contrast, these alterations were not observed in nmf333 mice.

In line, intrauterine hypoxia has been associated with defects in lung development which affected alveolarization, gas exchange, and blood vessel growth, and was characterized by reduced proliferation of airway smooth muscle cells, inflammation and increased airway smooth muscle thickness (Tong, Zhang et al. 2021). Moreover, it was shown that hypoxia exposure of newborn mice inhibits alveolar development and causes pulmonary arterial remodeling (Nicola, Ambalavanan et al. 2011).

Preterm infants which often undergo intermittent hypoxemic episodes have been described to show signs of damaged lung endothelial cells together with mitochondrial DNA damage. This might contribute to impairment of growth and maturation of pulmonary vessels and to the development of PH in the adult (Damianos, Kulandavelu et al. 2022).

Furthermore, it has been suggested that increased ROS in response to fetal hypoxia would contribute to delayed lung maturation although in vivo proof of principle studies are scarce (Tong, Zhang et al. 2021).

Interestingly, it was reported that chronic hypoxia reduced NOX4 mRNA levels in fetal lambs while it induced expression of antioxidant genes (McGillick, Orgeig et al. 2017). Other studies showed that NOX4 can be induced by hypoxia in pulmonary artery smooth muscle cells (Ismail, Sturrock et al. 2009, Diebold, Petry et al. 2010). Although the reasons for these conflicting data are not clear to date, they might relate to the length of hypoxic exposure and to species specific responses.

At the molecular level, we could show that fetal hypoxia reduced surfactant A expression in WT lungs at E17.5, but not in nmf333 lungs. In line, the number of PAS positive alveolar cells which are not yet able to produce surfactant (Roy, Rahmani et al. 2011) was increased in lungs from hypoxic WT embryos but not from hypoxic nmf333 embryos indicating that NADPH oxidases mediate decreased surfactant levels in response to transient fetal hypoxia.

In support, fetal hypoxia has been shown to downregulate surfactant proteins (Gortner, Hilgendorff et al. 2005, Saini, Harkema et al. 2008, Sardesai, Biniwale et al. 2017). For example, 72 hours of hypoxia from E14 to E17 (Gortner, Hilgendorff et al. 2005), but also 24 h of hypoxia at 10% oxygen from E16.5-17.5 (Tsao and Wei 2013) led to decreased surfactant

protein levels. In humans, decreased surfactant production is a frequent complication especially of preterm delivery associated with IUGR but has also been related respiratory distress syndrome in the newborn associated with intrauterine hypoxia (Compernolle, Brusselmans et al. 2002).

Interestingly, surfactant A levels remained reduced in lungs from WT adult offspring exposed to fetal hypoxia while NADPH oxidase expression was increased similar to the situation when adult mice were exposed to chronic hypoxia. However, surfactant A levels remained unchanged in lungs from nmf333 mice under these conditions.

While short term hypoxia exposure during adulthood has been reported to enhance surfactant protein A expression in rat lungs (Tripathi, Kumar et al. 2021), hypoxia decreased surfactant levels in cell culture (Ito, Ahmad et al. 2011), and surfactant levels were negatively correlated with sleep apnea (Lu, Abulimiti et al. 2018), a disorder which is associated with intermittent hypoxia and possibly pulmonary hypertension. However, while decreased surfactant levels are clearly associated with pulmonary hypertension of the newborn, their impact on the pathogenesis of adult PH still requires further studies (Konduri and Lakshminrusimha 2021).

Although we did not determine ROS levels in the fetal and adult lungs, the findings that NADPH oxidase expression was increased in lungs post-hypoxia and nmf333 mice were protected against the hypoxia-induced reduction in surfactant A levels points to a role of NADPH oxidases and ROS in this response. In line, ROS induced by toxic silica nanoparticles have been shown to decrease the levels of surfactant proteins A and B (Yang, Yang et al. 2022) although the sources of ROS have not been investigated.

Therapeutically, synthetic and animal-derived surfactants (bovine or porcine) are under investigation to support faster weaning of newborns with PH from ventilatory support and to decrease mortality (Sardesai, Biniwale et al. 2017). Our findings that p22phox-dependent NADPH oxidases might contribute to decreased surfactant production suggest them as an interesting new therapeutic target in conditions of low surfactant levels.

7.5 Transient fetal hypoxia leads to signs of pulmonary hypertension dependent on p22phox

In this study, we could show that adult wildtype animals challenged by transient fetal hypoxia for 24 h from E10.5 to E11.5 developed signs of pulmonary hypertension in adulthood including

increased RVP, right ventricular hypertrophy and pulmonary vascular remodelling as well as thickening of the alveolar septae which can develop as a consequence of elevated pressure in the lung (Hopkins and McLoughlin 2002). In contrast, nmf333 mice were protected. Furthermore, levels of β-MHC, a well-known remodelling marker in the adult heart (Cox and Marsh 2014), were not only increased in the fetal heart, but also in the adult right ventricle of WT, but not of nmf333 mice, indicating fetal programming of cardiac remodelling which was promoted by NADPH oxidases.

This response was similar to the adult response to chronic hypoxia challenge, a known condition to induce pulmonary hypertension. Under these conditions loss of p22phox or NOX2 has been shown to protect against the development of PH (Liu, Zelko et al. 2006, Nisbet, Graves et al. 2009, Zhang, Trautz et al. 2019).

In line, pulmonary-artery pressure responses to high-altitude exposure have been shown to be more pronounced in young adults previously suffering from transient perinatal hypoxic pulmonary hypertension suggesting that a perinatal hypoxic insult would enhance the susceptibility to hypoxia induced PH later in life (Sartori, Allemann et al. 1999). However, in our study exposure of offspring from hypoxic pregnancies to chronic hypoxia in adulthood did not further increase the signs of PH indicating that fetal and adult-onset hypoxia did not act additively to induce PH.

While we could show that fetal hypoxia for one day was sufficient to induce PH in adulthood, other studies could show programming of PH in the offspring only after prolonged periods of fetal hypoxia (Papamatheakis, Blood et al. 2013).

For example, adult mice which were exposed to hypoxia from E14.5 to postnatal day 4 developed increased RVP, RV hypertrophy and increased pulmonary vascular resistance (Mundo et al., 2021). Similarly, exposure of rats to high altitude during entire pregnancy resulted in the development of PH in the offspring (Krishnan, Stearman et al. 2020). In addition, newborn sheep from high altitude pregnancies developed PH (Kamitomo, Longo et al. 1992, Herrera, Riquelme et al. 2010, Blood, Terry et al. 2013).

In line with these experimental data, young offspring of mothers with preeclampsia displayed marked vascular dysfunction in the pulmonary circulation, as evidenced by a roughly 30% higher pulmonary artery pressure, but also signs of systemic vascular dysfunction as indicated by a 30% smaller FMD of the brachial artery than in control subjects (Jayet, Rimoldi et al. 2010, von Ehr and von Versen-Hoynck 2016). Similarly, exposure to gestational hypoxia for 6 days (E15-21) resulted in cardiac diastolic dysfunction and aortic stiffness in adult mice (Kumar,

Morton et al. 2020). Cardiac impairment following chronic fetal hypoxia has also been described in large mammals like sheep (Giussani, Camm et al. 2012, Giussani, Niu et al. 2014). Another study reported that fetal hypoxia from E15 to E21 not only resulted in the development of PH by 12 months of age, but also in LV diastolic dysfunction (Rueda-Clausen, Morton et al. 2009, Aljunaidy, Morton et al. 2018).

In contrast, in our study, mean LV pressure was not significantly changed in any of the groups, while these findings indicate that PH did not develop secondary to left ventricular dysfunction, the reasons for the conflicting data still need to be elucidated but might relate to time and duration of fetal hypoxia.

In support of our study, however, offspring from preeclamptic pregnancies showed in addition to increased pulmonary arterial pressure increased levels of thiobarbituric acid-reactive substances as an indicator of lipid peroxidation in the blood suggesting oxidative stress (Jayet, Rimoldi et al. 2010). ROS have also been suggested to play a role in fetal programming of other cardiac and renal dysfunctions. There is an excellent review by Rodriguez-Rodriguez et. al about the role of oxidative stress in fetal programming (Rodriguez-Rodriguez, Ramiro-Cortijo et al. 2018). For example, treatment with vitamin C or melatonin reversed the increased vasoconstrictor response and increased umbilical blood flow observed in animal pregnancies affected by hypoxia (Thakor, Richter et al. 2010). Comparable effects were also observed with a xanthine oxidase inhibitor (allopurinol) (Kane, Hansell et al. 2014). Antioxidant treatments also prevented renal or cardiovascular damage in response to placental insufficiency or to malnutrition during fetal development (Elmes, Gardner et al. 2007, Luzardo, Silva et al. 2011, Rexhaj, Bloch et al. 2011). Furthermore, cardiac hypertrophy in response to nutrient restriction during fetal development was associated with increased NADPH oxidase expression in the heart prior to the development of hypertension (Rodriguez-Rodriguez, Lopez de Pablo et al. 2017).

The above-mentioned findings in have encouraged clinical trials exploring the possible benefits of antioxidative therapy in high risk human pregnancies (Rodriguez-Rodriguez, Ramiro-Cortijo et al. 2018). Unfortunately, the results were not as comparable as expected. Some studies not only failed to demonstrate improved pregnancy or fetal outcomes but even resulted in increased rates of complications (Morton and Brodsky 2016). This antioxidant paradox has been accounted for by means of various facts (Halliwell 2013). Firstly, laboratory animals seem to be more susceptible to antioxidative supplements than humans. Secondly, some antioxidants like polyphenols and ascorbate could lead to pro-oxidant effects under certain circumstances, related to the presence of transition metals. Thirdly, many clinical trials with

antioxidative supplements have not evaluated the baseline nutritional status (Halliwell 2013, Rodriguez-Rodriguez, Ramiro-Cortijo et al. 2018). However, although inhibitors of NADPH oxidases are in development, these substances have not been studied yet extensively in the context of fetal programming (Cifuentes-Pagano, Meijles et al. 2015, Zielonka, Zielonka et al. 2019, Treuer, Faundez et al. 2023).

Overall, our study shows new insights that transient fetal hypoxia promotes the development of pulmonary hypertension in the adult offspring in WT mice. The functional loss of p22phox and therefore lower ROS production by NADPH oxidases is a preventive factor, making it an interesting new target to prevent the pathological consequences of fetal hypoxia.

7.6 Limitations of the study

Overall, our study gave new insights about the detrimental effects of ROS produced by NADPH oxidases induced by transient fetal hypoxia on cardiopulmonary development and their impact on programming of pulmonary hypertension in the adult offspring. Next, it would be of a high interest to explore the epigenetic programming and regulations due to transient fetal hypoxia. For example, miRNA sequencing should be performed to identify possible ROS regulated miRNAs as potential therapeutic targets.

Furthermore, there are a number of studies that also show alterations in the placenta after transient fetal hypoxia. It would be of interest to see whether the protective effects seen in the nmf333 mice are partly caused by better umbilical blood flow and less placental malformations in nmf333 mice.

Furthermore, expression analyses were performed in tissues derived from whole embryos leaving the possibility that expression of cardiac markers and NADPH oxidases as well as ROS levels were not dysregulated in the fetal heart but in other organs and structures. Further analyses should aim to directly analyse expression levels and ROS generation in the isolated fetal heart at E11.5.

Another interesting parameter in our study which was not evaluated is the mortality rate after transient fetal hypoxia. As we showed, surfactant levels were significantly decreased in WT embryos after transient fetal hypoxia exposure, but not in the adult offspring. As it is known that a lack of surfactant can lead to RDS in the newborn (Sardesai, Biniwale et al. 2017), it

would be interesting to monitor the mortality rate of the newborn, especially in the WT group which was exposed to transient fetal hypoxia.

To evaluate cardiac dysfunction in more detail in offspring mice, echocardiography would have been a valuable addition.

Furthermore, our study was focussed on the effects of fetal hypoxia on heart and lungs. Further studies are required to study in the impact of fetal hypoxia and NADPH oxidases on other organ systems.

8 Conclusion

The findings of this study clearly show that transient fetal hypoxia affects cardiac and pulmonary development and promotes the development of PH in adulthood. Mechanistically, this study points to a role of ROS derived from p22phox-dependent NADPH oxidases in mediating fetal programming of PH. Targeting NADPH oxidases in pregnancies complicated by fetal hypoxia might be a promising approach to prevent the development of PH in the adult offspring.

9 References

Agarwal, A., A. Aponte-Mellado, B. J. Premkumar, A. Shaman and S. Gupta (2012). "The effects of oxidative stress on female reproduction: a review." Reprod Biol Endocrinol **10**: 49.

Ago, T., T. Kitazono, J. Kuroda, Y. Kumai, M. Kamouchi, H. Ooboshi, M. Wakisaka, T. Kawahara, K. Rokutan, S. Ibayashi and M. Iida (2005). "NAD(P)H oxidases in rat basilar arterial endothelial cells." Stroke **36**(5): 1040-1046.

Aljunaidy, M. M., J. S. Morton, R. Kirschenman, T. Phillips, C. P. Case, C. M. Cooke and S. T. Davidge (2018). "Maternal treatment with a placental-targeted antioxidant (MitoQ) impacts offspring cardiovascular function in a rat model of prenatal hypoxia." Pharmacol Res **134**: 332-342.

Badran, M., B. A. Yassin, D. T. S. Lin, M. S. Kobor, N. Ayas and I. Laher (2019). "Gestational intermittent hypoxia induces endothelial dysfunction, reduces perivascular adiponectin and causes epigenetic changes in adult male offspring." J Physiol **597**(22): 5349-5364.

Bae, S., Y. Xiao, G. Li, C. A. Casiano and L. Zhang (2003). "Effect of maternal chronic hypoxic exposure during gestation on apoptosis in fetal rat heart." Am J Physiol Heart Circ Physiol **285**(3): H983-990.

Baehner, R. L., S. Millar-Groff and P. Bringas (1999). "Developmental expression of NADPH phagocytic oxidase components in mouse embryos." Pediatr Res **46**(2): 152-157.

Banfi, B., A. Maturana, S. Jaconi, S. Arnaudeau, T. Laforge, B. Sinha, E. Ligeti, N. Demaurex and K. H. Krause (2000). "A mammalian H+ channel generated through alternative splicing of the NADPH oxidase homolog NOH-1." Science **287**(5450): 138-142.

Banfi, B., F. Tirone, I. Durussel, J. Knisz, P. Moskwa, G. Z. Molnar, K. H. Krause and J. A. Cox (2004). "Mechanism of Ca2+ activation of the NADPH oxidase 5 (NOX5)." J Biol Chem **279**(18): 18583-18591.

Barbosky, L., D. K. Lawrence, G. Karunamuni, J. C. Wikenheiser, Y. Q. Doughman, R. P. Visconti, J. B. Burch and M. Watanabe (2006). "Apoptosis in the developing mouse heart." Dev Dyn **235**(9): 2592-2602.

Bartsch, C., M. M. Bekhite, A. Wolheim, M. Richter, C. Ruhe, B. Wissuwa, A. Marciniak, J. Muller, R. Heller, H. R. Figulla, H. Sauer and M. Wartenberg (2011). "NADPH oxidase and eNOS control cardiomyogenesis in mouse embryonic stem cells on ascorbic acid treatment." Free Radic Biol Med **51**(2): 432-443.

Bedard, K. and K. H. Krause (2007). "The NOX family of ROS-generating NADPH oxidases: physiology and pathophysiology." Physiol Rev **87**(1): 245-313.

Behringer, R., M. Gertsenstein, K. V. Nagy and A. Nagy (2016). "Differentiating Mouse Embryonic Stem Cells into Embryoid Bodies by Hanging-Drop Cultures." Cold Spring Harb Protoc **2016**(12).

Bekhite, M. M., V. Muller, S. H. Troger, J. P. Muller, H. R. Figulla, H. Sauer and M. Wartenberg (2016). "Involvement of phosphoinositide 3-kinase class IA (PI3K 110alpha) and NADPH oxidase 1 (NOX1) in regulation of vascular differentiation induced by vascular endothelial growth factor (VEGF) in mouse embryonic stem cells." Cell Tissue Res **364**(1): 159-174.

Bin, Z., L. G. Sheng, Z. C. Gang, J. Hong, C. Jun, Y. Bo and S. Hui (2006). "Efficient cardiomyocyte differentiation of embryonic stem cells by bone morphogenetic protein-2 combined with visceral endoderm-like cells." Cell Biol Int **30**(10): 769-776.

Blood, A. B., M. H. Terry, T. A. Merritt, D. G. Papamatheakis, Q. Blood, J. M. Ross, G. G. Power, L. D. Longo and S. M. Wilson (2013). "Effect of chronic perinatal hypoxia on the role of rho-kinase in pulmonary artery contraction in newborn lambs." Am J Physiol Regul Integr Comp Physiol **304**(2): R136-146.

Brain, K. L., B. J. Allison, Y. Niu, C. M. Cross, N. Itani, A. D. Kane, E. A. Herrera, K. L. Skeffington, K. J. Botting and D. A. Giussani (2019). "Intervention against hypertension in the next generation programmed by developmental hypoxia." PLoS Biol **17**(1): e2006552.

Browne, V. A., C. G. Julian, L. Toledo-Jaldin, D. Cioffi-Ragan, E. Vargas and L. G. Moore (2015). "Uterine artery blood flow, fetal hypoxia and fetal growth." Philos Trans R Soc Lond B Biol Sci **370**(1663): 20140068.
Bueno-Beti, C., L. Hadri, R. J. Hajjar and Y. Sassi (2018). "The Sugen 5416/Hypoxia Mouse Model of Pulmonary Arterial Hypertension." Methods Mol Biol **1816**: 243-252.
Buggisch, M., B. Ateghang, C. Ruhe, C. Strobel, S. Lange, M. Wartenberg and H. Sauer (2007). "Stimulation of ES-cell-derived cardiomyogenesis and neonatal cardiac cell proliferation by reactive oxygen species and NADPH oxidase." J Cell Sci **120**(Pt 5): 885-894.
Buvelot, H., V. Jaquet and K. H. Krause (2019). "Mammalian NADPH Oxidases." Methods Mol Biol **1982**: 17-36.
Buvelot, H., K. M. Posfay-Barbe, P. Linder, J. Schrenzel and K. H. Krause (2017). "Staphylococcus aureus, phagocyte NADPH oxidase and chronic granulomatous disease." FEMS Microbiol Rev **41**(2): 139-157.
Cabiscol, E., J. Tamarit and J. Ros (2000). "Oxidative stress in bacteria and protein damage by reactive oxygen species." Int Microbiol **3**(1): 3-8.
Cahill, L. S., Y. Q. Zhou, M. Seed, C. K. Macgowan and J. G. Sled (2014). "Brain sparing in fetal mice: BOLD MRI and Doppler ultrasound show blood redistribution during hypoxia." J Cereb Blood Flow Metab **34**(6): 1082-1088.
Chao, C. M., E. El Agha, C. Tiozzo, P. Minoo and S. Bellusci (2015). "A breath of fresh air on the mesenchyme: impact of impaired mesenchymal development on the pathogenesis of bronchopulmonary dysplasia." Front Med (Lausanne) **2**: 27.
Chen, H. F., H. C. Kuo, S. P. Lin, C. L. Chien, M. S. Chiang and H. N. Ho (2010). "Hypoxic culture maintains self-renewal and enhances embryoid body formation of human embryonic stem cells." Tissue Eng Part A **16**(9): 2901-2913.
Chen, X., L. Zhang and C. Wang (2019). "Prenatal hypoxia-induced epigenomic and transcriptomic reprogramming in rat fetal and adult offspring hearts." Sci Data **6**(1): 238.
Chu, A., D. Gozal, R. Cortese and Y. Wang (2015). "Cardiovascular dysfunction in adult mice following postnatal intermittent hypoxia." Pediatr Res **77**(3): 425-433.
Cifuentes-Pagano, M. E., D. N. Meijles and P. J. Pagano (2015). "Nox Inhibitors & Therapies: Rational Design of Peptidic and Small Molecule Inhibitors." Curr Pharm Des **21**(41): 6023-6035.
Colston, J. T., S. D. de la Rosa, J. R. Strader, M. A. Anderson and G. L. Freeman (2005). "H2O2 activates Nox4 through PLA2-dependent arachidonic acid production in adult cardiac fibroblasts." FEBS Lett **579**(11): 2533-2540.
Colvin, K. L. and M. E. Yeager (2014). "Animal Models of Pulmonary Hypertension: Matching Disease Mechanisms to Etiology of the Human Disease." J Pulm Respir Med **4**(4).
Compernolle, V., K. Brusselmans, T. Acker, P. Hoet, M. Tjwa, H. Beck, S. Plaisance, Y. Dor, E. Keshet, F. Lupu, B. Nemery, M. Dewerchin, P. Van Veldhoven, K. Plate, L. Moons, D. Collen and P. Carmeliet (2002). "Loss of HIF-2alpha and inhibition of VEGF impair fetal lung maturation, whereas treatment with VEGF prevents fatal respiratory distress in premature mice." Nat Med **8**(7): 702-710.
Compernolle, V., K. Brusselmans, D. Franco, A. Moorman, M. Dewerchin, D. Collen and P. Carmeliet (2003). "Cardia bifida, defective heart development and abnormal neural crest migration in embryos lacking hypoxia-inducible factor-1alpha." Cardiovasc Res **60**(3): 569-579.
Correa, A., D. M. Levis, S. C. Tinker and J. D. Cragan (2015). "Maternal cigarette smoking and congenital heart defects." J Pediatr **166**(4): 801-804.
Cox, E. J. and S. A. Marsh (2014). "A systematic review of fetal genes as biomarkers of cardiac hypertrophy in rodent models of diabetes." PLoS One **9**(3): e92903.
Damianos, A., S. Kulandavelu, P. Chen, P. Nwajei, S. Batlahally, M. Sharma, S. Alvarez-Cubela, J. Dominguez-Bendala, R. Zambrano, J. Huang, J. M. Hare, A. Schmidt, S. Wu, M. Benny, N. Claure and K. Young (2022). "Neonatal intermittent hypoxia persistently impairs lung

vascular development and induces long-term lung mitochondrial DNA damage." J Appl Physiol (1985) **133**(5): 1031-1041.
Davie, N., S. J. Haleen, P. D. Upton, J. M. Polak, M. H. Yacoub, N. W. Morrell and J. Wharton (2002). "ET(A) and ET(B) receptors modulate the proliferation of human pulmonary artery smooth muscle cells." Am J Respir Crit Care Med **165**(3): 398-405.
De Deken, X., D. Wang, M. C. Many, S. Costagliola, F. Libert, G. Vassart, J. E. Dumont and F. Miot (2000). "Cloning of two human thyroid cDNAs encoding new members of the NADPH oxidase family." J Biol Chem **275**(30): 23227-23233.
deMello, D. E., D. Sawyer, N. Galvin and L. M. Reid (1997). "Early fetal development of lung vasculature." Am J Respir Cell Mol Biol **16**(5): 568-581.
Di Minno, A., L. Turnu, B. Porro, I. Squellerio, V. Cavalca, E. Tremoli and M. N. Di Minno (2016). "8-Hydroxy-2-Deoxyguanosine Levels and Cardiovascular Disease: A Systematic Review and Meta-Analysis of the Literature." Antioxid Redox Signal **24**(10): 548-555.
Diebold, I., A. Petry, J. Hess and A. Gorlach (2010). "The NADPH oxidase subunit NOX4 is a new target gene of the hypoxia-inducible factor-1." Mol Biol Cell **21**(12): 2087-2096.
Ding, L., X. G. Liang, Y. Hu, D. Y. Zhu and Y. J. Lou (2008). "Involvement of p38MAPK and reactive oxygen species in icariin-induced cardiomyocyte differentiation of murine embryonic stem cells in vitro." Stem Cells Dev **17**(4): 751-760.
Dodson, M. W., L. M. Brown and C. G. Elliott (2018). "Pulmonary Arterial Hypertension." Heart Fail Clin **14**(3): 255-269.
Drager, L. F., J. C. Jun and V. Y. Polotsky (2010). "Metabolic consequences of intermittent hypoxia: relevance to obstructive sleep apnea." Best Pract Res Clin Endocrinol Metab **24**(5): 843-851.
Dschietzig, T., C. Richter, C. Bartsch, C. Bohme, D. Heinze, F. Ott, F. Zartnack, G. Baumann and K. Stangl (2001). "Flow-induced pressure differentially regulates endothelin-1, urotensin II, adrenomedullin, and relaxin in pulmonary vascular endothelium." Biochem Biophys Res Commun **289**(1): 245-251.
Ducsay, C. A., R. Goyal, W. J. Pearce, S. Wilson, X. Q. Hu and L. Zhang (2018). "Gestational Hypoxia and Developmental Plasticity." Physiol Rev **98**(3): 1241-1334.
Dunlap, B. and G. Weyer (2016). "Pulmonary Hypertension: Diagnosis and Treatment." Am Fam Physician **94**(6): 463-469.
Egea, J., I. Fabregat, Y. M. Frapart, P. Ghezzi, A. Gorlach, T. Kietzmann, K. Kubaichuk, U. G. Knaus, M. G. Lopez, G. Olaso-Gonzalez, A. Petry, R. Schulz, J. Vina, P. Winyard, K. Abbas, O. S. Ademowo, C. B. Afonso, I. Andreadou, H. Antelmann, F. Antunes, M. Aslan, M. M. Bachschmid, R. M. Barbosa, V. Belousov, C. Berndt, D. Bernlohr, E. Bertran, A. Bindoli, S. P. Bottari, P. M. Brito, G. Carrara, A. I. Casas, A. Chatzi, N. Chondrogianni, M. Conrad, M. S. Cooke, J. G. Costa, A. Cuadrado, P. My-Chan Dang, B. De Smet, B. Debelec-Butuner, I. H. K. Dias, J. D. Dunn, A. J. Edson, M. El Assar, J. El-Benna, P. Ferdinandy, A. S. Fernandes, K. E. Fladmark, U. Forstermann, R. Giniatullin, Z. Giricz, A. Gorbe, H. Griffiths, V. Hampl, A. Hanf, J. Herget, P. Hernansanz-Agustin, M. Hillion, J. Huang, S. Ilikay, P. Jansen-Durr, V. Jaquet, J. A. Joles, B. Kalyanaraman, D. Kaminskyy, M. Karbaschi, M. Kleanthous, L. O. Klotz, B. Korac, K. S. Korkmaz, R. Koziel, D. Kracun, K. H. Krause, V. Kren, T. Krieg, J. Laranjinha, A. Lazou, H. Li, A. Martinez-Ruiz, R. Matsui, G. J. McBean, S. P. Meredith, J. Messens, V. Miguel, Y. Mikhed, I. Milisav, L. Milkovic, A. Miranda-Vizuete, M. Mojovic, M. Monsalve, P. A. Mouthuy, J. Mulvey, T. Munzel, V. Muzykantov, I. T. N. Nguyen, M. Oelze, N. G. Oliveira, C. M. Palmeira, N. Papaevgeniou, A. Pavicevic, B. Pedre, F. Peyrot, M. Phylactides, G. G. Pircalabioru, A. R. Pitt, H. E. Poulsen, I. Prieto, M. P. Rigobello, N. Robledinos-Anton, L. Rodriguez-Manas, A. P. Rolo, F. Rousset, T. Ruskovska, N. Saraiva, S. Sasson, K. Schroder, K. Semen, T. Seredenina, A. Shakirzyanova, G. L. Smith, T. Soldati, B. C. Sousa, C. M. Spickett, A. Stancic, M. J. Stasia, H. Steinbrenner, V. Stepanic, S. Steven, K. Tokatlidis, E. Tuncay, B. Turan, F. Ursini, J. Vacek, O. Vajnerova, K. Valentova, F. Van Breusegem, L. Varisli, E. A. Veal, A. S. Yalcin, O. Yelisyeyeva, N. Zarkovic, M. Zatloukalova, J. Zielonka, R. M. Touyz, A. Papapetropoulos, T. Grune, S. Lamas, H. Schmidt, F. Di Lisa and A. Daiber (2018).

"Corrigendum to "European contribution to the study of ROS: A summary of the findings and prospects for the future from the COST action BM1203 (EU-ROS)" [Redox Biol. 13 (2017) 94-162]." Redox Biol **14**: 694-696.
Elbatreek, M. H., H. Mucke and H. Schmidt (2021). "NOX Inhibitors: From Bench to Naxibs to Bedside." Handb Exp Pharmacol **264**: 145-168.
Ellmark, S. H., G. J. Dusting, M. N. Fui, N. Guzzo-Pernell and G. R. Drummond (2005). "The contribution of Nox4 to NADPH oxidase activity in mouse vascular smooth muscle." Cardiovasc Res **65**(2): 495-504.
Elmes, M. J., D. S. Gardner and S. C. Langley-Evans (2007). "Fetal exposure to a maternal low-protein diet is associated with altered left ventricular pressure response to ischaemia-reperfusion injury." Br J Nutr **98**(1): 93-100.
Escobar, J., K. Teramo, V. Stefanovic, S. Andersson, M. A. Asensi, A. Arduini, E. Cubells, J. Sastre and M. Vento (2013). "Amniotic fluid oxidative and nitrosative stress biomarkers correlate with fetal chronic hypoxia in diabetic pregnancies." Neonatology **103**(3): 193-198.
Fischer, H. (2009). "Mechanisms and function of DUOX in epithelia of the lung." Antioxid Redox Signal **11**(10): 2453-2465.
Formanowicz, D., A. Malinska, M. Nowicki, K. Kowalska, K. Gruca-Stryjak, G. Breborowicz and K. Korybalska (2019). "Preeclampsia with Intrauterine Growth Restriction Generates Morphological Changes in Endothelial Cells Associated with Mitochondrial Swelling-An In Vitro Study." J Clin Med **8**(11).
Forough, R., C. Scarcello and M. Perkins (2011). "Cardiac biomarkers: a focus on cardiac regeneration." J Tehran Heart Cent **6**(4): 179-186.
Frank, H., J. Mlczoch, K. Huber, E. Schuster, H. P. Gurtner and M. Kneussl (1997). "The effect of anticoagulant therapy in primary and anorectic drug-induced pulmonary hypertension." Chest **112**(3): 714-721.
Frasch, M. G. and D. A. Giussani (2020). "Impact of Chronic Fetal Hypoxia and Inflammation on Cardiac Pacemaker Cell Development." Cells **9**(3).
Frasch, M. G., C. L. Herry, Y. Niu and D. A. Giussani (2020). "First evidence that intrinsic fetal heart rate variability exists and is affected by hypoxic pregnancy." J Physiol **598**(2): 249-263.
Galie, N., M. Humbert, J. L. Vachiery, S. Gibbs, I. Lang, A. Torbicki, G. Simonneau, A. Peacock, A. Vonk Noordegraaf, M. Beghetti, A. Ghofrani, M. A. Gomez Sanchez, G. Hansmann, W. Klepetko, P. Lancellotti, M. Matucci, T. McDonagh, L. A. Pierard, P. T. Trindade, M. Zompatori and M. Hoeper (2015). "2015 ESC/ERS Guidelines for the diagnosis and treatment of pulmonary hypertension: The Joint Task Force for the Diagnosis and Treatment of Pulmonary Hypertension of the European Society of Cardiology (ESC) and the European Respiratory Society (ERS): Endorsed by: Association for European Paediatric and Congenital Cardiology (AEPC), International Society for Heart and Lung Transplantation (ISHLT)." Eur Respir J **46**(4): 903-975.
Galie, N., M. Humbert, J. L. Vachiery, S. Gibbs, I. Lang, A. Torbicki, G. Simonneau, A. Peacock, A. Vonk Noordegraaf, M. Beghetti, A. Ghofrani, M. A. Gomez Sanchez, G. Hansmann, W. Klepetko, P. Lancellotti, M. Matucci, T. McDonagh, L. A. Pierard, P. T. Trindade, M. Zompatori and M. Hoeper (2016). "2015 ESC/ERS Guidelines for the Diagnosis and Treatment of Pulmonary Hypertension." Rev Esp Cardiol (Engl Ed) **69**(2): 177.
Geiszt, M., J. B. Kopp, P. Varnai and T. L. Leto (2000). "Identification of renox, an NAD(P)H oxidase in kidney." Proc Natl Acad Sci U S A **97**(14): 8010-8014.
Ghouleh, I. A., S. Sahoo, D. N. Meijles, J. H. Amaral, D. S. de Jesus, J. Sembrat, M. Rojas, D. A. Goncharov, E. A. Goncharova and P. J. Pagano (2017). "Endothelial Nox1 oxidase assembly in human pulmonary arterial hypertension; driver of Gremlin1-mediated proliferation." Clin Sci (Lond) **131**(15): 2019-2035.
Gittenberger-de Groot, A. C., M. M. Bartelings, R. E. Poelmann, M. C. Haak and M. R. Jongbloed (2013). "Embryology of the heart and its impact on understanding fetal and neonatal heart disease." Semin Fetal Neonatal Med **18**(5): 237-244.

Giussani, D. A. (2021). "Breath of Life: Heart Disease Link to Developmental Hypoxia." Circulation **144**(17): 1429-1443.
Giussani, D. A., L. Bennet, A. N. Sferruzzi-Perri, O. R. Vaughan and A. L. Fowden (2016). "Hypoxia, fetal and neonatal physiology: 100 years on from Sir Joseph Barcroft." J Physiol **594**(5): 1105-1111.
Giussani, D. A., E. J. Camm, Y. Niu, H. G. Richter, C. E. Blanco, R. Gottschalk, E. Z. Blake, K. A. Horder, A. S. Thakor, J. A. Hansell, A. D. Kane, F. B. Wooding, C. M. Cross and E. A. Herrera (2012). "Developmental programming of cardiovascular dysfunction by prenatal hypoxia and oxidative stress." PLoS One **7**(2): e31017.
Giussani, D. A., Y. Niu, E. A. Herrera, H. G. Richter, E. J. Camm, A. S. Thakor, A. D. Kane, J. A. Hansell, K. L. Brain, K. L. Skeffington, N. Itani, F. B. Wooding, C. M. Cross and B. J. Allison (2014). "Heart disease link to fetal hypoxia and oxidative stress." Adv Exp Med Biol **814**: 77-87.
Gortner, L., A. Hilgendorff, T. Bahner, M. Ebsen, I. Reiss and S. Rudloff (2005). "Hypoxia-induced intrauterine growth retardation: effects on pulmonary development and surfactant protein transcription." Biol Neonate **88**(2): 129-135.
Gupta, P., M. Narang, B. D. Banerjee and S. Basu (2004). "Oxidative stress in term small for gestational age neonates born to undernourished mothers: a case control study." BMC Pediatr **4**: 14.
Halliwell, B. (2013). "The antioxidant paradox: less paradoxical now?" Br J Clin Pharmacol **75**(3): 637-644.
Herrera, E. A., R. A. Riquelme, G. Ebensperger, R. V. Reyes, C. E. Ulloa, G. Cabello, B. J. Krause, J. T. Parer, D. A. Giussani and A. J. Llanos (2010). "Long-term exposure to high-altitude chronic hypoxia during gestation induces neonatal pulmonary hypertension at sea level." Am J Physiol Regul Integr Comp Physiol **299**(6): R1676-1684.
Herriges, M. and E. E. Morrisey (2014). "Lung development: orchestrating the generation and regeneration of a complex organ." Development **141**(3): 502-513.
Hislop, A. (2005). "Developmental biology of the pulmonary circulation." Paediatr Respir Rev **6**(1): 35-43.
Hoeper, M. M., H. A. Ghofrani, E. Grunig, H. Klose, H. Olschewski and S. Rosenkranz (2017). "Pulmonary Hypertension." Dtsch Arztebl Int **114**(5): 73-84.
Hong, K. H., Y. J. Lee, E. Lee, S. O. Park, C. Han, H. Beppu, E. Li, M. K. Raizada, K. D. Bloch and S. P. Oh (2008). "Genetic ablation of the BMPR2 gene in pulmonary endothelium is sufficient to predispose to pulmonary arterial hypertension." Circulation **118**(7): 722-730.
Hopkins, N. and P. McLoughlin (2002). "The structural basis of pulmonary hypertension in chronic lung disease: remodelling, rarefaction or angiogenesis?" J Anat **201**(4): 335-348.
Hu, C., Z. Wu, Z. Huang, X. Hao, S. Wang, J. Deng, Y. Yin and C. Tan (2021). "Nox2 impairs VEGF-A-induced angiogenesis in placenta via mitochondrial ROS-STAT3 pathway." Redox Biol **45**: 102051.
Huang, L., X. Chen, C. Dasgupta, W. Chen, R. Song, C. Wang and L. Zhang (2019). "Foetal hypoxia impacts methylome and transcriptome in developmental programming of heart disease." Cardiovasc Res **115**(8): 1306-1319.
Humbert, M., N. W. Morrell, S. L. Archer, K. R. Stenmark, M. R. MacLean, I. M. Lang, B. W. Christman, E. K. Weir, O. Eickelberg, N. F. Voelkel and M. Rabinovitch (2004). "Cellular and molecular pathobiology of pulmonary arterial hypertension." J Am Coll Cardiol **43**(12 Suppl S): 13S-24S.
Infantes, E. C., A. B. Prados, I. D. Contreras, G. M. Cahuana, A. Hmadcha, F. M. Bermudo, B. Soria, J. R. Huaman and F. J. Bergua (2015). "Nitric Oxide And Hypoxia Response In Pluripotent Stem Cells." Redox Biol **5**: 417-418.
Ismail, S., A. Sturrock, P. Wu, B. Cahill, K. Norman, T. Huecksteadt, K. Sanders, T. Kennedy and J. Hoidal (2009). "NOX4 mediates hypoxia-induced proliferation of human pulmonary artery smooth muscle cells: the role of autocrine production of transforming growth factor-beta1

and insulin-like growth factor binding protein-3." Am J Physiol Lung Cell Mol Physiol **296**(3): L489-499.
Ito, Y., A. Ahmad, E. Kewley and R. J. Mason (2011). "Hypoxia-inducible factor regulates expression of surfactant protein in alveolar type II cells in vitro." Am J Respir Cell Mol Biol **45**(5): 938-945.
Jayet, P. Y., S. F. Rimoldi, T. Stuber, C. S. Salmon, D. Hutter, E. Rexhaj, S. Thalmann, M. Schwab, P. Turini, C. Sartori-Cucchia, P. Nicod, M. Villena, Y. Allemann, U. Scherrer and C. Sartori (2010). "Pulmonary and systemic vascular dysfunction in young offspring of mothers with preeclampsia." Circulation **122**(5): 488-494.
Jeffery, T. K. and N. W. Morrell (2002). "Molecular and cellular basis of pulmonary vascular remodeling in pulmonary hypertension." Prog Cardiovasc Dis **45**(3): 173-202.
Jeffreys, R. M., W. Stepanchak, B. Lopez, J. Hardis and J. F. Clapp, 3rd (2006). "Uterine blood flow during supine rest and exercise after 28 weeks of gestation." Bjog **113**(11): 1239-1247.
Jensen, G. M. and L. G. Moore (1997). "The effect of high altitude and other risk factors on birthweight: independent or interactive effects?" Am J Public Health **87**(6): 1003-1007.
Jing, Z. C., X. Q. Xu, Z. Y. Han, Y. Wu, K. W. Deng, H. Wang, Z. W. Wang, X. S. Cheng, B. Xu, S. S. Hu, R. T. Hui and Y. J. Yang (2007). "Registry and survival study in chinese patients with idiopathic and familial pulmonary arterial hypertension." Chest **132**(2): 373-379.
Julian, C. G., E. Vargas, J. F. Armaza, M. J. Wilson, S. Niermeyer and L. G. Moore (2007). "High-altitude ancestry protects against hypoxia-associated reductions in fetal growth." Arch Dis Child Fetal Neonatal Ed **92**(5): F372-377.
Julian, C. G., M. J. Wilson, M. Lopez, H. Yamashiro, W. Tellez, A. Rodriguez, A. W. Bigham, M. D. Shriver, C. Rodriguez, E. Vargas and L. G. Moore (2009). "Augmented uterine artery blood flow and oxygen delivery protect Andeans from altitude-associated reductions in fetal growth." Am J Physiol Regul Integr Comp Physiol **296**(5): R1564-1575.
Julian, C. G., M. J. Wilson and L. G. Moore (2009). "Evolutionary adaptation to high altitude: a view from in utero." Am J Hum Biol **21**(5): 614-622.
Kamitomo, M., L. D. Longo and R. D. Gilbert (1992). "Right and left ventricular function in fetal sheep exposed to long-term high-altitude hypoxemia." Am J Physiol **262**(2 Pt 2): H399-405.
Kane, A. D., J. A. Hansell, E. A. Herrera, B. J. Allison, Y. Niu, K. L. Brain, J. J. Kaandorp, J. B. Derks and D. A. Giussani (2014). "Xanthine oxidase and the fetal cardiovascular defence to hypoxia in late gestation ovine pregnancy." J Physiol **592**(3): 475-489.
Karowicz-Bilinska, A., J. Suzin and P. Sieroszewski (2002). "Evaluation of oxidative stress indices during treatment in pregnant women with intrauterine growth retardation." Med Sci Monit **8**(3): CR211-216.
Katsuyama, M., C. Fan and C. Yabe-Nishimura (2002). "NADPH oxidase is involved in prostaglandin F2alpha-induced hypertrophy of vascular smooth muscle cells: induction of NOX1 by PGF2alpha." J Biol Chem **277**(16): 13438-13442.
Kawahara, T., D. Ritsick, G. Cheng and J. D. Lambeth (2005). "Point mutations in the proline-rich region of p22phox are dominant inhibitors of Nox1- and Nox2-dependent reactive oxygen generation." J Biol Chem **280**(36): 31859-31869.
Keyes, L. E., J. F. Armaza, S. Niermeyer, E. Vargas, D. A. Young and L. G. Moore (2003). "Intrauterine growth restriction, preeclampsia, and intrauterine mortality at high altitude in Bolivia." Pediatr Res **54**(1): 20-25.
Khalyfa, A., R. Cortese, Z. Qiao, H. Ye, R. Bao, J. Andrade and D. Gozal (2017). "Late gestational intermittent hypoxia induces metabolic and epigenetic changes in male adult offspring mice." J Physiol **595**(8): 2551-2568.
Khayrullina, G., S. Bermudez and K. R. Byrnes (2015). "Inhibition of NOX2 reduces locomotor impairment, inflammation, and oxidative stress after spinal cord injury." J Neuroinflammation **12**: 172.
Kim, J., J. Kim, H. J. Lim, S. Lee, Y. S. Bae and J. Kim (2022). "Nox4-IGF2 Axis Promotes Differentiation of Embryoid Body Cells Into Derivatives of the Three Embryonic Germ Layers." Stem Cell Rev Rep **18**(3): 1181-1192.

Konduri, G. G. and S. Lakshminrusimha (2021). "Surf early to higher tides: surfactant therapy to optimize tidal volume, lung recruitment, and iNO response." J Perinatol **41**(1): 1-3.
Kovo, M., L. Schreiber, O. Elyashiv, A. Ben-Haroush, G. Abraham and J. Bar (2015). "Pregnancy outcome and placental findings in pregnancies complicated by fetal growth restriction with and without preeclampsia." Reprod Sci **22**(3): 316-321.
Krampl, E. (2002). "Pregnancy at high altitude." Ultrasound Obstet Gynecol **19**(6): 535-539.
Krishnan, A., R. Samtani, P. Dhanantwari, E. Lee, S. Yamada, K. Shiota, M. T. Donofrio, L. Leatherbury and C. W. Lo (2014). "A detailed comparison of mouse and human cardiac development." Pediatr Res **76**(6): 500-507.
Krishnan, S., R. S. Stearman, L. Zeng, A. Fisher, E. A. Mickler, B. H. Rodriguez, E. R. Simpson, T. Cook, J. E. Slaven, M. Ivan, M. W. Geraci, T. Lahm and R. S. Tepper (2020). "Transcriptomic modifications in developmental cardiopulmonary adaptations to chronic hypoxia using a murine model of simulated high-altitude exposure." Am J Physiol Lung Cell Mol Physiol **319**(3): L456-L470.
Kublickiene, K. R., B. Lindblom, K. Kruger and H. Nisell (2000). "Preeclampsia: evidence for impaired shear stress-mediated nitric oxide release in uterine circulation." Am J Obstet Gynecol **183**(1): 160-166.
Kublickiene, K. R., H. Nisell, L. Poston, K. Kruger and B. Lindblom (2000). "Modulation of vascular tone by nitric oxide and endothelin 1 in myometrial resistance arteries from pregnant women at term." Am J Obstet Gynecol **182**(1 Pt 1): 87-93.
Kumar, P., J. S. Morton, A. Shah, V. Do, C. Sergi, J. Serrano-Lomelin, S. T. Davidge, D. Beker, J. Levasseur and L. K. Hornberger (2020). "Intrauterine exposure to chronic hypoxia in the rat leads to progressive diastolic function and increased aortic stiffness from early postnatal developmental stages." Physiol Rep **8**(1): e14327.
Lau, E. M. T., E. Giannoulatou, D. S. Celermajer and M. Humbert (2017). "Epidemiology and treatment of pulmonary arterial hypertension." Nat Rev Cardiol **14**(10): 603-614.
Lee, J. H., Y. M. Yoo, B. Lee, S. Jeong, D. N. Tran and E. B. Jeung (2021). "Melatonin mitigates the adverse effect of hypoxia during myocardial differentiation in mouse embryonic stem cells." J Vet Sci **22**(4): e54.
Lee, Y. S., J. Byun, J. A. Kim, J. S. Lee, K. L. Kim, Y. L. Suh, J. M. Kim, H. S. Jang, J. Y. Lee, I. S. Shin, W. Suh, E. S. Jeon and D. K. Kim (2005). "Monocrotaline-induced pulmonary hypertension correlates with upregulation of connective tissue growth factor expression in the lung." Exp Mol Med **37**(1): 27-35.
Li, G., S. Bae and L. Zhang (2004). "Effect of prenatal hypoxia on heat stress-mediated cardioprotection in adult rat heart." Am J Physiol Heart Circ Physiol **286**(5): H1712-1719.
Li, G., Y. Xiao, J. L. Estrella, C. A. Ducsay, R. D. Gilbert and L. Zhang (2003). "Effect of fetal hypoxia on heart susceptibility to ischemia and reperfusion injury in the adult rat." J Soc Gynecol Investig **10**(5): 265-274.
Li, J., M. Stouffs, L. Serrander, B. Banfi, E. Bettiol, Y. Charnay, K. Steger, K. H. Krause and M. E. Jaconi (2006). "The NADPH oxidase NOX4 drives cardiac differentiation: Role in regulating cardiac transcription factors and MAP kinase activation." Mol Biol Cell **17**(9): 3978-3988.
Lichty, J. A. (1957). "Neonatal mortality and prematurity in Colorado." Rocky Mt Med J **54**(3): 251-254.
Lichty, J. A., R. Y. Ting, P. D. Bruns and E. Dyar (1957). "Studies of babies born at high altitudes. I. Relation of altitude to birth weight." AMA J Dis Child **93**(6): 666-669.
Ling, Y., M. K. Johnson, D. G. Kiely, R. Condliffe, C. A. Elliot, J. S. Gibbs, L. S. Howard, J. Pepke-Zaba, K. K. Sheares, P. A. Corris, A. J. Fisher, J. L. Lordan, S. Gaine, J. G. Coghlan, S. J. Wort, M. A. Gatzoulis and A. J. Peacock (2012). "Changing demographics, epidemiology, and survival of incident pulmonary arterial hypertension: results from the pulmonary hypertension registry of the United Kingdom and Ireland." Am J Respir Crit Care Med **186**(8): 790-796.

Liu, J. Q., I. N. Zelko, E. M. Erbynn, J. S. Sham and R. J. Folz (2006). "Hypoxic pulmonary hypertension: role of superoxide and NADPH oxidase (gp91phox)." Am J Physiol Lung Cell Mol Physiol **290**(1): L2-10.
Long, L., M. L. Ormiston, X. Yang, M. Southwood, S. Graf, R. D. Machado, M. Mueller, B. Kinzel, L. M. Yung, J. M. Wilkinson, S. D. Moore, K. M. Drake, M. A. Aldred, P. B. Yu, P. D. Upton and N. W. Morrell (2015). "Selective enhancement of endothelial BMPR-II with BMP9 reverses pulmonary arterial hypertension." Nat Med **21**(7): 777-785.
Lu, D., A. Abulimiti, T. Wu, A. Abudureyim and N. Li (2018). "Pulmonary surfactant-associated proteins and inflammatory factors in obstructive sleep apnea." Sleep Breath **22**(1): 99-107.
Lueder, F. L., S. B. Kim, C. A. Buroker, S. A. Bangalore and E. S. Ogata (1995). "Chronic maternal hypoxia retards fetal growth and increases glucose utilization of select fetal tissues in the rat." Metabolism **44**(4): 532-537.
Luo, Z. C., Y. J. Zhao, F. Ouyang, Z. J. Yang, Y. N. Guo and J. Zhang (2013). "Diabetes and perinatal mortality in twin pregnancies." PLoS One **8**(9): e75354.
Luzardo, R., P. A. Silva, M. Einicker-Lamas, S. Ortiz-Costa, G. do Carmo Mda, L. D. Vieira-Filho, A. D. Paixao, L. S. Lara and A. Vieyra (2011). "Metabolic programming during lactation stimulates renal Na+ transport in the adult offspring due to an early impact on local angiotensin II pathways." PLoS One **6**(7): e21232.
Maisonneuve, E., E. Delvin, A. Edgard, L. Morin, J. Dube, I. Boucoiran, J. M. Moutquin, J. C. Fouron, S. Klam, E. Levy and L. Leduc (2015). "Oxidative conditions prevail in severe IUGR with vascular disease and Doppler anomalies." J Matern Fetal Neonatal Med **28**(12): 1471-1475.
Maraldi, T., C. Angeloni, C. Prata and S. Hrelia (2021). "NADPH Oxidases: Redox Regulators of Stem Cell Fate and Function." Antioxidants (Basel) **10**(6).
Martin, C., A. Y. Yu, B. H. Jiang, L. Davis, D. Kimberly, A. R. Hohimer and G. L. Semenza (1998). "Cardiac hypertrophy in chronically anemic fetal sheep: Increased vascularization is associated with increased myocardial expression of vascular endothelial growth factor and hypoxia-inducible factor 1." Am J Obstet Gynecol **178**(3): 527-534.
Martinet, W., M. W. Knaapen, G. R. De Meyer, A. G. Herman and M. M. Kockx (2002). "Elevated levels of oxidative DNA damage and DNA repair enzymes in human atherosclerotic plaques." Circulation **106**(8): 927-932.
Martyn, K. D., L. M. Frederick, K. von Loehneysen, M. C. Dinauer and U. G. Knaus (2006). "Functional analysis of Nox4 reveals unique characteristics compared to other NADPH oxidases." Cell Signal **18**(1): 69-82.
Mateev, S., A. H. Sillau, R. Mouser, R. E. McCullough, M. M. White, D. A. Young and L. G. Moore (2003). "Chronic hypoxia opposes pregnancy-induced increase in uterine artery vasodilator response to flow." Am J Physiol Heart Circ Physiol **284**(3): H820-829.
Mathiesen, E. R., L. Ringholm and P. Damm (2011). "Stillbirth in diabetic pregnancies." Best Pract Res Clin Obstet Gynaecol **25**(1): 105-111.
Matthai, C., R. Horvat, M. Noe, F. Nagele, A. Radjabi, M. van Trotsenburg, J. Huber and A. Kolbus (2006). "Oct-4 expression in human endometrium." Mol Hum Reprod **12**(1): 7-10.
McGillick, E. V., S. Orgeig, D. A. Giussani and J. L. Morrison (2017). "Chronic hypoxaemia as a molecular regulator of fetal lung development: implications for risk of respiratory complications at birth." Paediatr Respir Rev **21**: 3-10.
Mehta, A. R. and P. R. Mehta (2008). "The hypoxia of high altitude causes restricted fetal growth in chick embryos with the extent of this effect depending on maternal altitudinal status." J Physiol **586**(6): 1469-1471.
Meng, X., P. Zhang and L. Zhang (2020). "Fetal Hypoxia Impacts on Proliferation and Differentiation of Sca-1(+) Cardiac Progenitor Cells and Maturation of Cardiomyocytes: A Role of MicroRNA-210." Genes (Basel) **11**(3).
Meyerholz, D. K., J. A. DeGraaff, J. M. Gallup, A. K. Olivier and M. R. Ackermann (2006). "Depletion of alveolar glycogen corresponds with immunohistochemical development of CD208 antigen expression in perinatal lamb lung." J Histochem Cytochem **54**(11): 1247-1253.

Mikhed, Y., A. Gorlach, U. G. Knaus and A. Daiber (2015). "Redox regulation of genome stability by effects on gene expression, epigenetic pathways and DNA damage/repair." Redox Biol **5**: 275-289.
Millan, I., J. D. Pinero-Ramos, I. Lara, A. Parra-Llorca, I. Torres-Cuevas and M. Vento (2018). "Oxidative Stress in the Newborn Period: Useful Biomarkers in the Clinical Setting." Antioxidants (Basel) **7**(12).
Moore, L. G. (2003). "Fetal growth restriction and maternal oxygen transport during high altitude pregnancy." High Alt Med Biol **4**(2): 141-156.
Moore, L. G., S. M. Charles and C. G. Julian (2011). "Humans at high altitude: hypoxia and fetal growth." Respir Physiol Neurobiol **178**(1): 181-190.
Moore, L. G., S. Zamudio, J. Zhuang, S. Sun and T. Droma (2001). "Oxygen transport in tibetan women during pregnancy at 3,658 m." Am J Phys Anthropol **114**(1): 42-53.
Morton, S. U. and D. Brodsky (2016). "Fetal Physiology and the Transition to Extrauterine Life." Clin Perinatol **43**(3): 395-407.
Murphy-Marshman, H., K. Quensel, X. Shi-Wen, R. Barnfield, J. Kelly, A. Peidl, R. J. Stratton and A. Leask (2017). "Antioxidants and NOX1/NOX4 inhibition blocks TGFbeta1-induced CCN2 and alpha-SMA expression in dermal and gingival fibroblasts." PLoS One **12**(10): e0186740.
Murray, S. A., J. L. Morgan, C. Kane, Y. Sharma, C. S. Heffner, J. Lake and L. R. Donahue (2010). "Mouse gestation length is genetically determined." PLoS One **5**(8): e12418.
Nakano, Y., C. M. Longo-Guess, D. E. Bergstrom, W. M. Nauseef, S. M. Jones and B. Banfi (2008). "Mutation of the Cyba gene encoding p22phox causes vestibular and immune defects in mice." J Clin Invest **118**(3): 1176-1185.
Nanka, O., P. Valasek, M. Dvorakova and M. Grim (2006). "Experimental hypoxia and embryonic angiogenesis." Dev Dyn **235**(3): 723-733.
Newman, J. H. (2005). "Pulmonary hypertension." Am J Respir Crit Care Med **172**(9): 1072-1077.
Nicola, T., N. Ambalavanan, W. Zhang, M. L. James, V. Rehan, B. Halloran, N. Olave, A. Bulger, S. Oparil and Y. F. Chen (2011). "Hypoxia-induced inhibition of lung development is attenuated by the peroxisome proliferator-activated receptor-gamma agonist rosiglitazone." Am J Physiol Lung Cell Mol Physiol **301**(1): L125-134.
Nisbet, R. E., A. S. Graves, D. J. Kleinhenz, H. L. Rupnow, A. L. Reed, T. H. Fan, P. O. Mitchell, R. L. Sutliff and C. M. Hart (2009). "The role of NADPH oxidase in chronic intermittent hypoxia-induced pulmonary hypertension in mice." Am J Respir Cell Mol Biol **40**(5): 601-609.
Okada, K., Y. Tanaka, M. Bernstein, W. Zhang, G. A. Patterson and M. D. Botney (1997). "Pulmonary hemodynamics modify the rat pulmonary artery response to injury. A neointimal model of pulmonary hypertension." Am J Pathol **151**(4): 1019-1025.
Osol, G. and M. Mandala (2009). "Maternal uterine vascular remodeling during pregnancy." Physiology (Bethesda) **24**: 58-71.
Osterman, H., I. Lindgren, T. Lindstrom and J. Altimiras (2015). "Chronic hypoxia during development does not trigger pathologic remodeling of the chicken embryonic heart but reduces cardiomyocyte number." Am J Physiol Regul Integr Comp Physiol **309**(10): R1204-1214.
Paffenholz, R., R. A. Bergstrom, F. Pasutto, P. Wabnitz, R. J. Munroe, W. Jagla, U. Heinzmann, A. Marquardt, A. Bareiss, J. Laufs, A. Russ, G. Stumm, J. C. Schimenti and D. E. Bergstrom (2004). "Vestibular defects in head-tilt mice result from mutations in Nox3, encoding an NADPH oxidase." Genes Dev **18**(5): 486-491.
Paik, Y. H. and D. A. Brenner (2011). "NADPH oxidase mediated oxidative stress in hepatic fibrogenesis." Korean J Hepatol **17**(4): 251-257.
Pan, H., G. H. Deutsch, S. E. Wert, S. Ontology and N. M. A. o. L. D. P. Consortium (2019). "Comprehensive anatomic ontologies for lung development: A comparison of alveolar formation and maturation within mouse and human lung." J Biomed Semantics **10**(1): 18.

Panday, A., M. K. Sahoo, D. Osorio and S. Batra (2015). "NADPH oxidases: an overview from structure to innate immunity-associated pathologies." Cell Mol Immunol **12**(1): 5-23.
Papamatheakis, D. G., A. B. Blood, J. H. Kim and S. M. Wilson (2013). "Antenatal hypoxia and pulmonary vascular function and remodeling." Curr Vasc Pharmacol **11**(5): 616-640.
Patel, D., R. Alhawaj and M. S. Wolin (2014). "Exposure of mice to chronic hypoxia attenuates pulmonary arterial contractile responses to acute hypoxia by increases in extracellular hydrogen peroxide." Am J Physiol Regul Integr Comp Physiol **307**(4): R426-433.
Patterson, A. J., M. Chen, Q. Xue, D. Xiao and L. Zhang (2010). "Chronic prenatal hypoxia induces epigenetic programming of PKC{epsilon} gene repression in rat hearts." Circ Res **107**(3): 365-373.
Patterson, A. J., D. Xiao, F. Xiong, B. Dixon and L. Zhang (2012). "Hypoxia-derived oxidative stress mediates epigenetic repression of PKCepsilon gene in foetal rat hearts." Cardiovasc Res **93**(2): 302-310.
Patterson, A. J. and L. Zhang (2010). "Hypoxia and fetal heart development." Curr Mol Med **10**(7): 653-666.
Pearson, J. T. (2015). "Cardiac responses to hypoxia and reoxygenation in Drosophila. New insights into evolutionarily conserved gene responses. Focus on "Cardiac responses to hypoxia and reoxygenation in Drosophila"." Am J Physiol Regul Integr Comp Physiol **309**(11): R1344-1346.
Peng, T., Y. Tian, C. J. Boogerd, M. M. Lu, R. S. Kadzik, K. M. Stewart, S. M. Evans and E. E. Morrisey (2013). "Coordination of heart and lung co-development by a multipotent cardiopulmonary progenitor." Nature **500**(7464): 589-592.
Pennington, K. A., J. M. Schlitt, D. L. Jackson, L. C. Schulz and D. J. Schust (2012). "Preeclampsia: multiple approaches for a multifactorial disease." Dis Model Mech **5**(1): 9-18.
Pepke-Zaba, J., P. Jansa, N. H. Kim, R. Naeije and G. Simonneau (2013). "Chronic thromboembolic pulmonary hypertension: role of medical therapy." Eur Respir J **41**(4): 985-990.
Perjes, A., A. M. Kubin, A. Konyi, S. Szabados, A. Cziraki, R. Skoumal, H. Ruskoaho and I. Szokodi (2012). "Physiological regulation of cardiac contractility by endogenous reactive oxygen species." Acta Physiol (Oxf) **205**(1): 26-40.
Pfaffl, M. W., G. W. Horgan and L. Dempfle (2002). "Relative expression software tool (REST) for group-wise comparison and statistical analysis of relative expression results in real-time PCR." Nucleic Acids Res **30**(9): e36.
R-Development-Core-Team (2006). "R: A language and environment for statistiacl computing." R Foundation for Statistical Computing, Vienna, Austria.
Ramirez, D. C., S. E. Gomez-Mejiba and R. P. Mason (2007). "Immuno-spin trapping analyses of DNA radicals." Nat Protoc **2**(3): 512-522.
Rashid, C. S., A. Bansal and R. A. Simmons (2018). "Oxidative Stress, Intrauterine Growth Restriction, and Developmental Programming of Type 2 Diabetes." Physiology (Bethesda) **33**(5): 348-359.
Razeghi, P., M. F. Essop, J. M. Huss, S. Abbasi, N. Manga and H. Taegtmeyer (2003). "Hypoxia-induced switches of myosin heavy chain iso-gene expression in rat heart." Biochem Biophys Res Commun **303**(4): 1024-1027.
Ream, M., A. M. Ray, R. Chandra and D. M. Chikaraishi (2008). "Early fetal hypoxia leads to growth restriction and myocardial thinning." Am J Physiol Regul Integr Comp Physiol **295**(2): R583-595.
Rexhaj, E., J. Bloch, P. Y. Jayet, S. F. Rimoldi, P. Dessen, C. Mathieu, J. F. Tolsa, P. Nicod, U. Scherrer and C. Sartori (2011). "Fetal programming of pulmonary vascular dysfunction in mice: role of epigenetic mechanisms." Am J Physiol Heart Circ Physiol **301**(1): H247-252.
Robin, E., F. Marcillac and E. Raddatz (2015). "A hypoxic episode during cardiogenesis downregulates the adenosinergic system and alters the myocardial anoxic tolerance." Am J Physiol Regul Integr Comp Physiol **308**(7): R614-626.

Rockwell, L. C., E. C. Dempsey and L. G. Moore (2006). "Chronic hypoxia diminishes the proliferative response of Guinea pig uterine artery vascular smooth muscle cells in vitro." High Alt Med Biol **7**(3): 237-244.
Rodriguez-Rodriguez, P., A. L. Lopez de Pablo, C. F. Garcia-Prieto, B. Somoza, B. Quintana-Villamandos, J. J. Gomez de Diego, P. Y. Gutierrez-Arzapalo, D. Ramiro-Cortijo, M. C. Gonzalez and S. M. Arribas (2017). "Long term effects of fetal undernutrition on rat heart. Role of hypertension and oxidative stress." PLoS One **12**(2): e0171544.
Rodriguez-Rodriguez, P., D. Ramiro-Cortijo, C. G. Reyes-Hernandez, A. L. Lopez de Pablo, M. C. Gonzalez and S. M. Arribas (2018). "Implication of Oxidative Stress in Fetal Programming of Cardiovascular Disease." Front Physiol **9**: 602.
Roy, M. G., M. Rahmani, J. R. Hernandez, S. N. Alexander, C. Ehre, S. B. Ho and C. M. Evans (2011). "Mucin production during prenatal and postnatal murine lung development." Am J Respir Cell Mol Biol **44**(6): 755-760.
Rueda-Clausen, C. F., V. W. Dolinsky, J. S. Morton, S. D. Proctor, J. R. B. Dyck and S. T. Davidge (2011). "Hypoxia-Induced Intrauterine Growth Restriction Increases the Susceptibility of Rats to High-Fat Diet–Induced Metabolic Syndrome." Diabetes **60**(2): 507-516.
Rueda-Clausen, C. F., J. S. Morton and S. T. Davidge (2009). "Effects of hypoxia-induced intrauterine growth restriction on cardiopulmonary structure and function during adulthood." Cardiovasc Res **81**(4): 713-722.
Rueda-Clausen, C. F., J. L. Stanley, D. F. Thambiraj, R. Poudel, S. T. Davidge and P. N. Baker (2014). "Effect of prenatal hypoxia in transgenic mouse models of preeclampsia and fetal growth restriction." Reprod Sci **21**(4): 492-502.
Ryan, J. J., T. Thenappan, N. Luo, T. Ha, A. R. Patel, S. Rich and S. L. Archer (2012). "The WHO classification of pulmonary hypertension: A case-based imaging compendium." Pulm Circ **2**(1): 107-121.
Rybalkin, S. D., C. Yan, K. E. Bornfeldt and J. A. Beavo (2003). "Cyclic GMP phosphodiesterases and regulation of smooth muscle function." Circ Res **93**(4): 280-291.
Saini, Y., J. R. Harkema and J. J. LaPres (2008). "HIF1alpha is essential for normal intrauterine differentiation of alveolar epithelium and surfactant production in the newborn lung of mice." J Biol Chem **283**(48): 33650-33657.
Saker, M., N. Soulimane Mokhtari, S. A. Merzouk, H. Merzouk, B. Belarbi and M. Narce (2008). "Oxidant and antioxidant status in mothers and their newborns according to birthweight." Eur J Obstet Gynecol Reprod Biol **141**(2): 95-99.
Sardesai, S., M. Biniwale, F. Wertheimer, A. Garingo and R. Ramanathan (2017). "Evolution of surfactant therapy for respiratory distress syndrome: past, present, and future." Pediatr Res **81**(1-2): 240-248.
Sartori, C., Y. Allemann, L. Trueb, A. Delabays, P. Nicod and U. Scherrer (1999). "Augmented vasoreactivity in adult life associated with perinatal vascular insult." Lancet **353**(9171): 2205-2207.
Sauer, H., G. Rahimi, J. Hescheler and M. Wartenberg (2000). "Role of reactive oxygen species and phosphatidylinositol 3-kinase in cardiomyocyte differentiation of embryonic stem cells." FEBS Lett **476**(3): 218-223.
Sauer, H., C. Ruhe, J. P. Muller, M. Schmelter, R. D'Souza and M. Wartenberg (2008). "Reactive oxygen species and upregulation of NADPH oxidases in mechanotransduction of embryonic stem cells." Methods Mol Biol **477**: 397-418.
Schmiedl, A., T. Roolfs, E. Tutdibi, L. Gortner and D. Monz (2017). "Influence of prenatal hypoxia and postnatal hyperoxia on morphologic lung maturation in mice." PLoS One **12**(4).
Shati, A. A., M. S. A. Zaki, Y. A. Alqahtani, M. A. Haidara, M. A. Alshehri, A. F. Dawood and R. A. Eid (2022). "Intermittent Short-Duration Re-oxygenation Attenuates Cardiac Changes in Response to Hypoxia: Histological, Ultrastructural and Oxidant/Antioxidant Parameters." Br J Biomed Sci **79**: 10150.

Shimomura, S., H. Inoue, Y. Arai, S. Nakagawa, Y. Fujii, T. Kishida, M. Shin-Ya, S. Ichimaru, S. Tsuchida, O. Mazda and T. Kubo (2022). "Hypoxia promotes differentiation of pure cartilage from human induced pluripotent stem cells." Mol Med Rep **26**(1).
Smith, K. L. M., A. Swiderska, M. C. Lock, L. Graham, W. Iswari, T. Choudhary, D. Thomas, H. M. Kowash, M. Desforges, E. C. Cottrell, A. W. Trafford, D. A. Giussani and G. L. J. Galli (2022). "Chronic developmental hypoxia alters mitochondrial oxidative capacity and reactive oxygen species production in the fetal rat heart in a sex-dependent manner." J Pineal Res **73**(3): e12821.
Smith, L. J., K. O. McKay, P. P. van Asperen, H. Selvadurai and D. A. Fitzgerald (2010). "Normal development of the lung and premature birth." Paediatr Respir Rev **11**(3): 135-142.
Stasch, J. P. and O. V. Evgenov (2013). "Soluble guanylate cyclase stimulators in pulmonary hypertension." Handb Exp Pharmacol **218**: 279-313.
Steiner, M. K., O. L. Syrkina, N. Kolliputi, E. J. Mark, C. A. Hales and A. B. Waxman (2009). "Interleukin-6 overexpression induces pulmonary hypertension." Circ Res **104**(2): 236-244, 228p following 244.
Stiebellehner, L., J. K. Belknap, B. Ensley, A. Tucker, E. C. Orton, J. T. Reeves and K. R. Stenmark (1998). "Lung endothelial cell proliferation in normal and pulmonary hypertensive neonatal calves." Am J Physiol **275**(3): L593-600.
Sugishita, Y., D. W. Leifer, F. Agani, M. Watanabe and S. A. Fisher (2004). "Hypoxia-responsive signaling regulates the apoptosis-dependent remodeling of the embryonic avian cardiac outflow tract." Dev Biol **273**(2): 285-296.
Suzuki, N. (2015). "Erythropoietin gene expression: developmental-stage specificity, cell-type specificity, and hypoxia inducibility." Tohoku J Exp Med **235**(3): 233-240.
Szanto, I., L. Rubbia-Brandt, P. Kiss, K. Steger, B. Banfi, E. Kovari, F. Herrmann, A. Hadengue and K. H. Krause (2005). "Expression of NOX1, a superoxide-generating NADPH oxidase, in colon cancer and inflammatory bowel disease." J Pathol **207**(2): 164-176.
Szekeres, F. L. M., E. Walum, P. Wikstrom and A. Arner (2021). "A small molecule inhibitor of Nox2 and Nox4 improves contractile function after ischemia-reperfusion in the mouse heart." Sci Rep **11**(1): 11970.
Taraseviciene-Stewart, L., Y. Kasahara, L. Alger, P. Hirth, G. Mc Mahon, J. Waltenberger, N. F. Voelkel and R. M. Tuder (2001). "Inhibition of the VEGF receptor 2 combined with chronic hypoxia causes cell death-dependent pulmonary endothelial cell proliferation and severe pulmonary hypertension." FASEB J **15**(2): 427-438.
Ten Have-Opbroek, A. A. (1991). "Lung development in the mouse embryo." Exp Lung Res **17**(2): 111-130.
Terada, R., S. Warren, J. T. Lu, K. R. Chien, A. Wessels and H. Kasahara (2011). "Ablation of Nkx2-5 at mid-embryonic stage results in premature lethality and cardiac malformation." Cardiovasc Res **91**(2): 289-299.
Thakor, A. S., H. G. Richter, A. D. Kane, C. Dunster, F. J. Kelly, L. Poston and D. A. Giussani (2010). "Redox modulation of the fetal cardiovascular defence to hypoxaemia." J Physiol **588**(Pt 21): 4235-4247.
Tong, Y., S. Zhang, S. Riddle, L. Zhang, R. Song and D. Yue (2021). "Intrauterine Hypoxia and Epigenetic Programming in Lung Development and Disease." Biomedicines **9**(8).
Torres-Cuevas, I., A. Parra-Llorca, A. Sanchez-Illana, A. Nunez-Ramiro, J. Kuligowski, C. Chafer-Pericas, M. Cernada, J. Escobar and M. Vento (2017). "Oxygen and oxidative stress in the perinatal period." Redox Biol **12**: 674-681.
Treuer, A. V., M. Faundez, R. Ebensperger, E. Hovelmeyer, A. Vergara-Jaque, Y. Perera-Sardina, M. Gutierrez, R. Fuentealba and D. R. Gonzalez (2023). "New NADPH Oxidase 2 Inhibitors Display Potent Activity against Oxidative Stress by Targeting p22(phox)-p47(phox) Interactions." Antioxidants (Basel) **12**(7).
Tripathi, A., B. Kumar and S. S. K. Sagi (2021). "Hypoxia-mediated alterations in pulmonary surfactant protein expressions: Beneficial effects of quercetin prophylaxis." Respir Physiol Neurobiol **291**: 103695.

Tsao, P. N. and S. C. Wei (2013). "Prenatal hypoxia downregulates the expression of pulmonary vascular endothelial growth factor and its receptors in fetal mice." Neonatology **103**(4): 300-307.
Vargas, M., E. Vargas, C. G. Julian, J. F. Armaza, A. Rodriguez, W. Tellez, S. Niermeyer, M. Wilson, E. Parra, M. Shriver and L. G. Moore (2007). "Determinants of blood oxygenation during pregnancy in Andean and European residents of high altitude." Am J Physiol Regul Integr Comp Physiol **293**(3): R1303-1312.
Vento, M. and K. Teramo (2013). "Evaluating the fetus at risk for cardiopulmonary compromise." Semin Fetal Neonatal Med **18**(6): 324-329.
Villar, J., M. Purwar, M. Merialdi, N. Zavaleta, N. Thi Nhu Ngoc, J. Anthony, A. De Greeff, L. Poston, A. Shennan, W. H. O. V. C and E. t. g. Vitamin (2009). "World Health Organisation multicentre randomised trial of supplementation with vitamins C and E among pregnant women at high risk for pre-eclampsia in populations of low nutritional status from developing countries." BJOG **116**(6): 780-788.
von Ehr, J. and F. von Versen-Hoynck (2016). "Implications of maternal conditions and pregnancy course on offspring's medical problems in adult life." Arch Gynecol Obstet **294**(4): 673-679.
Walton, S. L., R. R. Singh, T. Tan, T. M. Paravicini and K. M. Moritz (2016). "Late gestational hypoxia and a postnatal high salt diet programs endothelial dysfunction and arterial stiffness in adult mouse offspring." J Physiol **594**(5): 1451-1463.
Wang, P., Z. X. Tan, L. Fu, Y. J. Fan, B. Luo, Z. H. Zhang, S. Xu, Y. H. Chen, H. Zhao and D. X. Xu (2020). "Gestational vitamin D deficiency impairs fetal lung development through suppressing type II pneumocyte differentiation." Reprod Toxicol **94**: 40-47.
Wang, Q., R. S. Reiter, Q. Q. Huang, J. P. Jin and J. J. Lin (2001). "Comparative studies on the expression patterns of three troponin T genes during mouse development." Anat Rec **263**(1): 72-84.
Watanabe, M., A. Jafri and S. A. Fisher (2001). "Apoptosis is required for the proper formation of the ventriculo-arterial connections." Dev Biol **240**(1): 274-288.
Wessels, A. and D. Sedmera (2003). "Developmental anatomy of the heart: a tale of mice and man." Physiol Genomics **15**(3): 165-176.
White, M. M., R. E. McCullough, R. Dyckes, A. D. Robertson and L. G. Moore (2000). "Chronic hypoxia, pregnancy, and endothelium-mediated relaxation in guinea pig uterine and thoracic arteries." Am J Physiol Heart Circ Physiol **278**(6): H2069-2075.
Wilson, M. J., M. Lopez, M. Vargas, C. Julian, W. Tellez, A. Rodriguez, A. Bigham, J. F. Armaza, S. Niermeyer, M. Shriver, E. Vargas and L. G. Moore (2007). "Greater uterine artery blood flow during pregnancy in multigenerational (Andean) than shorter-term (European) high-altitude residents." Am J Physiol Regul Integr Comp Physiol **293**(3): R1313-1324.
Wu, W., J. He and X. Shao (2020). "Incidence and mortality trend of congenital heart disease at the global, regional, and national level, 1990-2017." Medicine (Baltimore) **99**(23): e20593.
Xu, Y., S. J. Williams, D. O'Brien and S. T. Davidge (2006). "Hypoxia or nutrient restriction during pregnancy in rats leads to progressive cardiac remodeling and impairs postischemic recovery in adult male offspring." FASEB J **20**(8): 1251-1253.
Xue, L., J. Y. Cai, J. Ma, Z. Huang, M. X. Guo, L. Z. Fu, Y. B. Shi and W. X. Li (2013). "Global expression profiling reveals genetic programs underlying the developmental divergence between mouse and human embryogenesis." BMC Genomics **14**: 568.
Xue, Q. and L. Zhang (2009). "Prenatal hypoxia causes a sex-dependent increase in heart susceptibility to ischemia and reperfusion injury in adult male offspring: role of protein kinase C epsilon." J Pharmacol Exp Ther **330**(2): 624-632.
Yang, X., P. Yang, J. Zhang, Y. Yang, M. Xiong, F. Shi, N. Li and Y. Jin (2022). "Silica nanoparticle exposure inhibits surfactant protein A and B in A549 cells through ROS-mediated JNK/c-Jun signaling pathway." Environ Toxicol **37**(9): 2291-2301.
Yi, E. S., H. Kim, H. Ahn, J. Strother, T. Morris, E. Masliah, L. A. Hansen, K. Park and P. J. Friedman (2000). "Distribution of obstructive intimal lesions and their cellular phenotypes in

chronic pulmonary hypertension. A morphometric and immunohistochemical study." Am J Respir Crit Care Med **162**(4 Pt 1): 1577-1586.
Zhang, Z., B. Trautz, D. Kracun, F. Vogel, M. Weitnauer, K. Hochkogler, A. Petry and A. Gorlach (2019). "Stabilization of p22phox by Hypoxia Promotes Pulmonary Hypertension." Antioxid Redox Signal **30**(1): 56-73.
Zhao, L., N. A. Mason, N. W. Morrell, B. Kojonazarov, A. Sadykov, A. Maripov, M. M. Mirrakhimov, A. Aldashev and M. R. Wilkins (2001). "Sildenafil inhibits hypoxia-induced pulmonary hypertension." Circulation **104**(4): 424-428.
Zielonka, J., M. Zielonka, G. Cheng, M. Hardy and B. Kalyanaraman (2019). "High-Throughput Screening of NOX Inhibitors." Methods Mol Biol **1982**: 429-446.

10 Acknowledgement

I would like to thank the DZHK for their financial and ideal support through a scholarship. My supervisor, Prof. Dr. med. Görlach, was essential in defining the path of my research. For this, I am extremely grateful. Prof. Dr. med Martin Halle and PD Dr. med. vet. Katja Steiger did also contribute to my research in an essential and excellent way and have always provided me with advice whenever needed. Also, I would like to thank Dr. rer. nat. Andreas Petry for his guidance through each step of the process. I would like to thank Prof. Dr. Moretti for providing the R1 mESC cells and excellent help in establishing the protocol in cell culture. Next, I would like to thank all my lab members for helping me out. I would like to thank my whole family for their support, especially my parents Barbara and Klaus Hochkogler and my parents-in-law Dr. med. Johanna Haufe and PD Dr. med. Mathias Haufe. At last, I would like to thank my husband Tobias Haufe. Without him this work would not have been accomplished.